SDSN Global Climate Hub

Report:

Post-fire flood hazards: Integrated modelling, protection measures, economic and policy implications

August 2025

Authors and affiliations:

Phoebe Koundouri[1,2,3], Angelos Alamanos[4], George Papaioannou[5], Vassiliki Markogianni[6], George Varlas[6], Mohammed Basheer[7], Nikolaos Nagkoulis[1], Angelos Plataniotis[1], Russell M. Wise[8], Stefanos Xenarios[8,9], Olympia Nisiforou[10], Anastasios Papadopoulos[6], Elias Dimitriou[6].

1. Sustainable Development Unit, ATHENA Research Center (RC), Athens, Greece

2. School of Economics DIEES and ReSEES Research Laboratory, Athens University of Economics and Business, Athens, Greece

3. Department of Earth Sciences, University of Cambridge, Cambridge, United Kingdom

4. Independent Researcher, Berlin, Germany

5. Department of Forestry and Management of the Environment and Natural Resources, Democritus University of Thrace, Orestiada, Greece

6. Hellenic Centre for Marine Research, Institute of Marine Biological Resources and Inland Waters, Anavissos, Attiki, Greece

7. Department of Civil & Mineral Engineering, University of Toronto, Toronto, Ontario, Canada

8. CSIRO Environment, Canberra, Australian Capital Territory, Australia

10. Nazarbayev University, Graduate School of Public Policy, Astana, Kazakhstan

Recommended citation:

Koundouri P, Alamanos A, Papaioannou G, Markogianni V, Varlas G, Basheer M, Nagkoulis N, Plataniotis A, Wise RM, Xenarios S, Nisiforou O, Papadopoulos A, Dimitriou E. (2025). Post-fire flood hazards: Integrated modelling, protection measures, and economic implications. Report, UN SDSN Global Climate Hub. August 2025, Athens, Greece.

The Global Climate Hub

The UN Sustainable Development Solutions Network's (SDSN) response to the multifaceted contemporary challenges is the Global Climate Hub (GCH), which came as an initiative for change, leveraging science-based solutions for a holistic and equitable sustainability transition [1,2]. These solutions are developed at regional, national, and sub-national level based both on the scientific expertise of its members, and the engagement with local policymakers (representatives of central and/or local government) – there are dedicated teams of GCH scientists specialized across various fields, working in research projects, as well as a network of SDSN National Hubs, facilitating communication, outreach, and solutions' implementation. The overall philosophy of the GCH can be summarized in the combination of five critical innovations, for developing acceptable and implementable sustainable pathways. These work as a framework for the analysis of any problem:

I. Cutting-edge models: This includes the use/development of system-dynamics based cross-sectoral simulation models.

II. Powerful digital AI-driven infrastructure that supports the handling of big data, their harmonization and management, as well as the coupling of the various models and the results' visualization. This facilitates the integration of the above models.

III. Development of the socio-economic narrative for the just and equitable implementation of the science-based pathways, a process fostering the co-ownership of the pathways across stakeholders, such as scientists and technology developers, policymakers, finance and business sectors, NGOs and civil society.

IV. Stakeholder engagement: Transformative participatory stakeholder approaches (workshop-based) for co-designing the pathways in detail.

V. Openness: The whole process of analyzing, co-designing, presenting and applying sustainable pathways supports the widespread adoption of the principles of Open Science and Open Access to data, models developed, and in general scientific infrastructure.

The GCH consists of nine separate units/working teams that have expertise to handle relevant research and practical applications (see the table below). These units are scientific areas, conceived as necessary 'steps' towards sustainability, as each one contributes a unique perspective and insight towards the development of customized strategies for climate neutrality, resilience, and sustainability.

All units operate under the philosophy of the five innovations explained in the previous section, together and always in coordination, to achieve the long-term goals.

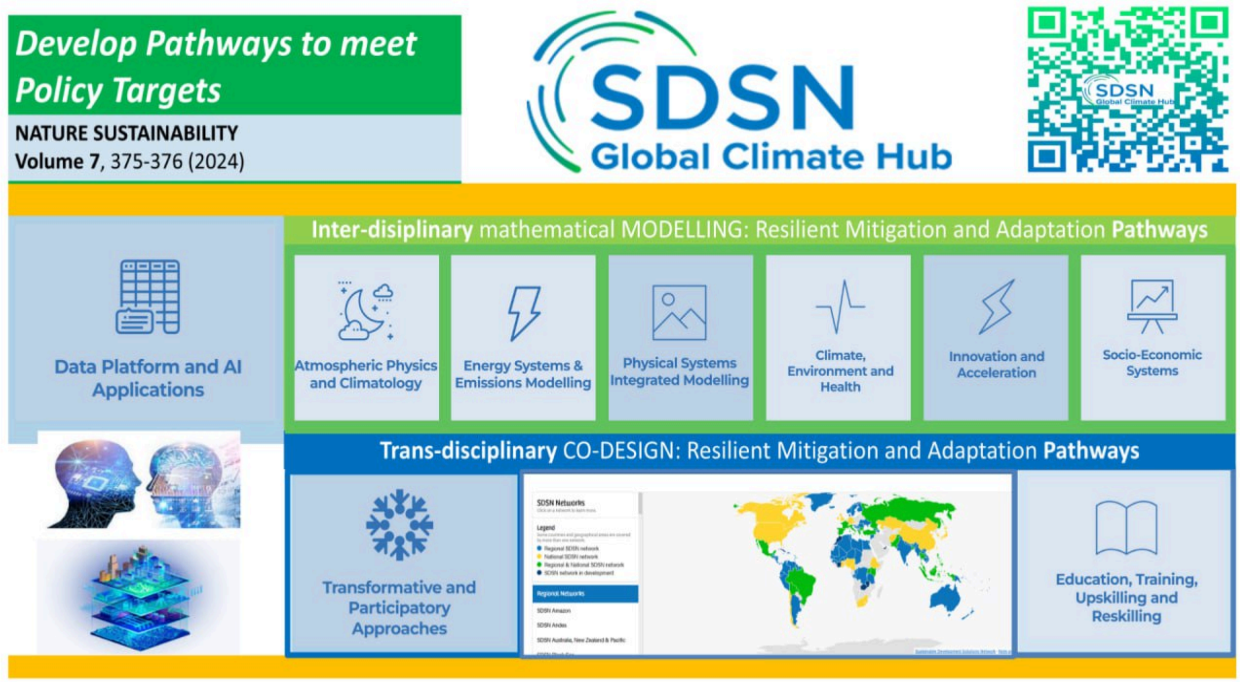

Figure a. The 9 units of the Global Climate Hub.

The GCH is hosted by Athens University of Economics and Business (AUEB) and the "Athena" Research and Innovation Center in Information, Communication, and Knowledge Technologies (ATHENA RC), both integral components of the Alliance of Excellence for Research and Innovation on Aephoria (AE4RIA – in Greek 'aephoria' is a synonymous concept to sustainable development). Within the GCH, AE4RIA plays a vital role in securing funding from competitive projects, ensuring the necessary resources to fulfill its multidimensional mission. The Research Centre for Atmospheric Physics and Climatology of the Academy of Athens also supports the GCH.

In this report we present a thorough study on an overlooked issue: post-fire floods and protection, along with a breadth of interrelated factors and modelling scenarios. A local case study is presented, and we argue on the generalization and transferability of the findings, by suggesting newly developed tools.

Executive Abstract:

Climate change-induced wildfires are increasingly prevalent, particularly during summer periods, with evident consequences in multiple regions worldwide. Wildfires affect and change the condition, functionality, and ecosystem services of the burned sites. Altered hydrologic processes make burnt areas more flood-prone. However, the actual effects of wildfires to flooding, the post-fire protection measures and their economic implications remain still overlooked issues. In this report, we cover these gaps in a multi-disciplinary way. More specifically:

PART A: We present a novel, integrated and interdisciplinary computational framework that we have developed for the accurate modelling of post-fire flash-flood events. The 2019 post-fire flood in Kineta, Central Greece is used as a case study-example.

The proposed approach assesses the fire impacts (burn extent and severity) with Remote Sensing techniques; 'recreates' real storms using the atmospheric model WRF-ARW; simulates the flood using the 2D HEC-RAS hydraulic-hydrodynamic model; and validates the results with remote sensing analysis on the flood extent. We detail the linking of those models, step-by-step, for the first time. We build upon the findings by reviewing, selecting and designing the most appropriate Post-fire Erosion and Flood-protection Treatments (PEFTs), and represent them within a Geographic Information System (GIS), which allows their incorporation to the HEC-RAS hydraulic model. The flood event is simulated under three scenarios: pre-fire; post-fire (real case, happened in November 2019), and post-fire with the PEFTs protection. Thus, for the first time, we reveal the effects of the fire on flooding (~25%), as well as the effectiveness of the suggested measures to mitigate the flood (completely offsetting the fire's effect).

In order to assess the economic implications of the potential flood protection interventions, we present also a detailed estimation of the: i) Costs of the proposed PEFTs, ii) The flood damage direct costs, which were estimated by a semi-automated AI-based approach using image segmentation and human-checks. The comparison of the costs reveals that protection could have cost just 13.6% of the direct damages.

Part B: Drawing from the inaction and poor protection of our real case study, we explore the governance gaps. We performed a knowledge-transfer exercise from similar cases in Australia (climate and governance similarities), based on the VRK (Values-Rules-Knowledge) framework. We provide a detailed stakeholder engagement roadmap targeting changes in anachronistic perceptions about the extreme phenomena, the understanding and application of solutions, and their communication as necessary, multi-benefit and cost-effective measures. These findings are applicable to other case studies, too.

Part C: For the facilitation of similar analyses nation-wide, we provide a national Greek inventory of design storms based on the official IDF (intensity-duration-frequency) Curves. For this purpose, we developed a novel tool called Catchment2Storm that provides customized design storms (return periods, durations, time intervals) using just the desired catchment's location. We comment on the results of its Greek-wide application, highlighting the need for localized design considerations in critical sites such as urban centers, ports, and agricultural areas.

Finally, we synthesize all the above into a concrete, agenda-setting list of policy recommendations to foster resilience to combined hazards.

CONTENTS

1 Background

1.1. Post-fire floods

Wildfires have become an increasingly pressing challenge, with the changing climate exacerbating their extent and severity worldwide [3,4]. This escalating trend threatens ecosystems and human communities, as evidenced by the recurring occurrence of record-high wildfire damages each summer [5–9]. Countries with drier climate, such as the Mediterranean ones, are particularly susceptible to wildfires, and the summer of 2023 served as compelling evidence [10,11]. Although wildfires are strongly felt during summer periods, the associated damages last longer, posing severe risks [12]. Wildfires notably alter the vegetation and land cover composition, and soil properties. These fundamental changes directly affect the hydrological behaviour of burnt catchments, removing their canopy cover, modifying their runoff patterns, heightening streamflow rates, and increasing sediment transport [13]. Thus, burnt areas are more vulnerable to extreme peak-flows [14,15].

Text Box 1:

Flood danger after wildfire – Informational Material from the US National Weather Service, warning for the Mesa Country[1].

[1] Source: https://www.mesacounty.us/departments-and-services/sheriff/divisions/emergency-services/wildland-fire-management/after/flood

The Mediterranean region, a climate change hotspot, has been particularly vulnerable to increasingly severe fire and flood events over the last years, while such threats are anticipated to become more prevalent in the future [16–18]. Thus, it is imperative to better understand the dynamics of such risks, as well as being proactive through continuous resilience-building efforts.

Such effects have been explored from the perspective of identifying the driving factors of post-fire flood risks [19], and the post-fire hazards considering infrastructure sedimentation to hypothetical watersheds [20,21]. Also, previous works have examined the hydrological response of burnt sites [22], their hydrological and soil-hydraulic properties [23], and the formulation of hydrological models tailored to post-fire runoff simulation [6,24,25].

Some studies have also analyzed the flood mapping of burnt sites through hydraulic modelling: Godara et al. [26] applied a rain-on-grid technique in the hydraulic model Telemac to explore the response of a Norwegian catchment to a design-flood. Chrysovergis et al. [27] studied a real post-fire event causing flood and erosion damages in Southern California, with the focus however being on the factors that caused the damages. Theochari and Baltas [28] analyzed the hydrological and hydraulic response of flood-susceptible areas of a burnt site in Evia island, Greece, to a design-storm. Furthermore, the effect of flood protection works on flood risk scenarios has been explored for the case of Mandra (Attica, Greece), which is often under fire risk [29,30]. The findings of all these studies converge, demonstrating the large extent of flooded areas, following fires that increase the soil imperviousness, the peak discharge, reduce the time to peak of rainfall events and also underlying the need for post-fire protection treatments and flood protection works. However, there are only a handful of studies focusing on the response of burnt catchments to real flood events, represented by hydrometeorologic-hydraulic models [31,32]. We aim to fill this gap by simulating a real storm that caused a flash flood in a Greek burnt catchment (Kineta in Central Greece), using meteorological modelling, combining it with remote sensing techniques for the assessment and validation of the fire and flood events, and mapping the flood with hydraulic-hydrodynamic modelling.

1.2. Simulating post-fire conditions, storms and flood events

A challenge in flood simulation studies is the accurate knowledge of the flooded areas, and additionally in our case, considering a post-fire flood, the accurate knowledge of the burnt area. New technologies such as Remote Sensing (RS) have been successfully used to provide detailed information on burn extent and severity [33–37], as well as flooded areas [38–41].

RS techniques are very common in studies relevant both to fires and floods, and in general, are particularly useful for obtaining ready-to-use information that is not available through on-site observations [32,41,42]. RS has been used to assess fire impacts such as burn severity [43], burn extent and site recovery [44], along various other applications [45]. Additionally, RS applications have been widely used for identifying flooded areas [46] with satisfactory performance and spatial detail [47,48].

In this work we leverage the use of RS to assess both the burn extent and severity, and the flooded parts of the study area. Burn severity and extent are critical factors that directly influence post-fire land use changes in the catchment, while the knowledge of the flooded area is essential for developing an accurate hydraulic model and validating it.

As mentioned, most studies considering post-fire floods use typical design storms, rather than the actual storm caused a real event. The simulation of the exact meteorological conditions of the event can be achieved though, by using meteorological modelling. In this work, the Advanced Weather and Research Forecasting (WRF-ARW) model enabled the precise representation of the flood event under real storm conditions [49,50]. The atmospheric model WRF-ARW has been used to simulate various meteorological conditions in Greece, demonstrating a satisfactory level of performance under different tests [51], including heavy precipitation events and storms, and their forecast [52–54]. Rainfall inputs from WRF-ARW have been coupled with land-hydrological models [55]. However, this report presents a novel approach, where the WRF-ARW weather model inputs are used directly for hydraulic modelling, exploiting the rain-on-grid technique of HEC-RAS [56], as it allows a higher level of spatial resolution reflecting the actual rainfall patterns and variability across the study area. Remote Sensing (RS) techniques were used for the identification of the flooded area (flood extent), and also for the impacts of the fire to the flood, through the determination of the burn extent and severity.

Text Box 2:

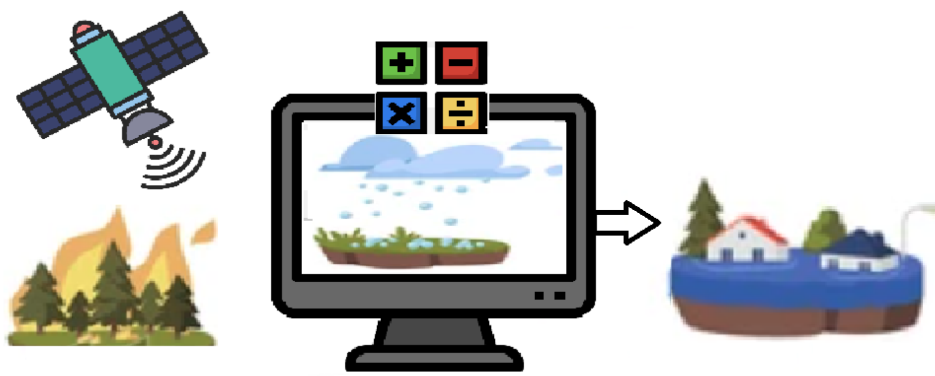

A schematic animation of the different components of our framework: Remote Sensing assessment (burnt conditions), atmospheric modelling (storm), and hydraulic simulations (flood).

For the simulation of the flood event, the hydraulic-hydrodynamic modelling has been conducted using the 2D Hydrologic Engineering Center's River Analysis System (HEC-RAS), one of the most commonly used software for that purpose [21,57–59]. HEC-RAS is a common software for flood inundation mapping [60] which has been successfully performed under various scales [54,61] and data availability conditions [21,32,62,63].

1.3. Post-fire Erosion and Flood-protection Treatments (PEFTs)

Watersheds receiving precipitation close to their usual-average levels, and have generally good hydrologic conditions, yield relatively small amounts of sediment, while their stream baseflow remains sustained for extended periods, or even the entire year. For example, in watersheds where hydrologic conditions are satisfactory (e.g., dominated by litter and vegetation, exceeding the 75% of their ground cover), only about 2% of rainfall becomes surface runoff, and erosion rates are low [64]. Even if such watersheds receive enough rainfall, sustainable annual streamflow conditions and little sediment production can be achieved when there are good hydrologic conditions [65].

However, this behaviour can significantly change after fires. Fires affect all watershed characteristics, including soils, vegetation, and land cover, which are critical to fundamental hydrologic processes such as runoff, streamflows, and sediment transport [65,66].

In particular, depending on the burn severity and the fire's duration, post-fire areas have reduced organic litter and vegetation covering the ground surface (even less than 10% of the ground), so there is very limited water retention. Subsequently, increased runoff leads to sediment transport, soil erosion, and water quality deterioration, even after mild precipitation events [67–69].

Robichaud et al. [70] find that the surface runoff can increase over 70% in such cases, while erosion can increase by three orders of magnitude. In general, after a fire, precipitation events have noticeable effects, such as the formation of water-repellent soils that cause immediate runoff, floods, roughness reduction, high peak flows, hydrological connectivity alteration, disruption of the infiltration processes, topographical alterations, delivery of sediment, post-fire debris flows and ash to streams [71–73]. The above negatively affect habitats, bridges, roads, buildings, and other infrastructures [74,75]. Water quality and channel stability are also severely affected, along with soil erosion, due to the movement of soil particles. Studies also show the effects of such post-fire cascade effects and the impacts on erosion, flood risks, sediment transport, and water quality [76,77]. The hillside slopes can also be affected, leading to the immediate occurrence of dry ravels after a fire event [78]. This further enhances the transport of surface materials through channels [79,80]. Many studies provided evidence that the most severe sediment losses occurred within the first year after the fire [81,82]. However, the magnitude of the damages can vary depending on multiple factors, such as climate, fire frequency, soil type, geology, topography (especially slopes), and vegetation [22,83]. Regarding water quality, Rust et al. [84] studied several sites in the western USA, and found that nutrient flux (different forms of nitrogen and phosphorus), major-ion flux, and metal concentrations are the most common pollutants in streams within the first five years after a fire. The importance of having good hydrologic and land cover conditions in watersheds will be more valuable in the future, as the changing climate increases the length of the fire weather seasons [85]. Considering all the consequences mentioned in the previous para-graph, one can understand how many co-benefits lie in the timely restoration of post-fire sites. As Girona-García et al. [72] noted, mitigating the prone areas to erosion and floods after fires is crucial to decreasing potential downstream risks and preserving the eco-systems' sustainability. In order to speed up a burned watershed's land cover restoration and thus boost its hydrological and erosion response [86], several practices have been developed, known as PEFTs. These can be cover-based and include barriers, mulch or hydromulch, erosion control mats, slit fences, seeding, or even in-channel treatments, such as check dams, grade stabilizers, in-channel tree felling, debris basins, channel deflectors, and stream channel armoring, while road and trail or even chemical treatments can be used. While the literature review highlights the importance of immediate action by applying various PEFTs, considerably less information is available about the operation and effectiveness of those PEFTs. The lack of consistency in evaluating and assessing the PEFTs' effectiveness is due to the highly variable influence of site-specific factors (climate, terrain slopes, land uses, burn severity, costs, etc.). The large dependence of a watershed's response to PEFTs on multiple factors that interact makes any evaluation of PEFTs challenging and the generalization of most findings almost impossible.

Text Box 3:

Examples of different post-fire recovery treatments, from the Watershed Center, US (2024)[2].

Thus, the literature is restricted to specific case studies on a regional or local scale, evaluating PEFTs under certain conditions. In this report, we provide a categorization and analysis of the effectiveness of PEFTs in relation to most factors reported by the existing literature, along with insights on their costs, from the available literature.

1.4. Design, Effectiveness, and Costs of PEFTs

PEFTs include several interventions that are quite case-specific, depending on the sites' physical characteristics, hence the literature around them is not rich or concise. The literature on PEFTs' performance is poor, with the majority of the studied cases are in the US, Spain and Portugal [72]. While there are some papers on the application of PEFTs, these refer to certain types of measures, mostly focusing on soil-erosion rather than flood hazards, and they are highly case-specific [72,87].

In one of the few examples evaluating the effectiveness of the PEFTs, Kastridis and Kamperidou [88] focus on two northern Greek basins where the applied measures referred to the cutting of burned trees, a total ban on grazing, and construction of log erosion barriers, log check-dams and contour branch barriers. They observed failures of these PEFTs, mainly due to the rush of construction and their poor implementation, which resulted in subsequent floods. The importance of the timely and proper

[2] Source: https://watershed.center/project/post-fire-ecological-recovery/

installation of PEFTs to enhance their efficiency in mitigating flood risks is also highlighted by Mitsopoulos et al. [30], studying another Greek burnt site. A similar study by Posner and Georgakakos [89] evaluated the feasibility and impact of check-dams (gabion-dams) and vegetation coverage PEFTs in the mountainous areas of Haiti, indicating that hillslope revegetation primarily impacts lower return period storms, while channel vegetation reduces peak discharge and delays flood peaks, and combined gabion dams and channel vegetation effects are non-linear and dependent on storm characteristics.

But, to our knowledge, there is no study simulating a real post-fire flood event along with the suitable PEFTs to test the effects of the fire and the role of PEFTs in the actual flooding. Even more scarce in academic literature are studies evaluating the PEFT costs, considering various components from installation to material and labour costs, probably due to the case- and context-specific nature of this problem. These costs are often argued to be the greatest obstacle for their implementation. For our case study, we provide detailed cost breakdowns in this report.

1.5. Economic Implications

From an engineering point of view, the post-fire flood resilience highly relies on the application of the necessary protection measures. From an economic or policy point of view however, the decision to apply the PEFTs is connected with the associated costs [90].

The costs for applying the necessary PEFTs and especially their comparison with the damage costs of a flood that can occur is a crucial analysis to reveal how beneficial the PEFTs can be in the long-run, and inform decision-making on flood protection. The estimation and comparison of a real- flood damage costs to the costs of the recommended protection measures is a challenging task that requires extensive data, specific for the studied case, and needs to be based on comprehensive modelling.

To our knowledge, it has not been performed in the literature so far. However, performing such an analysis can be highly valuable and informative, as the findings might be similar for several cases (e.g. comparable numbers/magnitudes of costs and damages). In this report, we present such an analysis, showing a detailed breakdown of both protection costs and flood damages.

1.6. Policy Debate and need for Capacity Building

The described situation is actually a complex problem, lying in the intersection of modelling and governance spaces, consisting of:

i) combined hazards (climate change, wildfires, floods) – where we do not always know the impacts and severity, or the ways they are linked and increase risks;

ii) post-fire erosion and flood protection works (PEFTs) – which are currently poorly studied, categorized, and there is limited information on their cost-effectiveness;

iii) a decision that has to be made on the level (investment and work) of post-fire protection treatments (mitigation).

In practice, this is a difficult problem, as often information is lacking on both three points. For example, we do not have a clear picture at the local scale, of the effect of a wildfire to a subsequent flood, the risks it can bring, what PEFTs exactly to consider, how effective they will be, how much they will cost, and if this investment is 'profitable'.

In reality, we often see cases being burnt and then flooded, even repeatedly, highlighting systematic failures [91]. In this report, we aim to bridge this governance gap with two ways:

- Interdisciplinary simulation modelling, aiming to shed light on the effect of a wildfire to a catchment, the simulation of extreme storms and floods that can occur, the design of specific and tailored PEFTs, and a thorough assessment of their costs and effectiveness, comparing it to the flood damages.
- Stakeholder capacity building support, and a detailed roadmap, drawing upon real cases. This is applicable to any country, based on state-of-the-art theories for stakeholder engagement to cover any governance gaps in science-to-policy uptake and flood protection.

1.7. Research approach summary

In this report, we aim to cover the research and policy gaps mentioned above by:

i) A detailed representation of a post-fire flood event in a typical Mediterranean site, combining atmospheric model with remote sensing and hydraulic modelling.

ii) Assessing the most appropriate PEFTs and modelling them spatially, as a recommended protection plan for the study area.

iii) Assessing their effectiveness for flood mitigation, by directly incorporating them in the hydraulic model.

iv) Estimating their costs, as well as comparing them with the estimated direct flood damage costs.

v) Analyze the drivers behind the current inaction in terms of flood protection, and reflect on them based on a transformation framework used for similar cases in Australia.

vi) Propose a capacity building roadmap, targeting existing flood governance gaps, applicable to similar cases.

Text Box 4:

Post-wildfire flood assessment and mitigation framework

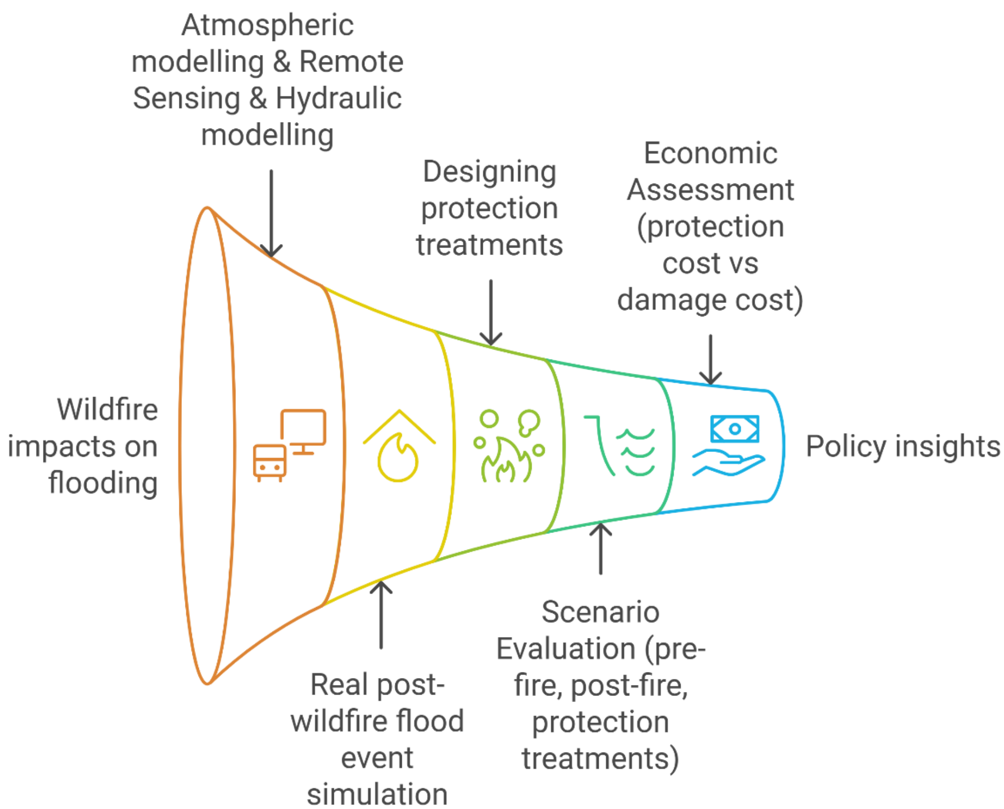

Schematic summary of our research approach, as described in the points above.

Each one of these analyses, and especially their combination, is a novel contribution with direct practical and policy insights to address the increasing threat of post-fire flood effects, both in terms of understanding and mitigation.

For each analysis, novel tools have been developed aiming to couple/link models.

The findings are easily transferable and the approach has an operational character, both in terms of modelling and stakeholder analysis.

1.8. Sustainability Implications

The presented approach consists of: i) methodological advances and combined models for the simulation of post-fire floods; ii) the assessment of protection works; iii) their economic implications in terms of costs of protection versus the flood damage costs; iv) a capacity building roadmap to bridge similar science-to-policy flood protection gaps.

All these four aspects are interdisciplinary and have multiple layers with implications for sustainability, resilience, climate change adaptation and mitigation, and science-supported policies. These principles are core elements for the Global Climate Hub's research [92,93]. These are essential insights not only for the study area, but for any area where such a thorough analysis can be carried out. These sustainability implications are briefly outlined below, in relation to the relevant Sustainable Development Goals (SDGs), which are the blueprint of the Hub [94,95].

- SDG1 – Poverty: Avoidance of consequences from combinations of disasters thanks to the implementation of the proposed mitigation measures. Resilience against flood risks is crucial to avoid the economic decline of the critical agricultural sector of the Mediterranean region [96].
- SDG2 – Hunger: Protection of agricultural crops from the loss of arable land as well as a large number of people who depend on agriculture [97,98].
- SDG3 – Health: The results of the implementation of the proposed system are directly related to the protection of human lives, as well as the avoidance of numerous diseases related to floods and extreme soil erosion events [99].
- SDG6 – Water and Sanitation: Through the identification of the risks in the study, municipal water supply and irrigation networks and sanitation facilities can also be protected, ensuring the availability and quality of water [100].
- SDG8 – Economy and Development: Economic development of areas that can avoid soil erosion and flood risks. Strengthening research and innovation, creating jobs, which can be achieved achieved through the creation of the proposed system [101,102].
- SDG9 – Infrastructure: Measures to strengthen areas facing increased risks from the natural disasters under investigation [103].
- SDG11 – Cities: Resilience to extreme events, protection of cities and settlements, allowing their continued development [104].
- SDG13 – Climate: Management of the impacts of climate change by reducing the number of affected people and preserving the sustainability of the area [105].
- SDG14 – Life Below Water & SDG15 – Life on Land: Avoidance of degradation and desertification of vulnerable areas, preservation of biodiversity, and avoidance of pollution of coastal areas due to protection from erosion and floods [8,37,106].
- SDG17 – Partnerships: Interdisciplinary nature of the proposal (methodologically and at the level of implementation and policy) with multiple benefits (see above), thus it can build bridges of cooperation for their implementation [107].

Structure of the report

Text Box 5:

The rest of this report is organized by presenting each step the approach, describing its methods and results in the same section, in order of application.

In particular:

- Study area, and research problem;

- Quantifying the wildfire’s impacts to the catchment’s flooding response;

- ‘Recreating’ a real storm;

- Representing the flood, and validating the result;

- Reviewing available PEFTs;

- Selecting and designing the most appropriate ones for the case study;

- Running scenarios to reveal the effectiveness of the PEFTs, and compare their flooding and economic performance;

- Specifically, for the economic performance, we compare the costs of PEFTs vs the flood damage costs, for each scenario;

The following schematic summarizes the modelling framework:

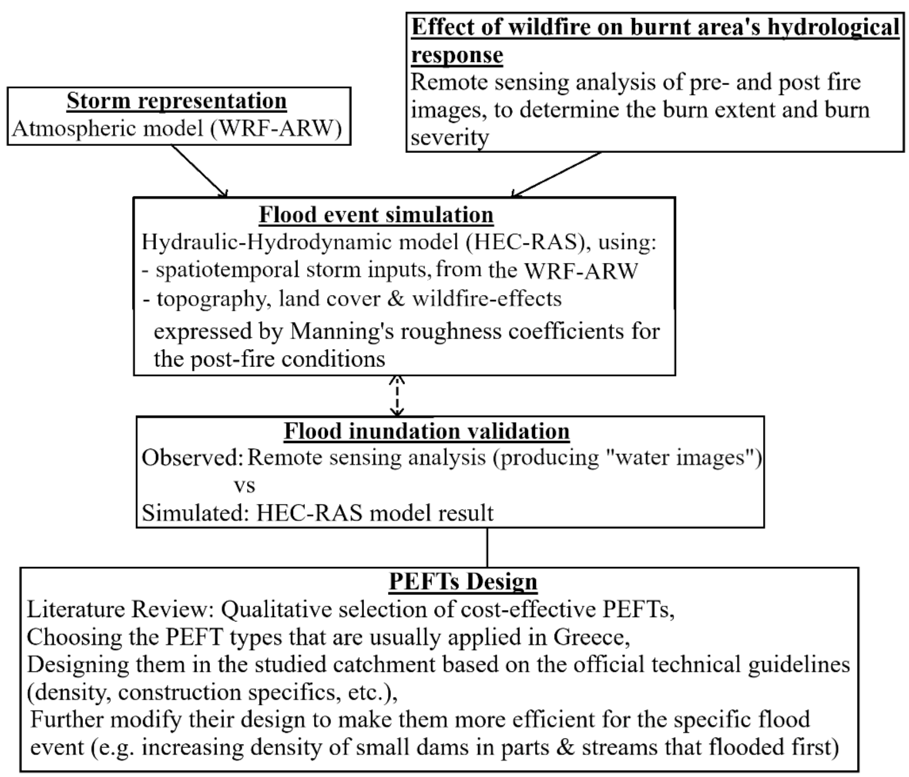

While more details on the technical parts will be provided in the next sections.

Drawing on the results of this framework, in the second part of the report, we:

- Present a governance assessment framework and analyze the existing gaps;

- Propose a stakeholder capacity building framework, targeted to fill those gaps.

The final part of this report presents the first step towards a national-scale resilience-building effort, by:

- Using design storms for future flood protection assessments.
- Applying a novel tool in all officially delineated Greek catchments (~11,000).

2 Post-fire flood in Kineta, Central Greece

A Mediterranean catchment was selected as an application area: Kineta catchment in western Attica, central Greece (Fig.1). Kineta catchment, covering approximately 40 km^2 is located in western Attica. Its northern part drains the Geraneia mountains towards its southern part, through the Pikas and two other, smaller, intermittent streams, where there is the coastal town of Kineta. A part of the Geraneia mountains is a Natura 2000 Protected Area.

The climate of the Kineta catchment has, like most Mediterranean areas, hot, dry summers and mild, wet winters [108,109]. The main land uses are forests (pine forest in the north, which was the main burned area), complex cultivation patterns with the various fields in the southern part, and the urban settlements (the coastal Kineta town).

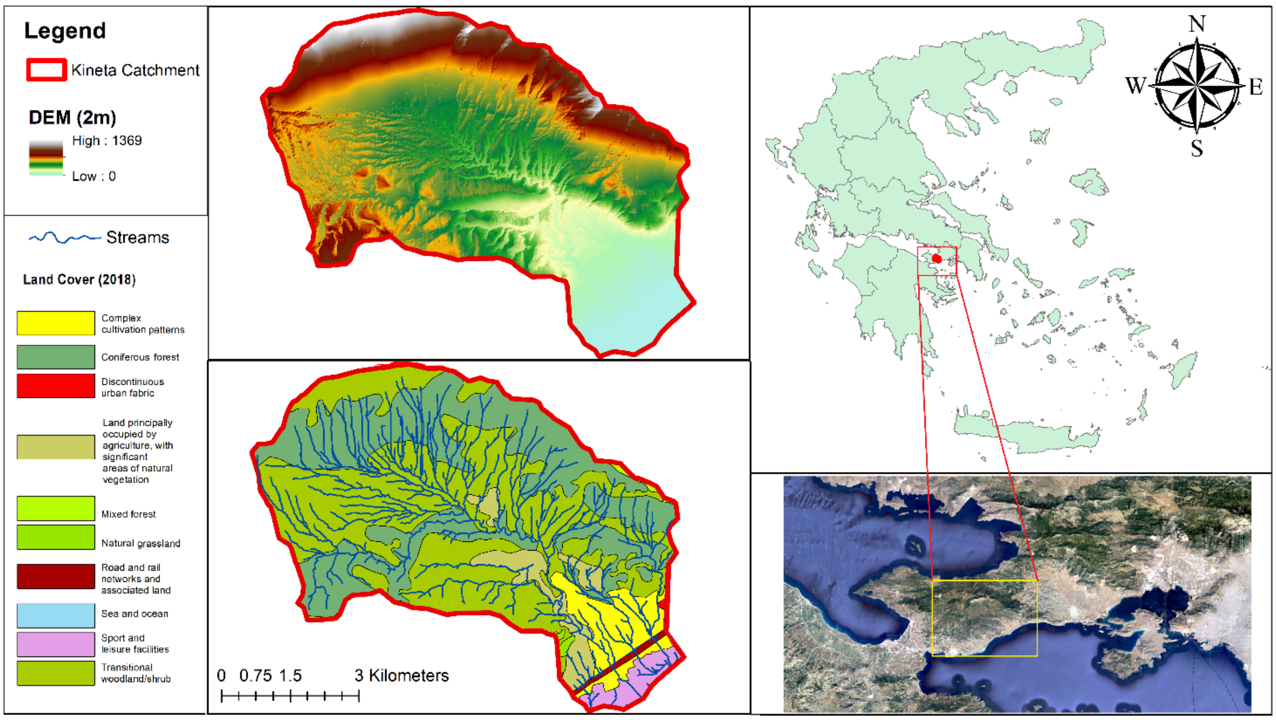

Figure 1: The map of the study area, showing the location of Kineta in Greece, and the catchment with the Digital Elevation Model (DEM), the river network, and the pre-fire land cover in 2018 (according to the CORINE classification) [58,110].

The Kineta area faces risks from fires, with notable incidents in 2017 and 2018 (Fig.2). On May 14, 2017, a fire broke out in the Panorama settlement in Agioi Theodoroi, Corinthia (northwest of Kineta), claiming two lives and causing two injuries. The fire reached close to the area's settlements and consumed one of them [111] On July 23, 2018, a large fire ravaged the pine forest of Geraneia Mountains above Kineta.

The fire was attributed to strong winds bringing power lines into contact, causing sparks that resulted in the ignition of dry grass [112], while there were also debates regarding the possibility of an organized arson [113]. The fire advanced and burned down the Panorama and Galini settlements, as well as houses in Kineta, causing 14 injuries.

Figure 2: A) Damages by the fire of 2017. Source: [111]. B) The burnt pine forest after the fire of 2018. Source: [114]. C, D) Damages by the fire of 2018. Source: [115].

Next year (2019), an extreme storm event, named 'Girionis' by the meteorologists, took place during November 24-26 and caused a destructive flash flood [116]. Among the findings of the subsequent visual inspection, was that the fire of 2018 played a key role in the magnitude of the flood damages [114]. After the fires in 2018, an inspection revealed that there were already loose sediments in significant quantities within the riverbeds [114]. The flood brought downstream a considerable amount of sediment (mud, trees, rocks, etc.) which, combined with the large volume of water, caused severe damages (Fig.3).

However, there is no comprehensive, data-driven assessment so far, investigating the mechanisms involved and under which this flood occurred.

Figure 3: Damages by the flood of 2019 to infrastructure, road networks, and the coastline of the Kineta area [111,114,115].

PART A: The modelling framework / techno-economic assessment

3 Assessing the fire's impact and mapping the burn severity through Remote Sensing techniques

For the identification of the 2018 fire impacts, three Sentinel 2 satellite imageries of pre-fire (1 image) and post-fire (2 images) were used for the mapping of the burnt area of the Kineta area, after the fire of 23 July 2018. Sentinel 2A Level 1C tiles (Tile ID: T34SFH) were acquired on 20 July 2018 (before the fire event) and 02 August 2018 and 16 October 2019 (after the fire event and before the flood event under investigation), and downloaded from the Copernicus Open Access Hub [117]. The selection of the Sentinel 2 imagery was based on the tiling grid which is available by the ESA [117] as a KML file, providing unique IDs for each tile (100 km x 100 km ortho-images in UTM/WGS84 projection). Followingly, Sentinel 2 images were pre-processed by being imported in the semi-automatic classification plugin (SCP) of the free and open-source cross-platform desktop Quantum Geographic Information System (Q-GIS), v. 3.6.3-Noosa to perform: (a) conversion of images from digital numbers (DN) to top-of-atmosphere reflectance (TOA) and (b) atmospheric correction (AC) by using the DOS1 method (an AC method widely used by the Earth Observation community) [118,119].

The study area was delineated by using the shapefile of the Kineta catchment including adjacent watersheds while the mapping of burnt areas has been conducted for two periods; the first one concerns the period between July and August 2018 and the second one the period between July 2018 and October 2019 with basic aim the detection of regrown vegetation.

Burnt areas were mapped based on the double calculation of Normalized Burn Ratio (NBR) (Equation 1) [120] for both of periods, by using bands B08 (NIR) and B12 (SWIR). This index uses the differences of reflected light between healthy and burnt vegetation based on the fact that green vegetation presents a very high reflectance in the NIR and low in the SWIR portion of the spectrum whilst recently burnt areas present low reflectance in the NIR and high in the SWIR [121]. NBR index takes values ranging from -1 to +1 with the healthy green and burnt vegetation presenting high and low values, respectively.

$$NBR = \frac{(\mathrm{NIR} - \mathrm{SWIR})}{(\mathrm{NIR} + \mathrm{SWIR})} \qquad (1)$$

Subsequently, the Change in Normalized Burn Ratio (Delta NBR-dNBR) [120] was twofold calculated to highlight the changes from the reference state, by subtracting the post-fire NBR values (02 August 2018 and 16 October 2019) from the reference NBR value of 20 July 2018 (Equation 2). In this way, burn severity is more accurately assessed than through the NBR index, as it is based on the measurement of per pixel changes in reflectance values.

$$dNBR = NBR\,prefire\ - NBRpostfire \qquad (2)$$

Followingly, according to Rahman et al. [122] a threshold value of +0.1 (proposed for Sentinel 2 images) was set to both dNBR files for each period to appropriately differentiate the burnt from unburnt areas along the study area. Conclusively, the resulted dNBR values were multiplied by 1000 and afterwards classified according to burn severity ranges proposed by the United States Geological Survey (USGS),

(Fig.4). Two-fold calculation of dNBR, highlighted initially the most affected-from-fire areas for each period and then the observed changes in burn severity levels from August 2018 to October 2019.

Severity Level	dNBR Range (scaled by 10^3)	dNBR Range (not scaled)
Enhanced Regrowth, high (post-fire)	-500 to -251	-0.500 to -0.251
Enhanced Regrowth, low (post-fire)	-250 to -101	-0.250 to -0.101
Unburned	-100 to +99	-0.100 to +0.99
Low Severity	+100 to +269	+0.100 to +0.269
Moderate-low Severity	+270 to +439	+0.270 to +0.439
Miderate-high Severity	+440 to +659	+0.440 to +0.659
High Severity	+660 to +1300	+0.660 to +1.300

Figure 4: Pictures of Kineta's Burn severity levels, following the categorization proposed by the relevant USGS Table.

Results:

The two-fold calculation of the dNBR indicated a vegetation regrowth between August 2018 and October 2019 with the percentages of unburnt areas and those characterized by low or low-moderate burn severity (2019) being increased compared to those of August 2018 (Fig.6). In addition, for both periods, burn severity classes covering the greatest areas are those subjected to moderate-high and moderate-low severity and the unburnt areas (2018) and moderate-low and low severity and unburnt area for October 2019, respectively. It should also be noted that areas affected by high burn severity in October 2019 are almost minimized compared to August of 2018 and are mainly replaced by areas impacted by moderate-low burn severity (Fig.5).

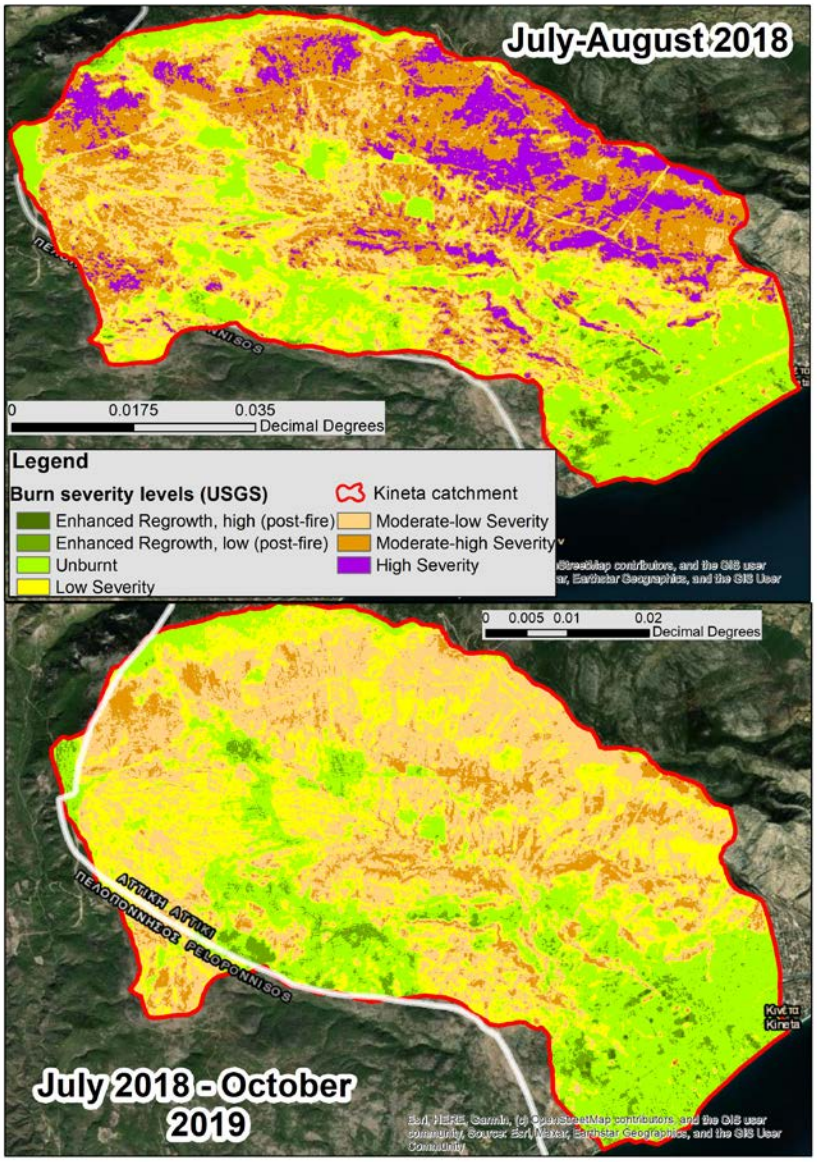

Figure 5: Results with the burn severity classes of the Kineta catchment during the fire (July-August 2018) and post-fire, before the flood event (Jul 2018 – October 2019) [58].

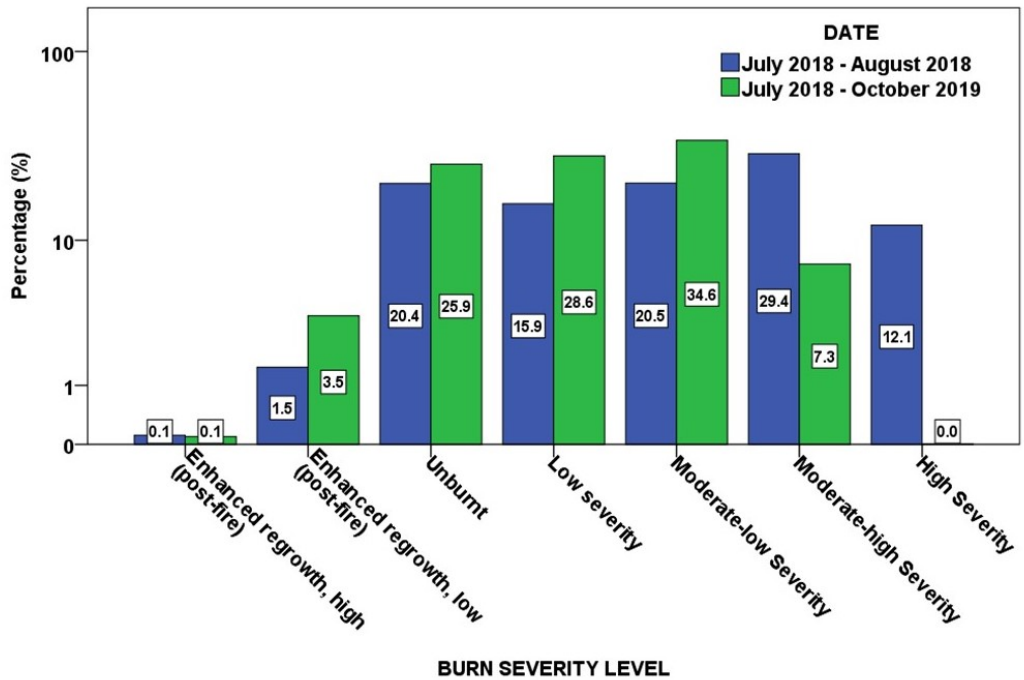

Figure 6: Percentage extent of burn severity classes (USGS) along the study area for both the studied time periods.

4 Representing the storm that caused the flood through the Atmospheric model WRF-ARW

The Advanced Weather and Research Forecasting (WRF-ARW) v4.2 model [49] was used to simulate the meteorological conditions resulting to the heavy precipitation event that caused the flash flood in Kineta. The model here was set up on three nested domains having horizontal grid spacings of 9 km × 9 km (644 × 360 grid points), 3 km × 3 km (292 × 286 grid points) and 1 km × 1 km (187 × 154 grid points), respectively. The third domain well covered the flooded area and some adjacent regions, the second domain covered Greece, and the first one covered a wide area including parts of Europe, Mediterranean, North Africa and West Asia, respectively.

The simulation was initialized on 24 November at 00:00 UTC (02:00 local time) to capture the atmospheric conditions prior to the flash flood and the simulation lasted 48 hours up to 26 November at 00:00 UTC (02:00 local time). The initial and boundary (every 6 hours) conditions of the simulation were constructed using operational analysis data of the Global Forecasting System (GFS) provided by the National Centers for Environmental Prediction (NCEP) on a horizontal grid spacing of 0.25° × 0.25°. The initial conditions involved atmospheric data at several atmospheric layers and near the surface as well as soil moisture and temperature. The sea surface temperature (SST) in the lower boundary conditions of the simulation were updated every 6 hours and they were constructed using real-time global (RTG) SST analysis data, also provided by the NCEP on a horizontal grid spacing of 0.083° × 0.083°. The ground processes were parameterized employing the unified Noah [123,124] land surface model. The long-wave and short-wave radiation processes were parameterized using the RRTMG scheme [125]. Also, the WSM 5-class scheme [126] was used to parameterize the cloud microphysics processes. Regarding the convective processes, the Grell-Freitas ensemble scheme [127] was employed in the calculations of the first domain (9 km × 9 km) while explicit resolve of convection was used in the second and third domains (3 km × 3 km and 1 km × 1 km). Moreover, the Yonsei University scheme (YSU) [128] and the revised Monin-Obukhov scheme were employed for the planetary boundary layer and the surface layer processes, respectively.

Results:

On 24-25 November, Greece was affected by severe weather conditions. A deep barometric low from the west brought heavy precipitation in many areas. More specifically, a cold front, accompanying the barometric low, passed through the night between 24 and 25 November causing torrential rainfall in Kineta and adjacent areas. A meteorological station of the National Observatory of Athens (NOA) network at Agioi Theodoroi located approximately 8 km west-southwest of Kineta recorded 206.8 mm of 2-day rainfall on 24-25 November (daily data available from 'meteo' – Greek weather portal [129]).

Text Box 6 **(animations – moving images)**:

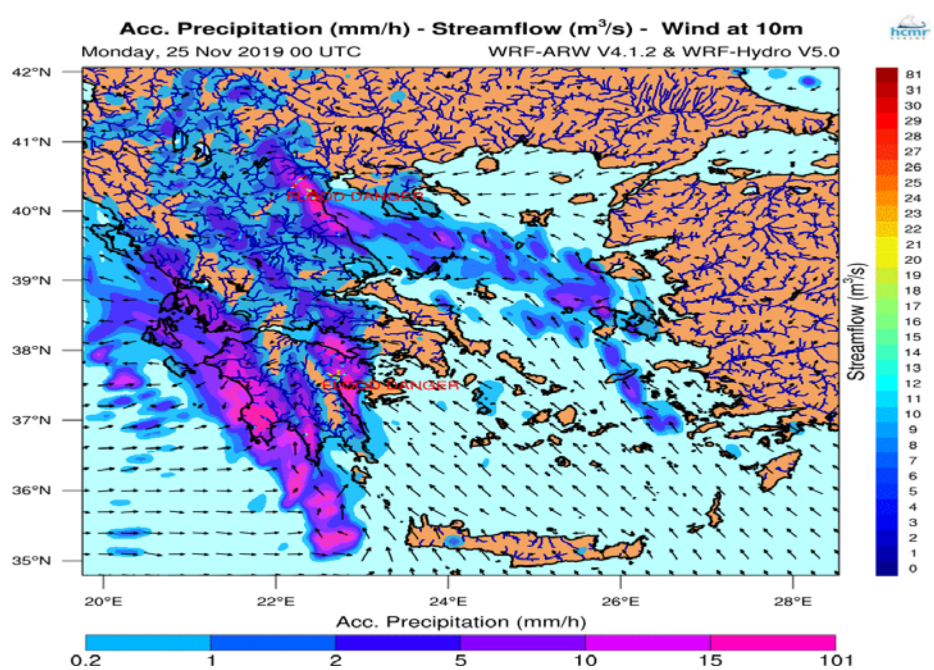

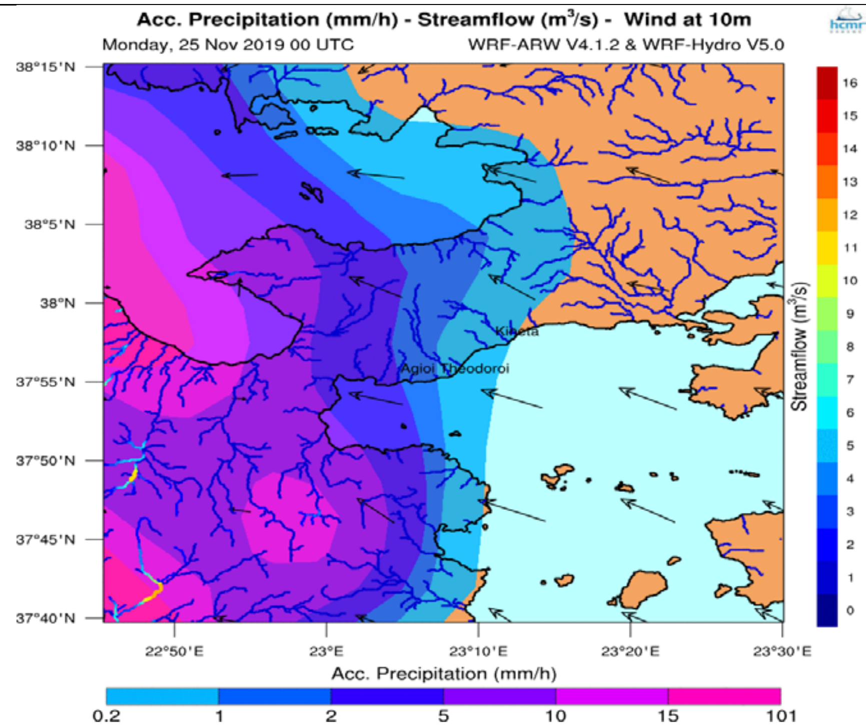

The modelling results of the accumulated precipitation and river streamflow for the Greek grid (upper), and the sub-section of the study area (lower), over time.

The WRF-ARW model simulation estimated 182.6 mm of 2-day rainfall at the same area, thus agreeing very well with the measurements. Most of the rain was simulated from 24 November at 20:00 UTC (22:00 local time) to 25 November at 06:00 UTC (08:00 local time) as shown in Fig.7a. Especially in the early morning of 25 November, a severe storm occurred around Kineta, as indicated by the pattern and intensity of the 1-h accumulated precipitation in Fig.7(b-d) for 03:00, 04:00, 05:00 and 06:00 local time respectively. The high rainfall rates caused significant increase of surface water runoff in the watershed upstream of Kineta, finally resulting to the devastating flash flood.

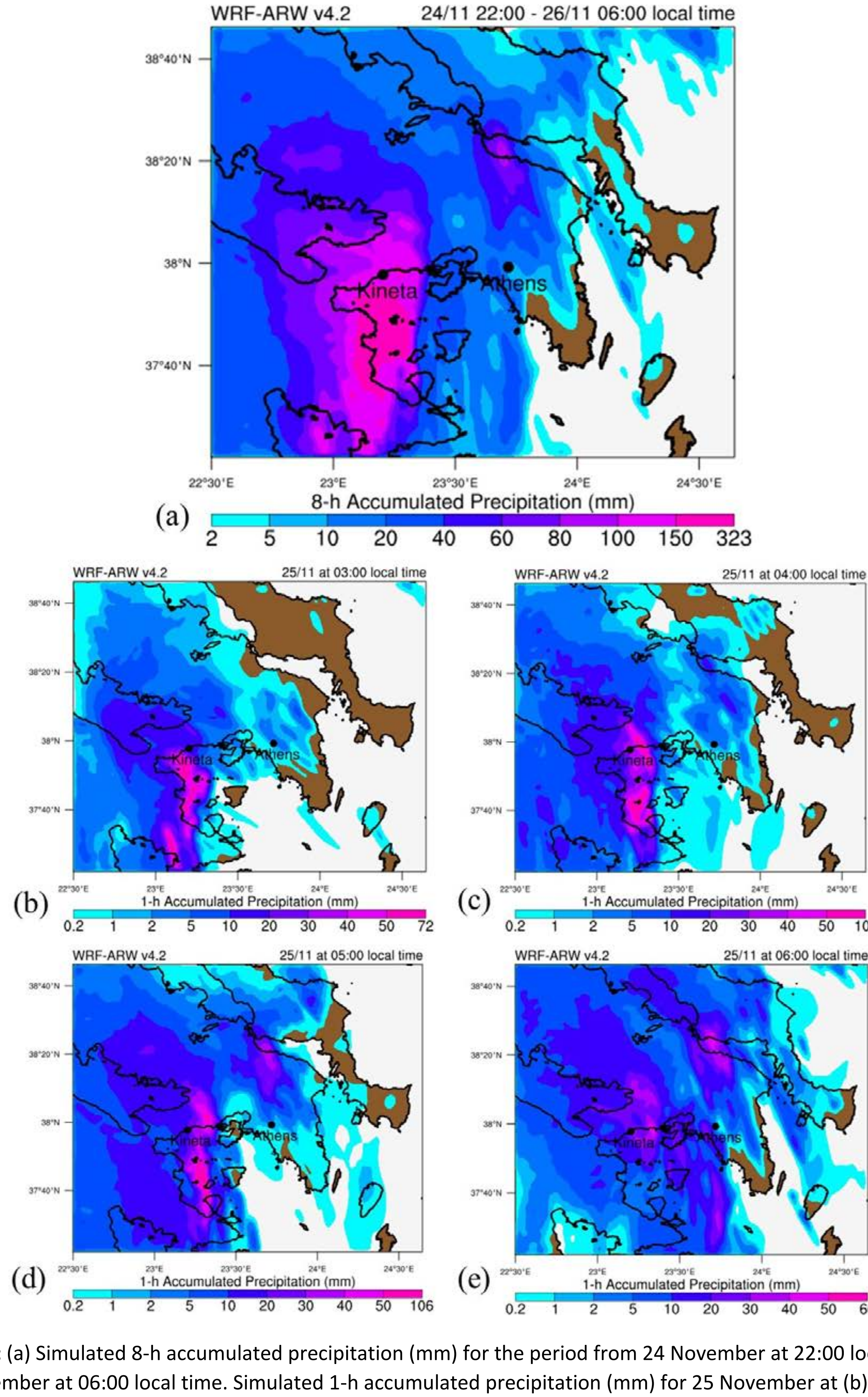

Figure 7: (a) Simulated 8-h accumulated precipitation (mm) for the period from 24 November at 22:00 local time to 25 November at 06:00 local time. Simulated 1-h accumulated precipitation (mm) for 25 November at (b) 03:00, (c) 04:00, (d) 05:00 and (e) 06:00 local time [58].

5 Delineation of flood inundated areas through Remote Sensing techniques

The RS analysis provided us with a map of the flood extent. One Sentinel 2 (S2) image of 25 November 2019 with processing level 1C and time 09:23:21:024Z was used to map flood inundated areas in Kineta while the flood event started on 24 November 2019. The S2 image was subjected to the same pre-processing procedure as those used for the mapping of burnt areas. Concerning the delineation of water on land, spectral indices containing visual bands with wavelength (μm) between 0.5 and 0.7 and near infrared spectra with a wave-length (μm) 0.7 to 1.1 have been proven the most successful [130,131]. Therefore, in this study several spectral indices (NDWI, MNDWI, AWEI, RSWIR1, and RSWIR2) have been evaluated by employing S2 bands. In addition to the spectral indices, the SWIR2, NIR and red bands were ascribed to Red, Green, and Blue values (RGB) respectively and converted to the HSV (Hue, Saturation, Value) colours using a standardized transformation [132]. According to Pekel et al. [133,134] water can be effectively delineated by defining a relation between H, S and V com-ponents while more information about the theoretical background and the equations used can be found in Konapala et al. [135].

Five water indices (WIs) were calculated on the S2 image of 25 November 2019, while the most significant task was to select the most representative threshold value for each WI. Analysis of their histograms indicates a different magnitude peak while positive indices' values normally correspond to water while negative or zero values correspond to soil or terrestrial vegetation. In addition, manual (subjective) adjustment of the thresholds is proven to achieve a more accurate result in the water delineation, which was performed based on the actual images (pictures) and drone videos from the visual inspection after the flood [114,136]. Then, after the application of the thresholds, each image file representing each distinct WI was binarized, putting as logical value (true) for values greater than the threshold and false for lower values.

Results:

For the mapping of the flood extent, all calculated WIs were compared, interpreted by using expert knowledge and visually checked, aligned to the 4 (Red)-3 (Green)-2 (Blue) natural composite of the respective S2 image. Intensified analysis highlighted the RSWIR2 (accompanied by the threshold value ≥ -0.1) as the best performing index for the detection of inundated areas (Fig.8), as it presented the most stable results.

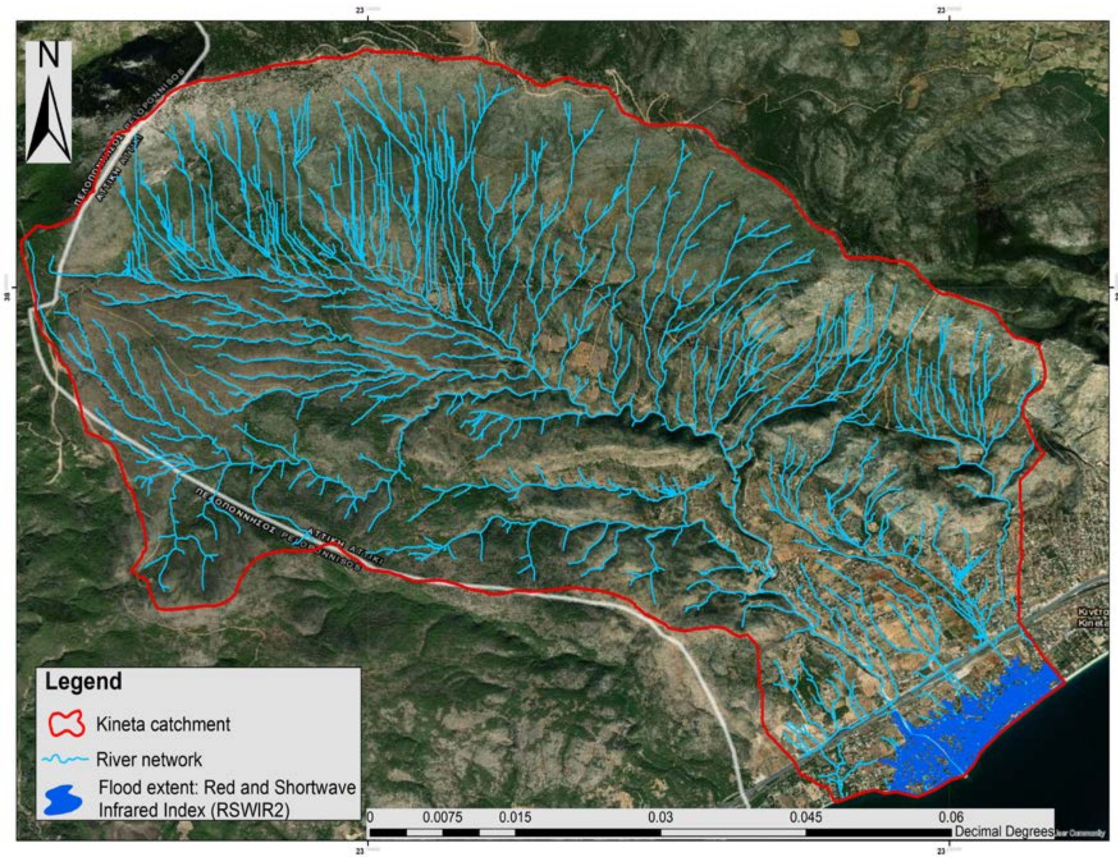

Figure 8: Flood extent mapped through RSWIR2 index calculation. The flood extent at the location of Kineta town was used as the validation polygon, to validate the flood model (next section) [58].

6 Simulation of the flood extent and water depth through hydraulic-hydrodynamic modelling

The hydraulic-hydrodynamic modelling has been conducted using the 2D Hydrologic Engineering Center's River Analysis System (HEC-RAS), to map the inundated areas of the studied catchment, and analyze the water depth and velocity during the studied event. The main components needed for precise flood inundation modelling and mapping, include the digital elevation model (DEM), stream channel characteristics (such as river flowpaths and banks), the hydraulic model setup (including initial and boundary conditions, roughness coefficients, and engineering structures), as well as the depiction of urban areas. A 2m resolution DEM was applied in this case, obtained by the National Cadastre and Mapping Agency S.A. (NCMA).

Roughness is a key input in flood inundation modelling, as it directly affects the flow conditions. The most common approach for the reasonable mapping of Manning's roughness coefficients (n) is the use of typical values for land cover data based on the literature, combined with personal judgment based on the area's characteristics. This approach was followed in this case, combining CORINE land cover data and typical values for pre- and post-fire land use categories, always considering the burn severity conditions. The spatially distributed roughness values used for the Kineta area were derived after testing considering the typical minimum, median, and maximum n values provided by the literature for similar areas and conditions (in particular: [25,137–145]), aiming to the optimum set of values. After the tests performed, two set of values of the n roughness coefficient have been defined (Table 1). These values were used in a spatially distributed format for the Kineta area and combined with the DEM, the 2D flow area computational grid, and the rain-on-grid input constituted the model setup for the initial (pre-fire) and the post-fire conditions, respectively. In Table 1, the Classification Category field corresponds to the CORINE 2018 land cover categories (CLC2018), combined with the different conditions derived from the RS observations (RS obs). So, the CLC2018 categories (e.g., Complex cultivation patterns, Coniferous forest, Mixed forest, etc.), were spatially combined with the RS observations (e.g., Enhanced regrowth high, Enhanced regrowth low, High severity, Low severity, Moderate-low severity, Moderate high severity, Unburnt), and produced the categories of the first column of Table 1. This actually shows us spatially all the different land cover categories (according to CORINE) with their different burn/recovered status (based on the RS observations).

Table 1: Manning's roughness n values for the pre-fire and post-fire scenario. The post-fire scenario corresponds to the actual simulated flood of November 2019.

Classification Category (CLC2018 & RS obs)	Manning's n (pre-fire scenario)	Manning's n (post-fire scenario)
Complex cultivation patterns enhanced regrowth, high (post fire)	0.650	0.4903
Complex cultivation patterns enhanced regrowth, low (post-fire)	0.650	0.1708
Complex cultivation patterns high severity	0.650	0.0110
Complex cultivation patterns low severity	0.650	0.4903
Complex cultivation patterns moderate-low severity	0.650	0.3305
Complex cultivation patterns moderate high severity	0.650	0.1708
Complex cultivation patterns unburnt	0.650	0.6500
Coniferous forest enhanced regrowth, high (post fire)	0.800	0.6028
Coniferous forest enhanced regrowth, low (post-fire)	0.800	0.2083
Coniferous forest high severity	0.800	0.0110
Coniferous forest low severity	0.800	0.6028
Coniferous forest moderate-low severity	0.800	0.4055
Coniferous forest moderate high severity	0.800	0.2083
Coniferous forest unburnt	0.800	0.8000
Discontinuous urban fabric enhanced regrowth, low (post-fire)	0.060	0.0233
Discontinuous urban fabric low severity	0.060	0.0478
Discontinuous urban fabric moderate-low severity	0.060	0.0355
Discontinuous urban fabric unburnt	0.060	0.0600
Land principally occupied by agriculture, with significant areas of natural vegetation enhanced regrowth, high (post fire)	0.050	0.0403
Land principally occupied by agriculture, with significant areas of natural vegetation enhanced regrowth, low (post-fire)	0.050	0.0208
Land principally occupied by agriculture, with significant areas of natural vegetation low severity	0.050	0.0403
Land principally occupied by agriculture, with significant areas of natural vegetation moderate-low severity	0.050	0.0305
Land principally occupied by agriculture, with significant areas of natural vegetation moderate high severity	0.050	0.0208

Classification Category (CLC2018 & RS obs)	Manning's n (pre-fire scenario)	Manning's n (post-fire scenario)
Land principally occupied by agriculture, with significant areas of natural vegetation unburnt	0.050	0.0500
Mixed forest enhanced regrowth, low (post-fire)	0.800	0.2083
Mixed forest high severity	0.800	0.0110
Mixed forest low severity	0.800	0.6028
Mixed forest moderate-low severity	0.800	0.4055
Mixed forest moderate high severity	0.800	0.2083
Mixed forest unburnt	0.800	0.8000
Natural grassland enhanced regrowth, high (post fire)	0.650	0.4903
Natural grassland enhanced regrowth, low (post-fire)	0.650	0.1708
Natural grassland low severity	0.650	0.4903
Natural grassland moderate-low severity	0.650	0.3305
Natural grassland unburnt	0.650	0.6500
Road and rail networks and associated land enhanced regrowth, high (post fire)	0.013	0.0130
Road and rail networks and associated land, enhanced regrowth, low (post-fire)	0.013	0.0130
Road and rail networks and associated land, low severity	0.013	0.0130
Road and rail networks and associated land, unburnt	0.013	0.0130
Sea and ocean, enhanced regrowth, high (post fire)	0.070	0.0700
Sea and ocean, enhanced regrowth, low (post-fire)	0.070	0.0700
Sea and ocean, low severity	0.070	0.0700
Sea and ocean, unburnt	0.070	0.0700
Sport and leisure facilities, enhanced regrowth, high (post fire)	0.025	0.0215
Sport and leisure facilities, enhanced regrowth, low (post-fire)	0.025	0.0145
Sport and leisure facilities, high severity	0.025	0.0110
Sport and leisure facilities, low severity	0.025	0.0215
Sport and leisure facilities, moderate-low severity	0.025	0.0180
Sport and leisure facilities, moderate high severity	0.025	0.0145
Sport and leisure facilities, unburnt	0.025	0.0250
Transitional woodland/shrub, enhanced regrowth, high (post fire)	0.800	0.6028
Transitional woodland/shrub, enhanced regrowth, low (post-fire)	0.800	0.2083
Transitional woodland/shrub, high severity	0.800	0.0110
Transitional woodland/shrub, low severity	0.800	0.6028
Transitional woodland/shrub, moderate-low severity	0.800	0.4055
Transitional woodland/shrub, moderate high severity	0.800	0.2083
Transitional woodland/shrub, unburnt	0.800	0.8000
Streams	0.060	0.0950

The 2D hydrodynamic calculations were based on a computational grid covering the study area, using a variable high-resolution mesh computation point. The small mesh spacing especially around streams, makes the computations more demanding, but ensures a high level of modelling detail.

Moreover, the hydraulic model considered the information retrieved from the visual inspection after the fire of 2018 and the flood of November 2019, as reported in the respective report, the news, and a drone video of the flooded area (as shown in Fig.9). This allowed us to:

- Create an accurate representation of the validation polygon of the areas that flooded within the town of Kineta, by refining the RS results of Fig.8 according to the relevant descriptions and photos. This improved, 'modified' validation polygon is shown in Fig.9, along with the relevant photos and references.

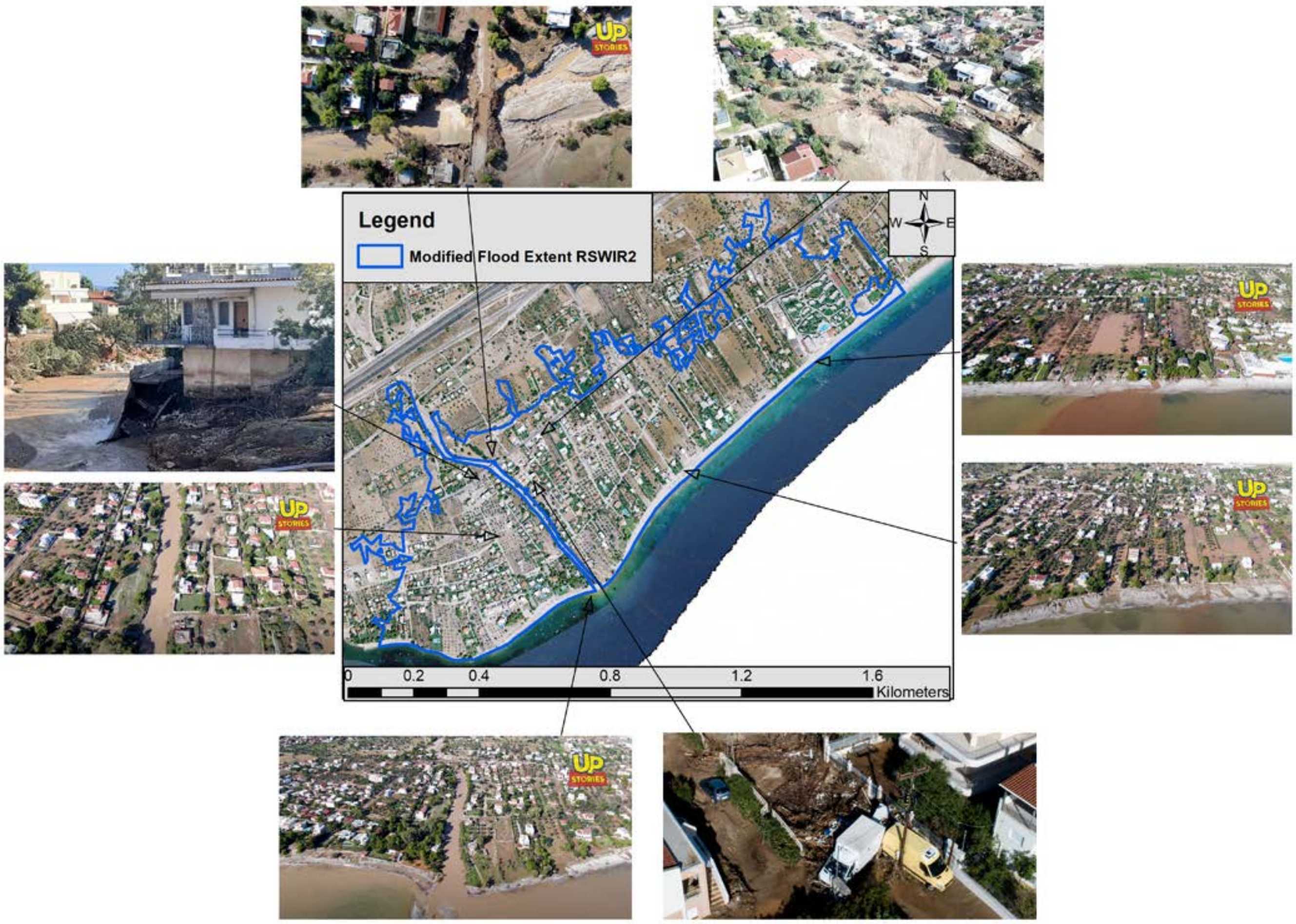

Figure 9: The actual flood extent, as extracted from the RS observations of Fig.8, and refined with the documented damages after the visual inspection of the flood event of November 2019 [114], sources from the Greek news [146] and a drone video by the UPstories team showing the aftermath of the flood [147].

- Consider the effect of the debris flow to the blocked drainage routes. In particular, after the fire, it was reported that considerable amount of rocks, mud and wood mass blocked the Pika stream's drainage passage before the Olympia highway, and an underground culvert at the two other smaller streams in the east (Fig. 10). Figures and further details justifying this can be found in the visual inspection's report [114]. These, under the initial (pre-fire) conditions were not blocked, so the hydraulic model took into account these changes:
    - In the pre-fire conditions, the Pika stream is considered to be a typical surface, open stream. While the other two streams have an orthogonal culvert 3 x 5 m for water drainage to the sea.

- In the post-fire conditions, these are blocked, so the Pika stream was blocked above the Olympia (Athens-Corinth) highway (using HEC-RAS's terrain modification toolbox), and the culvert is inactive.

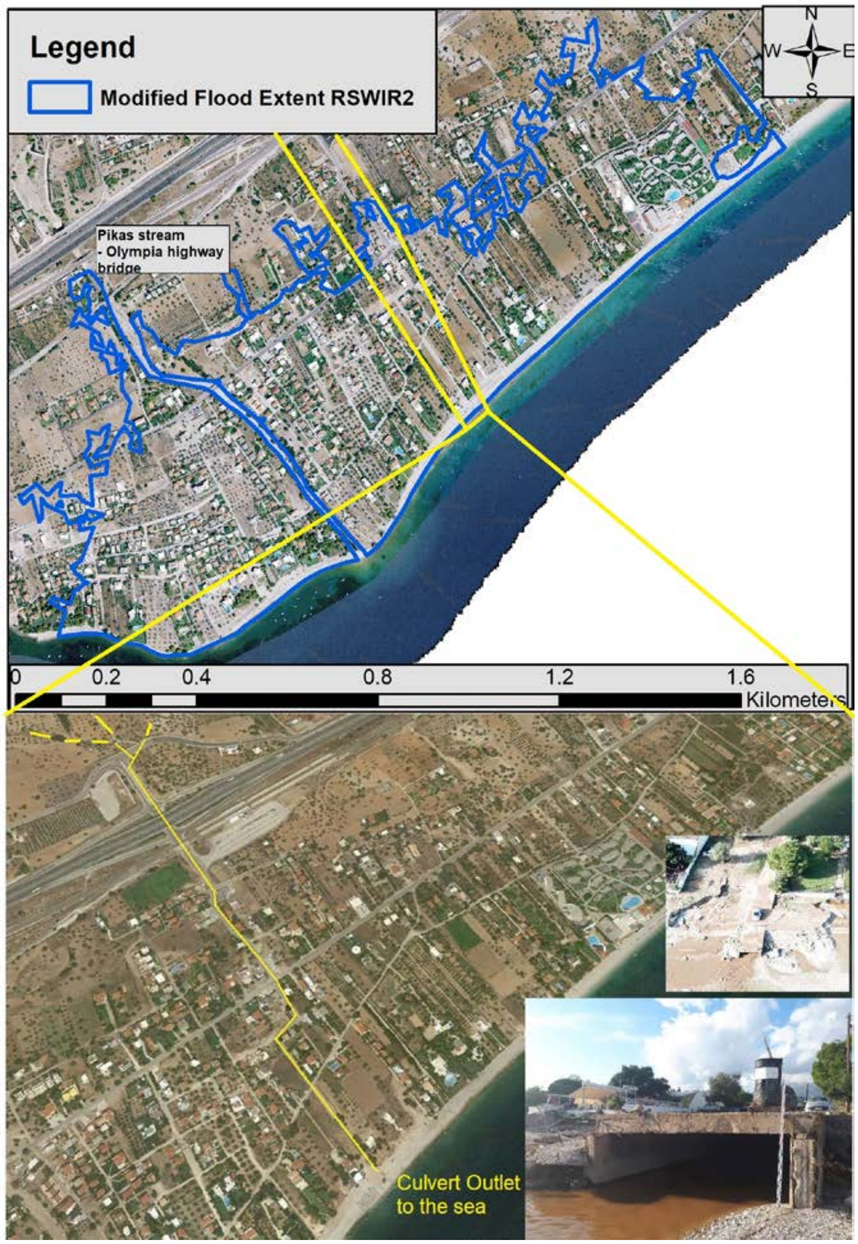

Figure 10: The location of the Pika stream – Olympia highway bridge (Athens-Corinth route), and in the second picture, there is the schematic of the underground culvert until its outlet to the sea. The post-fire flood of November 2019 blocked both drainage routes. Sources: [Google Earth; [114,146,147].

In these views from Fig.9 and 10, it is worth noting how many houses have been built close to the streams, maximizing thus their exposure risks from potential damage of a flood event.

The rain-on-grid technique was used, allowing us to apply spatially the detailed rainfall accompanying the storm that caused the flood event, as simulated by the WRF-ARW atmospheric model, on a grid over the Kineta catchment. The rain-on-grid is a relatively new technique that allows the user to apply spatial datasets of gridded precipitation to the study area, in contrast with the traditional point-observations [21,57]. The time-step of the rain-on-grid storm applied was 1 hour, so 20 spatial datasets (raster files – 20 grids from 24 November 2019 14:00:00 to 25 November 2019 09:00:00) representing the storm event were inserted in HEC-RAS. The simulation was configurated based on these inputs, as follows: the computation interval was set to 1 second, while the mapping, the hydrograph and the detailed output intervals were set to 5 minutes. The model provides the flood inundation (extent) and water depth for each time step of the simulated event, in both the pre-fire (hypothetically, if the same storm had happened before the fire), and the post-fire cases.

Text Box 7 (**animation – video**):

The link video1.mp4 leads to a video of the 2D simulation, see screenshot below:

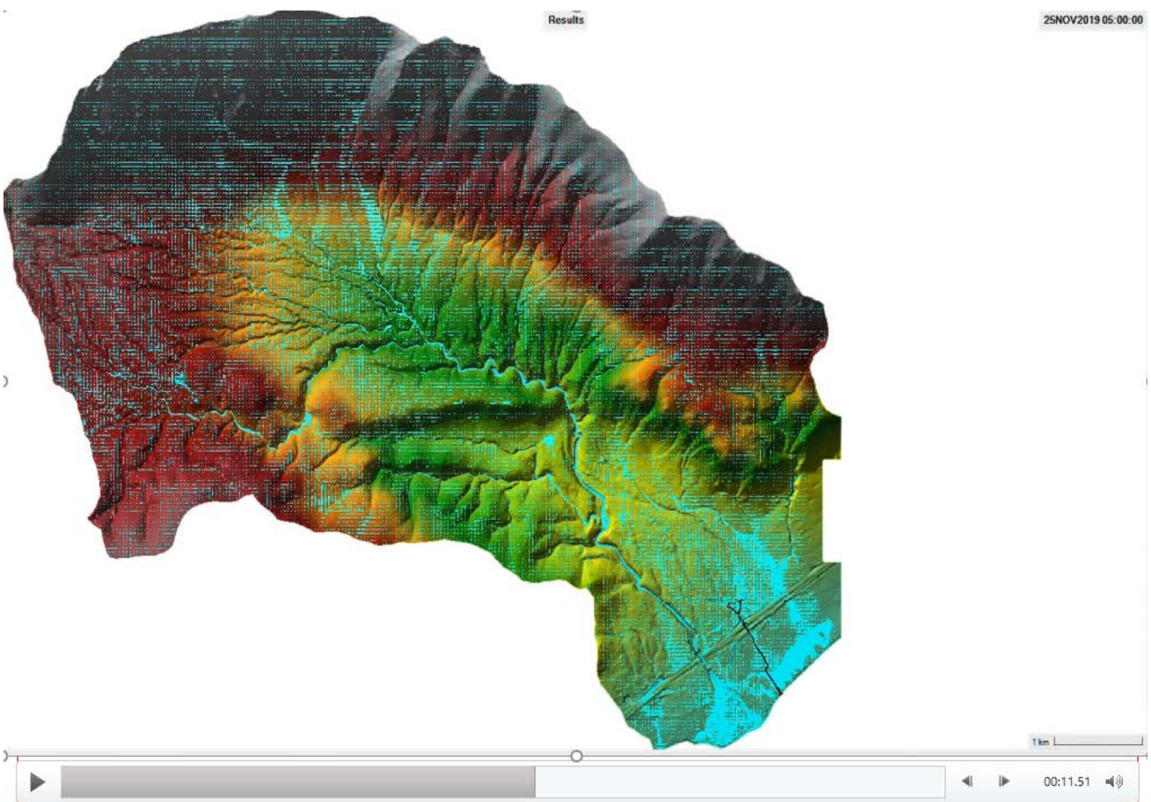

This is a useful output, as it shows the evolution of the flood, with several insights that cannot be seen from a static flood map (e.g. which parts of the catchment flooded first, from where they got the biggest amount of water, or how fast this happened).

The results of this simulation are shown in Fig.11, considering two initial[3] scenarios:

- Pre-fire – the same storm hits Kineta catchment, with the pre-fire Manning's coefficients and the streams not blocked with debris. This is a theoretical scenario in order to explore the fire's effect to the actual flood.
- Post-fire – the reality of what happened in Kineta: the simulated Girionis storm hits the area considering the post-fire Manning's coefficients and blocked streams from debris.

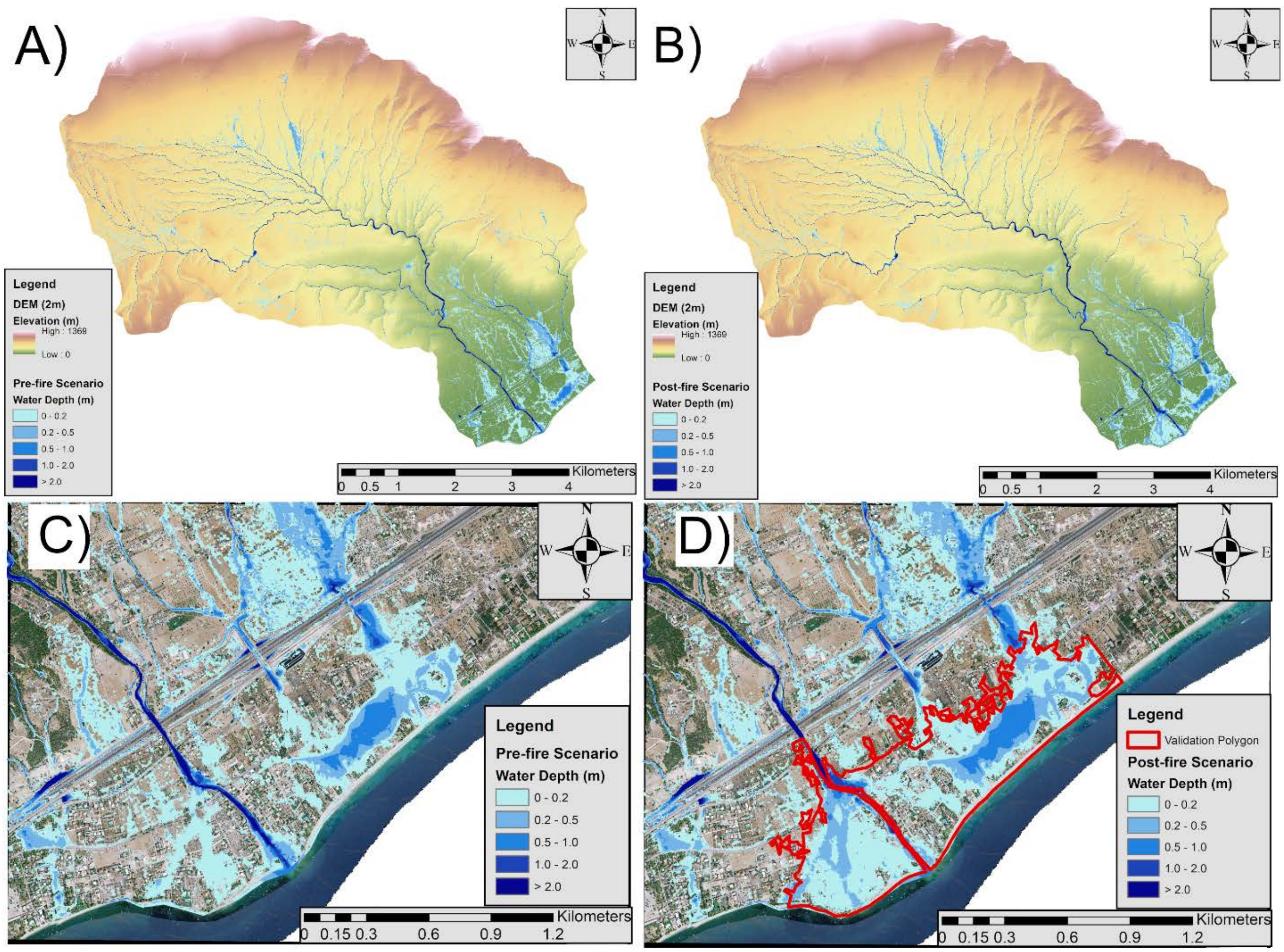

Figure 11: The results of the hydraulic-hydrodynamic model under the Girionis storm: Flood extent and depth for the pre-fire scenario (A, C) and the real post-fire conditions representing the flood event of November 2019 (B, D), over the validation polygon (D) [58].

[3] In the following sections, one more scenario is added, considering the application of PEFTs.

Model validation:

For the validation of the model, the results of Figure 11D were compared to the validation polygon of Figure 8 (also presented in Fig.11D with red colour).

In particular, the flooded area's polygon as obtained from the RS imagery was used (Figure 8) and assessed with typical indices that consider the flood ex-tent. In particular, the Critical Success Index (CSI), also known as threat score (TS) was used to assess the accuracy of the simulated inundated areas against the validation polygon [148–151]. The CSI can be estimated according to Equation (3):

$$\mathrm{CSI} = \frac{A}{A+B+C} \quad (3)$$

Where A is the correctly simulated flooded area (hits); B is the false-simulated flooded area (false alarms); C is the flooded area that is not predicted by the model (misses); and the term B at the numerator in Equation (3) is used to penalize the model's overprediction [152–154].

The CSI for the flood of November 2019 in Kineta was 0.65, which is a satisfactory value (CSIs above 0.5 are acceptable). The total simulated flood inundation area was found 451,848 m^2 (411,177 m^2 inside the validation polygon) for the pre-fire scenario, and 595,246 m^2 (549,308 m^2 inside the validation polygon) for the post-fire scenario. So, the actual effect of the fire on the flood extent is 143,398 m2 more flooding in total, with the 138,131 m^2 within the validation polygon.

This practically proves that if the Kineta pine forest has not been burned, and the streams were not then blocked, the flood extent would have been reduced by 25.1%. At the catchment scale, this might sound a small difference, however, for a small coastal town covering approximately 4.5 km^2, the 0.138 km^2 is not negligible. In any case, as mentioned in section's 3.1 results, the Girionis storm was indeed a severe phenomenon. This indicates a potential flood risk in the area, regardless of the fire, as the hydraulic model's results confirmed for the initial pre-fire conditions (Fig.11). This finding is in line with some historic flood events, as mentioned in the study area section. Moreover, the results of the RS analysis showed that the land cover and vegetation have recovered from August 2018 since October 2019, although not completely, but the high-burn severity areas were minimized.

An interesting finding is that the Pikas stream was not the main responsible for the flood. The water came in principle from the other two smaller streams in the eastern part of the catchment, and mainly the one in the east. These are intermittent streams, but it seems that the more abrupt slopes contributed to the increased streamflows. Another factor that contributed to the increased post-fire flood scenario was the streams being blocked by the debris flow.

The next step is to explore what kind of protection (PEFTs) could have been applied in Kineta.

7 Post-fire Erosion and Flood Protection Treatments (PEFTs): A literature-based assessment, and analysis of their suitability

There are many different kinds of PEFTs. All of them aim to speed up the recovery of burned watersheds, improving thus their response to hydrological processes and erosion. The way each PEFT tries to achieve this differs. The most common PTTs' categorization is based on which watershed element they are aiming to improve. According to Napper [155], PEFTs can be categorized per treatment type, such as land treatments, channel treatments, road and trail treatments. These are described as follows:

- Land treatments: Stabilizing burned areas can be accomplished using several land treatments by providing soil cover (reducing erosion), trapping sediment (reducing sedimentation), and/or reducing water-repellence (improving infiltration). These ways aim to speed up recovery while maintaining ecosystem functionality and integrity by limiting the expansion of unwanted species [156]. Land treatments can be cover-based (working on the land cover improvements, including seeding) or barrier-based (installed barriers to trap sediments, reduce excess flow, or slow runoff).
- Channel treatments: Channel treatments focus on mitigating the negative post-fire effects on water quality, loss of water control, lower water velocity, trapping sediment, and preserving channel characteristics. As a result, they are highly beneficial for downstream areas, minimizing the hazardous impact of potential high flows and flooding, erosion, deposition, and sediment transport.
- Road and Trail Treatments: Combined with the previous two types (land and channel treatments), road and trail treatments can reduce the post-fire effect on the transportation infrastructure. They also protect life, safety, and property, supporting thus critical natural or cultural resources.

Since the available information on PEFTs is so limited and not concisely presented, we conducted first a literature review: In the Annex of Papaioannou et al. [157] we provide a detailed overview of the most typical works under each type of treatment, along with a description, commenting on their suitability/ effectiveness. In this section, Table 2 highlights the main factors that one must consider when assessing the effectiveness and suitability per type of treatment.

Table 2. Different treatment types with the most common works, and comments on site suitability and effectiveness [157].

Type of Treatment	Typical works	Suitability and Effectiveness
Land – Cover-based	• Aerial Hydromulch • Ground Hydromulch • Straw Mulch • Slash Spreading • Erosion Control Mats, etc.	• Suitability: Areas with high-moderate burn severity; steep slopes; soils with high erodibility factor; low winds. • Effectiveness depends on: Proper installation, application rates, slope length and steepness, and wind conditions. Combinations of mulching and seeding is more effective in germination but not necessarily in surface cover. Wood-based mulches are equally or more effective than straw mulch in reducing post-fire erosion. Erosion Control Mats are costly solutions, with limited information about their effectiveness [155].
Land – Barriers	• Log Erosion Barriers • Fiber Rolls or Wattles • Silt Fences, etc.	• Suitability: Areas with high-moderate burn severity and highly erodible and water-repellent soils; slopes between 20% - 60%; accessible for maintenance and inspection. • Effectiveness depends on: Proper installation, slope, tree size and length. Barriers are more effective in low-intensity storms only [158]. Their maintenance requires significant effort and attention. Barrier construction remains a typical hillslope treatment with better effectiveness when combined with other treatments [157].
Land – Seeding	• Soil Scarification • Ploughing • Seeding, etc.	• Suitability: Areas with high-moderate burn severity and highly erodible slopes; vulnerable for invasive and noxious plants spreading. • Effectiveness: While there is limited available information, seeding is inefficient in reducing sediment yield compared to no treatment [158].

		Seeding (e.g. < 60% surface cover) is not very effective in the first year after a fire and is neutral in the following seasons. Combining seeding with mulch-treatments increases the germination potential.
Land - Chemical treatments	• Polyacrylamides (PAM) • other polymers	• Suitability: There is not adequate information to generalize their site suitability. Areas with very mild rainfall events are preferred, as they boost the vegetation development fast. • Effectiveness: Very few cases report their effectiveness, with no effects found on runoff and little erosion reduction achieved [159–161].
Channel - Barriers	• Check dams • In-Channel Tree Felling • Grade Stabilizers • Stream Channel Armoring • Channel Deflectors • Debris Basins, etc.	• Suitability: Areas with high burn severity; smooth slopes where sediment storage can be achieved; with <20 % ground cover; small catchments and drainage areas; where construction, maintenance, and inspection is accessible; high-risk value (road crossing, sensitive aquatic species) and need to protect the downstream areas. • Effectiveness: Channel barriers are more effective in smooth slopes, when used in series, and for mild storms and flows. They can reduce most of the runoff and also significant amounts of erosion, but they have short-term effectiveness and require maintenance following runoff events [162]. Debris basins are expensive treatments [155].
Road and Trail	• Outsloping • Rolling Dips • Overflow Structures • Culvert Modification • Trail Stabilization, etc.	• Suitability: Areas prone to flow concentration (e.g. mild slopes, bad drainage with undersized culverts) that need immediate protection from floods (important access, infrastructure, vulnerability, etc.). • Effectiveness: Limited data suggest that if properly designed and installed correctly, they provide significant benefits in terms of discharge, reduced sediment delivery to stream channels and less road maintenance [155,157].

It is worth noting that the costs of post-fire erosion and flood protection techniques can vary widely depending on factors such as the size and severity of the burn area, the steepness and slope of the terrain, the proximity to water bodies and infrastructure, the type of vegetation present, and the specific technique employed [158].

These factors affect only the costs, but also the effectiveness of most treatments. There is very limited information on the cost-effectiveness of PEFTs. A recent assessment based on 63 sites in Spain, Portugal, USA and Canada [163], finds that land treatments are the most cost-effective (e.g. straw mulch, wood-residue mulch, and hydromulch). The cost-effectiveness of barrier PEFTs was found to be low because their effectiveness is low related to the reduced erosion rates and they might have high implementation costs in some cases [163]. Concerning the barriers, it is noteworthy to mention that log erosion barriers had slightly better cost-effectiveness values than other barrier types [163]. Keeping in mind that the cost ranges can be highly variable, seeding PEFTs have in general low costs (but require considerable time and labour to implement), while chemical treatments erosion control mats are considered costly PEFTs. In certain cases, invasive plant management may also be necessary to prevent further damage to the ecosystem, but can be expensive. According to Girona-Garcia et al. [163], while all treatment types significantly reduce post-fire soil erosion, the cover and barrier treatments reduce significantly also the runoff. In particular, straw and wood mulches were much more effective in mitigating erosion than hydromulch. This finding is in line also with Robichaud et al. [70]. Mulch is generally more effective in short-duration and high-intensity rainfall events than erosion barrier treatments that provide little ground cover. However, the effectiveness of the different mulch types depends on several factors, e.g., application rates, while other measures (e.g. seeding) still have uncertain potential. Seeding can provide hardly little protection during the initial post-fire damaging runoff events, since it must grow first. For immediate protection from excess runoff and sediment transport, barrier treatments applied in the appropriate slopes were found to be effective. Channel and road treatments are effective when properly applied to serve certain purposes, namely, to avoid expected failures in certain channels, culverts and road passages at risk. Based on limited information, chemical treatments have been found to be inefficient for runoff and erosion reduction. According to Pizzeghello et al. [164] their effectiveness majorly depends on the occurrence of light rainfall events in order to allow vegetation to grow shortly after fire.

Text Box 8:

Examples of PEFTs, including (in order of appearance): Heli-mulching operations, contour-felled log, in-channel check dams (wooden); hillslope log debris dam[4].

As shown, there are many kinds of PEFTs. All of them aim to speed up the recovery of the burned site. Although each treatment of the categories presented has case-specific factors and potentially different site suitability, we can draw a general conclusion regarding their effectiveness:

- Land treatments can generally reduce runoff and/or sediment yields during the first rainfall events. Still, their effectiveness depends on several factors, such as the application rates, the proper installation (e.g., log barrier installation is vital for the effectiveness of the treatment [88]), post-fire climatological conditions (e.g., rainfall amount and intensity [157]), slope length and

[4] Source: Papaioannou et al. [157].

steepness-terrain gradient make/brand of tackifier, and the time (e.g., seeding does not provide instant protective effect, especially in the first year) [157].

- Channel treatments seem more efficient in gentle gradients and areas of low or moderate flows, as the risk of failure is lower. Moreover, channel treatment effectiveness is highly correlated with the adjacent areas' land treatments since these areas supply the channels with water and sediments [155]. However, specifically for check dams with finite storage capacity, their effectiveness is restricted due to their limited life expectancy (short-term sediment control solution) [165]. Moreover, channel treatment effectiveness is usually a function of the proper installation (e.g., log dams' installation is essential for the effectiveness of the treatment [88]), the appropriate positioning of the treatment (e.g., some channel treatments should be constructed in series), their maintenance (e.g., debris basin maintenance) [155] and the post-fire climatological conditions (e.g., rainfall amount and intensity affect the erosion, sediment transport, and deposition processes).
- Road and trail treatments may benefit road facilities and deliver less sediment into channels. However, similar to the channel treatment, the effectiveness of these treatments can be affected due to their poor installation and/or due to insufficient maintenance. On the other hand, there are limited data documenting their effectiveness [166].

Overall, the effectiveness of all treatment types is subject to large uncertainties due to the difficulty in monitoring their actual effect and the multiple factors that can affect it. Even listing and documenting these factors is not easy, as it would be an attempt to generalize several site-specific cases. According to Robichaud et al. [166] these factors can be divided into not-fire-dependent and fire-dependent, as their combination determines the actual watershed response and, subsequently, the effectiveness of the post-fire treatments [167]. These factors are presented and further discussed in Table 3.

Table 3. An overview of some important factors affecting the effectiveness of post-fire treatments where all factors, except the "treatment implementation-installation", are based on the analysis of Robichaud et al. [70], references therein, and Papaioannou et al. [157].

Factors	Description
	1. Factors Unrelated to Fire:
Rainfall characteristics, especially rainfall intensity	**a.** Intense, short-duration storms with high rainfall intensity and low rainfall volumes cause high stream peak flows, and substantial erosion episodes after fires. **b.** An increase in runoff, erosion rates, and stream flows means potentially lower effectiveness of any treatment.
Topography	**a.** Erosion rates are generally higher in bigger slopes and hillslope lengths (flow path). **b.** Drainage patterns and topographies that enhance erosion and peak flow concentration are more challenging for post-fire treatments.
Land use and management	**a.** In addition to natural elements like rainfall and topography, the extent of a watershed's reaction to a hydrological event is also influenced by manmade activities like road construction, fuel reduction, and timber harvesting. **b.** The cumulative effect of these anthropogenic activities can lead to the rise of runoff severity and, by extension, erosion, and flooding, posing important challenges for any treatment.
Treatment implementation-	**a.** The effectiveness of many post-fire treatments depends on the accuracy of the installation, the selected design type, the post-installation maintenance, and the level of experience of the personnel used for the treatments [7,49,53].

Factors	Description
installation and design matters	**b.** With proper treatment implementation, we can avoid failures and improve functionality and effectiveness over the long term.
	2. Fire-Dependent Factors:
Burn severity (also referred to as “fire severity”)	**a.** Burn severity can be seen as a measure of damage to ecosystem properties. It is usually expressed by the degree of soil heating and/or vegetation mortality or precisely the degree of overstory plant mortality. **b.** In general, higher burn severity is translated into larger and quicker watershed responses to rainfall, being thus more challenging for the post-fire treatments.
Soil burn severity	**a.** Soil burn severity expresses the fire effects of soil heating and the soil’s organic material consumption. Thus, higher soil burn severity leads to soil properties alteration resulting in soil infiltration reduction and high soil erodibility. **b.** Both these effects lead to an increase in surface runoff, higher peak flows, flow concentration, sediment transport, and erosion.
Amount of bare soil	**a.** A crucial factor for burn severity mapping is positively related to postfire erosion rates. **b.** Land cover treatments, such as natural or straw mulching, can reduce post-fire erosion.
Soil water repellency	**a.** Post-fire soil water repellency is associated with soil burn severity and reduced infiltration. **b.** Although its effects vary over space, time, and soil type, most relevant treatments aim to rewet the soil to minimize the soil water repellency and its negative consequences since it depends on soil moisture (it is reduced or absent following prolonged wet conditions).
Soil erodibility	**a.** The treatments' effectiveness is largely dependent on runoff, sediment transport, and soil erosion. Moreover, soil texture, structure, and organic matter content are important factors considering erosion resistance. **b.** Soil texture (namely its inorganic particles by size, such as sand, silt, and clay) is ordinarily unaffected by the fire. On the other hand, soil structure is affected by fire (namely, the arrangement of primary particles into aggregates). Therefore, soil structure can become disaggregated, making soil more erodible and reducing its infiltration capacity.
Time since the fire	**a.** This factor refers to the ecosystem's natural recovery (soil structure, vegetation, microclimate, etc.). For example, more significant and faster vegetation recovery means smaller instant surface runoff rates and reduced erosion rates. **b.** As discussed above, timely action with post-fire treatments can improve watersheds' overall response and avoid post-fire negative consequences.

The factors of Table 3 are the main and more generic ones, but are not the only ones relevant to the effectiveness of the post-fire treatments (for example roughness also changes after a fire, affecting the water retention and flow [140]). Finally, we should keep in mind that all these factors are interrelated, resulting in more complex cause-effect relations in terms of watershed responses (damage, runoff, erosion, etc.), and more complex relations on the treatment’s impact and effectiveness.

8 Designing PEFTs for the case of Kineta, Greece

The most important factors to consider when designing PEFTs, according to the studies reviewed are:

- the burn severity and extent, as it determines the damages caused;

- the climatic conditions, especially rainfall intensity and duration, as it determines the risk;
- the slopes and roughness; or in general, the terrain morphology (geomorphology) of the areas, as they affect the runoff and sediment movements, as well as the accessibility for applying the treatments reviewed;
- the proper application – installation of the works and their monitoring over time (e.g., annual time step) to ensure maximum efficiency;
- other site-specific factors, including social and behavioural aspects that define the response for human interventions and other criteria such as costs and rehabilitation efforts [168].

Thus, a combination of techniques will be the most efficient way (and also necessary) to mitigate and protect from erosion and flooding risks adequately.

For the case of Kineta, we started from the most common PEFTs as categorized above, namely, land treatments, channel treatments, and road and trail treatments.

The literature on specific treatments in Mediterranean sites is mainly focused on soil erosion, and there are very limited studies focusing specifically on flood protection. The most commonly applied PEFTs in Greece are barrier-based (land treatments) and channel-based (channel treatments), due to their relatively low costs, and ease of installation from local timber. In particular, these works include log-erosion barriers - LEBs (barrier-based) which are placed across the contours to retain peak flows and sediments, and wooden check-dams (channel-based), which are placed within the channels. Usually, these PEFTs aim to trap sediments, reduce excess flow, and slow runoff [169,170]. Depending on their placement spatially, they can offer sufficient protection to roads from floodwaters and sediments.

For the case of Kineta catchment, these PEFTs (LEBs and wooden check-dams) were assessed, according to the respective official Greek guidelines, to specify their recommended installation strategy. In particular, according to the Hellenic Technical Specification on the Technical Guidelines for erosion control structures, and relevant studies and technical reports describing the application of these PEFTs [171–173], the main criteria for their installation were retrieved:

- LEBs are suitable for areas with high-moderate burn severity (at the time after the fire, to target the most vulnerable areas), and slopes between 20% - 50%, while it is also common for many applications to consider the slope installation starting from 10%, with looser spacing till 20%). LEBs are typically installed every 8m along the contour lines, while in practice, longer distances are also considered (usually 10m or even 20m) to reduce the installation costs, the labour and maintenance requirements. They are usually 0.2 meters high.
- Wooden check-dams are constructed along channels of 1st and 2nd order streams (the small tributaries, because they are more controllable in smaller channel openings, due to the practicality of installing small wooden structures, where they exhibit higher durability). They are placed in constrictions of channels having an upstream widened bed and a slight stream slope (<20%), spaced at intervals of 50-100 meters (and always according to the expert of the on-field experts). They are usually 1 meter high.

These criteria, namely, burn severity categories (as occurred from the RS analysis – Fig.5), stream slopes and order (Fig.12A) were spatially visualized over the DEM of the study area in GIS, so the locations meeting the installation criteria for LEBs and wooden check-dams were identified.

The LEBs were installed in every 10m, along the contour lines according to the usual practice followed in Greece. At the spots where the LEBs meet a stream, we recommend the installation of wooden check dams within this stream, to ensure that the 'protection line' is not interrupted. Moreover, specifically for the studied catchment, instead of installing wooden check-dams in the channels of 1st and 2nd order streams, we recommend their installation in the 3rd order steams as well. The reason is the specific characteristics of the studied catchment, and in particular, its small size and the quite narrow morphology of the 3rd order streams. So, the wooden check-dams were placed in the 1st, 2nd and 3rd order streams, every approximately 10m contour lines, within the streams. Compared to the general guidelines, as mentioned in the bullet points above, it is worth noting that the PEFTs that we considered for the Kineta catchment are quite conservative, with a dense network of LEBs (slope from 10%-50%) and wooden check-dams, as can be seen from their spatial distribution (Fig.12B).

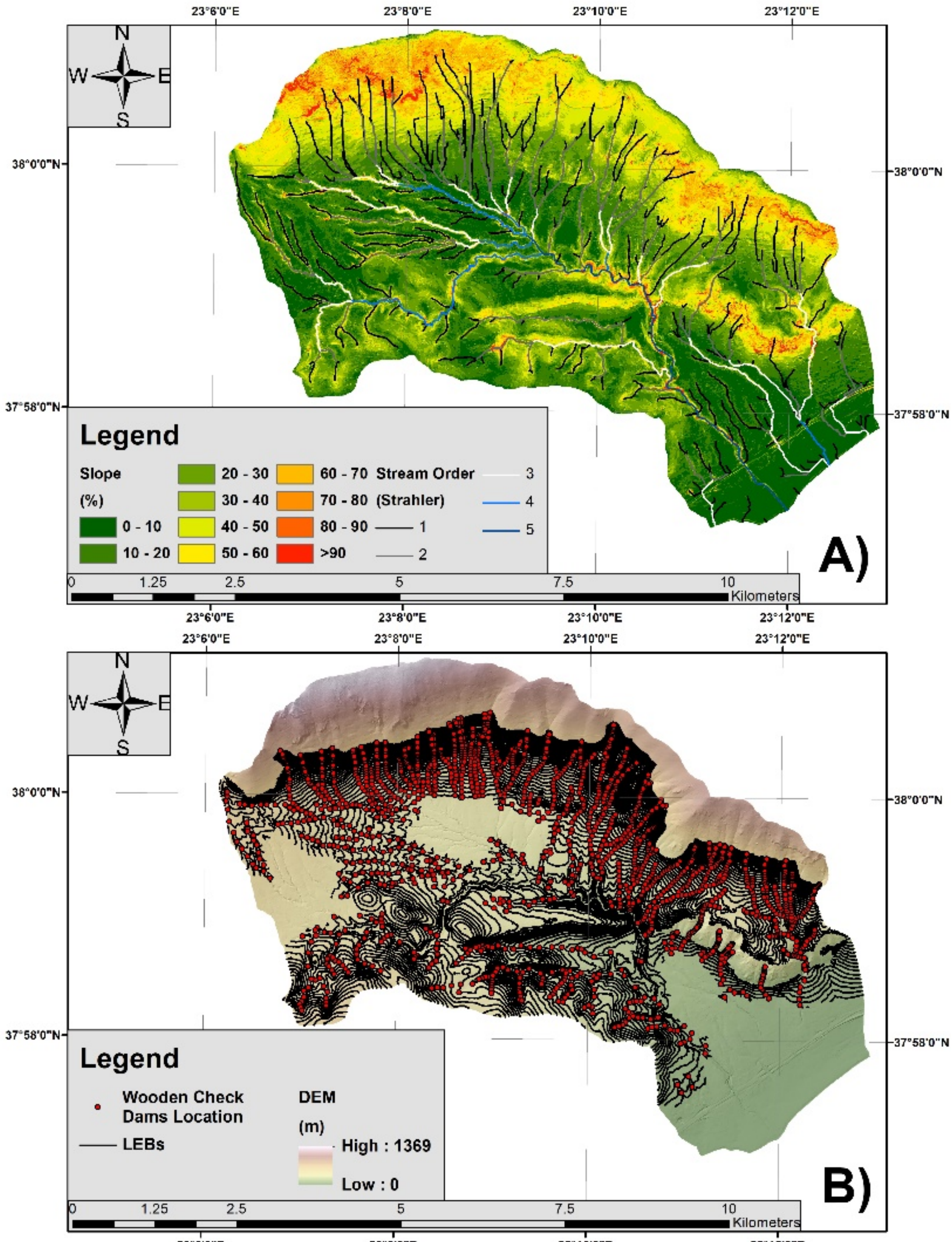

Figure 12: A) stream order and slope, and B) final map with the locations of LEBs, and wooden check-dams. Source: [174].

9 Scenario analysis: Pre-fire, Post-fire no protection, and Post-fire with protection

Besides the pre-fire and post-fire scenarios, a flood protection scenario was also considered, to quantify the PEFTs' effectiveness. The PEFTs scenario considers the application of the PEFTs, namely the LEBs and the wooden check-dams, as shown in Fig.12.

So, now the scenarios are the pre-fire and post-fire ones (as explain above), plus a post-fire PEFTs scenario. In summary:

- Pre-fire (same as above): same storm, pre-fire conditions with the respective Manning's n coefficients, and no PEFTs in place.
- Post-fire, No PEFTs (same as above, reality scenario): the same storm applies in the catchment with post-fire conditions, using the respective Manning's n coefficients, and no PEFTs in place. This is the reality of what happened in Kineta, so the results of this scenario were the ones that were validated, as shown in Fig.11.
- Post-fire, With PEFTs (protection scenario): the same storm applies in the catchment, with post-fire conditions, using the respective Manning's n coefficients. The suggested PEFTs now are included: Having designed the PEFTs spatially (Fig.12), we can modify the terrain of the HEC-RAS model accordingly. The terrain was modified to incorporate the suggested PEFTs according to Fig.12 using the R package "terra" to analyze the raster file with the designed PEFTs, the R package "sf" to analyze vectors (placing thus the LEBs and WCD in the defined intervals), and the R package "smoothr" for lines smoothing, making the PEFTs suggested installation realistic (see Text Box 9). The model in this scenario has a terrain with the designed network of LEBs and WCD in place. This is our suggested wish-case, where protection should be considered after the wildfire, to mitigate potential future floods. In this scenario, it was assumed that PEFTs works would retain debris, and thus, major culverts and bridges would not be blocked.

Text Box 9:

A central part of the protection scenario was to run the hydraulic model HEC-RAS with a terrain reflecting the protection scenario with the spatially designed PEFTs in place.
In order to incorporate the PEFTs (log-erosion barriers (LEBs) and wooden check-dams (WCD)) of Fig.12 in the terrain model, we used the R packages 'terra' to analyze rasters, 'sf' to analyze vectors and 'smoothr' for lines smoothing.
First, we exported the PEFTs layout (Fig.12) as a high-resolution raster mask. Using the R package 'terra', we loaded the original digital elevation model (DEM) and overlaid the PEFTs raster, adjusting elevation values where barriers and check-dams were to be installed. For each LEB, we raised the DEM by 0.2 m along the contour lines at 10 m spacing; for each WCD, we inserted 1 m high linear features within stream channels at specified intervals.
Next, the 'sf' package parsed the vector data, point and line shapefiles representing PEFTs locations, allowing precise georeferencing of structure footprints and extents. Finally, to avoid artificial hydrological artifacts caused by unnaturally jagged barrier alignments, or odd curves in the LEBs as they followed the contours of the DEM, we applied 'smoothr' to gently smooth linear features, preserving their designed geometry while ensuring flow continuity in the hydraulic mesh. The result is a modified terrain surface that realistically incorporates PEFTs elevations and geometries, ready for HEC-RAS's

rain-on-grid simulation, thus capturing how these treatments divert, slow, and attenuate post-fire flood flows.

The results of these scenarios were tested in terms of i) flood extent (area), ii) water depth, iii) water velocity, iv) flood maximum arrival time, and v) costs and damages (analyzed in the following sections).

10 Comparing the results of the scenarios: Insights on flood protection performance of PEFTs

The total simulated flood inundation area for the (real) post-fire case was 595,246 m^2, covering almost 24% of the town's total residential area. The pre-fire simulation resulted in a flood inundation area of 451,848 m^2 (Fig.13B and Fig.13D).

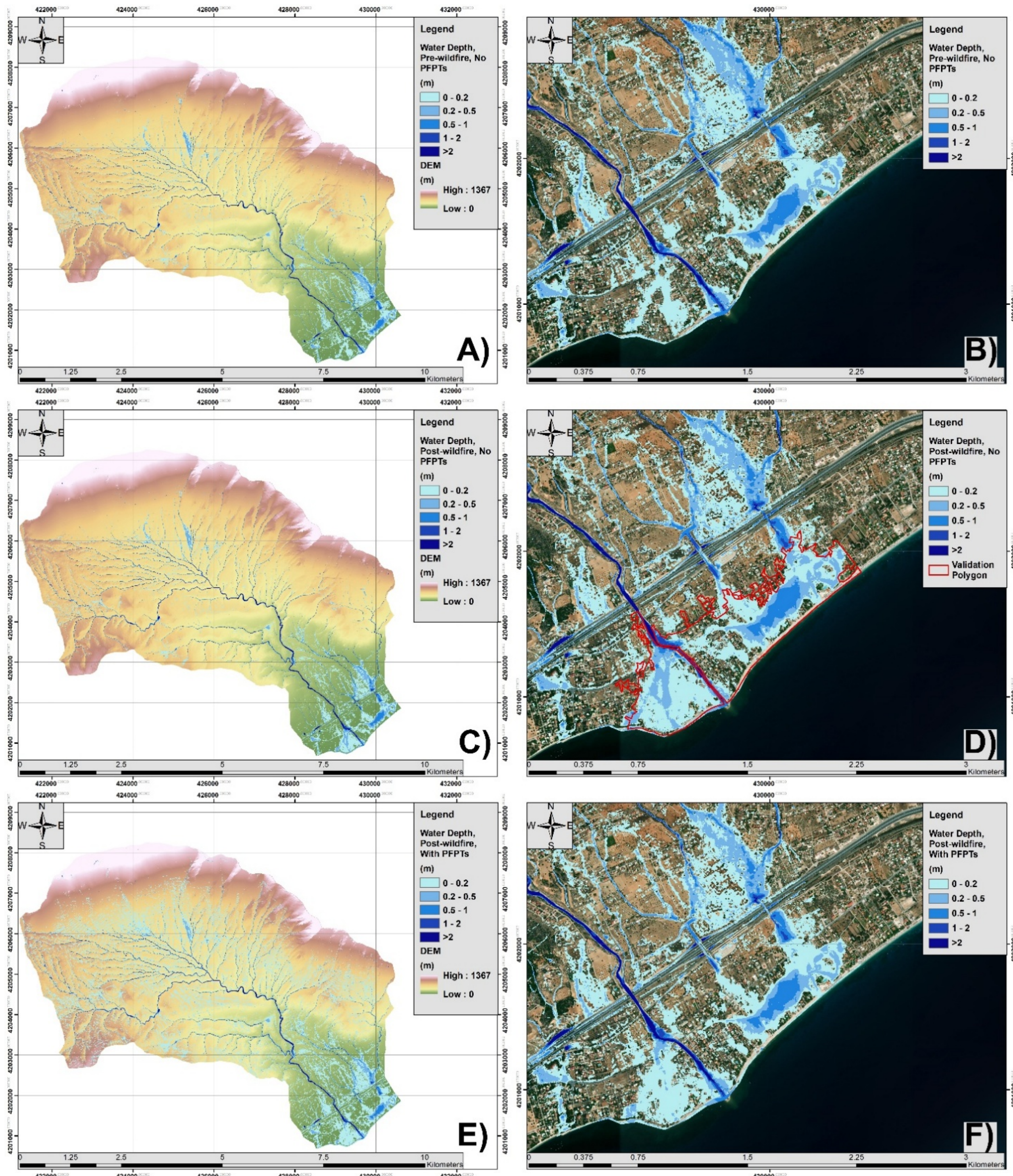

Figure 13: The extent of the flood in Kineta catchment (A),(C),(E) and the water extent and depth in the Kineta town (B),(D),(F). These are shown for the hypothetical Pre-fire scenario (A),(B); the real Post-fire, No PEFTs scenario (C),(D); and the hypothetical Post-fire, With PEFTs scenario (E),(F), respectively. The red “validation polygon” in Fig.S4D represents the boundary of the water extent as resulted from RS analysis. Source: [175].

Text Box 10:

The difference in the flood extents of pre-fire vs post-fire reflects the impact of the wildfire on the flooding, which is 143,398 m^2 (the one fifth of the flood ~ 25%), as also mentioned in the previous sections.

Here is the difference of the floods of the post-fire – pre-fire scenarios:

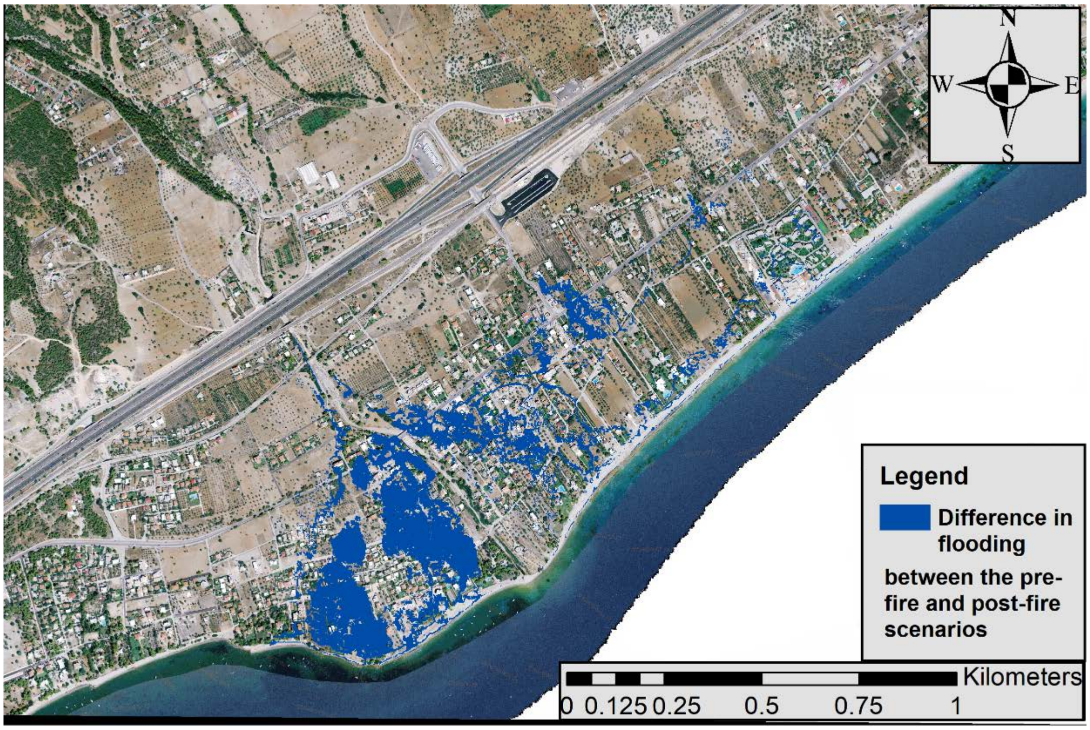

In simple words, if there was no fire the previous summer, the illustrated flood water would not have been there!

If the PEFTs were in place after the wildfire, the flood extent would have been 447,575m^2. Therefore, the effect of these recommended protection measures would have reduced the flood-inundated area by 147,671 m^2 (24.8%) (Fig.13F).

It is worth noting that this difference indicates that the effect of the wildfire could have been entirely avoided with the PEFTs.

As shown in Fig.14, the effect of the fire and of the PEFTs are also evident in terms of water velocity and flood arrival time. In fact, the proposed works could have offset significant parts of water velocity in other parts of the town, while delaying them.

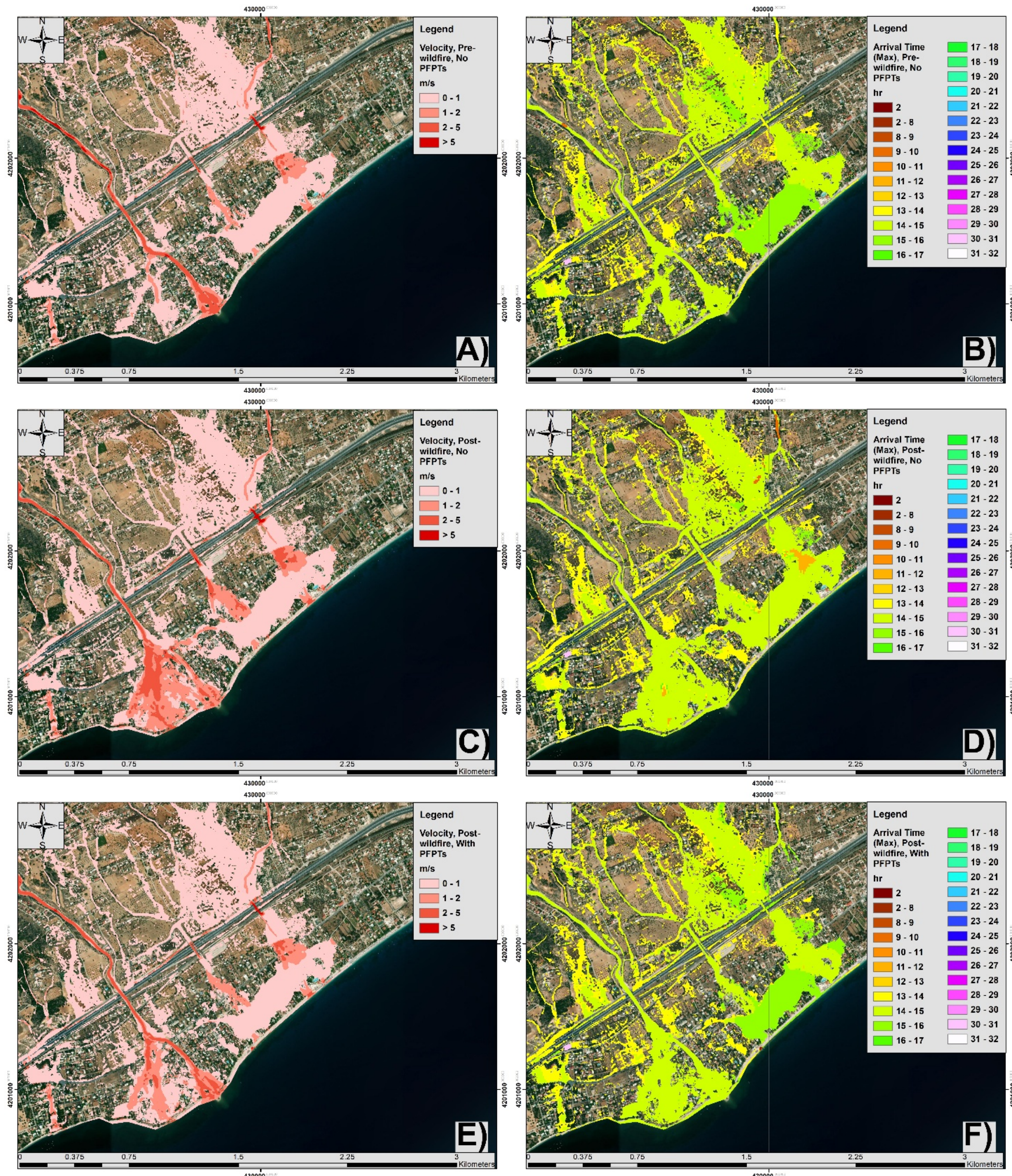

Figure 14: The water velocity (A),(C),(E), and the flood maximum arrival time in the Kineta town (B),(D),(F). These are shown for the hypothetical Pre-fire scenario (A),(B); the real Post-fire, No PEFTs scenario (C),(D); and the hypothetical Post-fire, With PEFTs scenario (E),(F), respectively. Source: [175].

In particular, Fig.15 shows the differences between the reality and the protection scenarios (isolating the effect of the PEFTs), as detailed in Fig.13 and Fig.14. We observe that the PEFTs lead to moderate reductions in peak water depths across much of the inundated zone, of around 0.1-0.3m, with the biggest differences being in the peripheral areas, and in the central stream (Fig.15A). Velocity reductions are spatially heterogeneous but pronounced where flow paths concentrate (Fig.15B). Yellow to orange zones (0.2-0.8 m/s reductions) follow main overland flow corridors, while even bigger reductions (1.0-1.6 m/s, red–pink) are observed in the main stream's flooding, and the rest of the broad flat areas exhibit minor reductions (0-0.2 m/s, pale yellow). Such reductions, especially to the west part, can significantly reduce infrastructure damages.

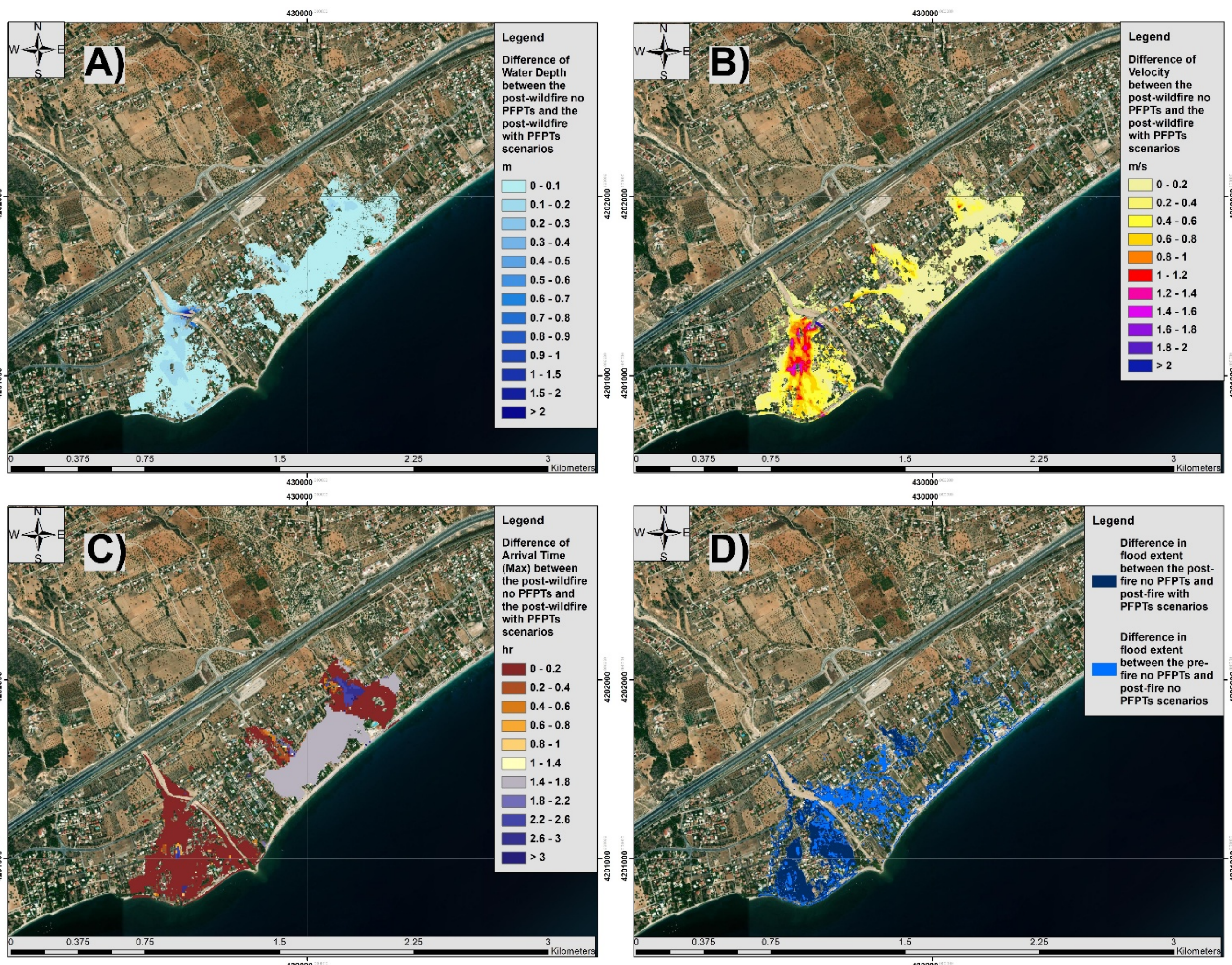

Figure 15: Assessment of the effect of the PEFTs on: A) Water depth, B) water velocity, C) Flood maximum arrival time, D) water extent. These are presented as the differences between the Post-fire No PFTs and Post-fire With PEFTs, while for the floodwater extent (D) we compare all scenarios. Source: [175].

The PEFTs introduce meaningful delays in flood wave arrival, as seen in the arrival-time difference map (Fig.15C). Peripheral urban areas and floodplain margins experience minimal delays (0-0.4 h, brown–light orange), while central zones downstream of barrier clusters show delays of 1.0-2.2 h (light purple to deep blue). The central part of the city, which appears to be the most flood-prone, had the largest delays due to PEFTs, and this is crucial for emergency response, evacuation, traffic management, and individual protection measures. Moreover, elongated travel times reduce flood peaks, lessen hydraulic loads on downstream structures, and allow more water to infiltrate or be retained, showcasing PEFTs' role in temporal flood risk mitigation.

Regarding the flood extent, the dark blue areas would have been inundated without PEFTs but remain dry when they're in place. The blue shading shows the additional flood extent caused by the wildfire (post-fire with PEFTs vs. pre-fire without PEFTs), underscoring how burn-induced changes expand inundation inland. This joint comparison illustrates that while the post-fire landscape is inherently more flood-prone, strategically placed PEFTs can reclaim substantial areas from inundation.

11 Economic analysis: Flood protection vs flood damage costs

From an engineering perspective, post-fire flood resilience heavily relies on the application of necessary protection measures. From an economic or policy perspective, however, the decision to apply the PEFTs is connected to the associated costs [174]. We assess the direct economic implications of the proposed PEFTs' application by estimating their total implementation cost and comparing them with the direct cost of avoided damage.

Flood protection cost

Our estimations for PEFTs consider the necessary material and transportation costs, as well as the installation and labour costs. This information was obtained from the Greek guidelines, which provide detailed cost breakdowns for such works.

More specifically:

Following the recent destructive fires at large areas in Thrace, Northern Greece during the summer of 2023 [176,177], the Greek Ministry of Environment and Energy has issued a detailed set of studies reporting the on-site installation of post-fire restoration works in forests, including the associated costs [178]. The same approach is followed in this paper to estimate the cost for the implementation of the suggested PEFTs (LEBs and wooden check-dams). The cost analysis reported (based on the joint Ministerial Decisions of the Greek Ministries of Infrastructure and Transport and Environment and Energy, on the application of Forestry works), takes into account the costs of logging (i.e. timber), their transportation, and installation (construction), both for LEBs and wooden check-dams (as presented in Table 4). The values refer to €2023 and the use of pine trees is considered as timber, which is also common in the Kineta mountainous area.

Table 4. Cost analysis for LEBs and wooden check-dams, considering costs of materials (timber), transportation, and installation (construction), in values of 2023 [178].

Logging costs (for pine trees 2m long x 0.2m diameter)
Timber cost: 7.99€
Increase 10% for burnt sites: 0.80€
Increase 10% due to execution by the same work group: 0.80€
Allowance 5% for travel expenses for a distance of 0-50km: 0.40€
Good performance bonus 5%: 0.40€
Employer's Insurance 24.44%: 2.54€

Logging cost: 12.93€/m^3
Displacement and transport costs (for pine-trees 2m long x 0.2m diameter)
Transport cost for distances less than 200m: 8.98€
Increase 10% for burnt sites: 0.90€
Increase 10% due to execution by the same work group: 0.90€
Allowance 5% for travel expenses for a distance of 0-50km: 0.44€
Good performance bonus 5%: 0.45€
Employer's Insurance: 24.44% 2.85€

Transport costs: 14.53€/m^3
Estimation of LEBs construction cost per meter installed
Volume of a unit log (1m long x 0.2m diameter): 0.0314
Increase 10% for losses coverage and supporting brackets: 0.0345
Volume per meter installed: 0.066m3/m
Logging cost = 12.93€/m^3 · 0.066 m^3/m = 0.85€/m
Transport cost = 14.53€/m^3 · 0.066 m^3/m = 0.96€/m
Labour cost of an unskilled worker for digging, construction and installation 3.06€/m
----
Total cost per meter of LEBs installed: 4.87€/m
Estimation of wooden check-dam cost per square meter installed
The volume of timber required for a typical trapezoid wooden check-dam, using unit logs of typical dimensions as above, and supporting brackets and a log, tied with wires is estimated to be 1.635m^3
Logging cost = 12.93€/m^3 · 1.635m^3 = 21.14€/wooden check-dam
Transport cost = 14.53€/m^3 · 1.635m^3 = 23.76€/wooden check-dam
Labour cost of an unskilled worker and a logger for tools, digging, construction and installation 172.38€/m
----
Total cost of a wooden checked-dam of open surface of 3.5m^2 = 172.38/ 3.5 = 49.25 €/m^2

Based on these estimations, the costs for the PEFTs designed for the Kineta catchment would be 4.87€ per meter of LEBs installed, and 49.25 €/m^2 of wooden check dams. The spatial model for the proposed PEFTs (Fig.12) resulted in 636,049 m of LEBs and 2065 wooden check dams (of an average installed area of 3.5 m^2). Therefore, their total cost would be:

- 4.87€/m · 636,049 m of LEBs installed = €3.1mill, plus
- 49.25 €/m^2 · 2065 wooden check dams ·3.5 m^2 each = 355,954€,

Which, in total, sums to **€3.45mill.**

Flood damage direct costs

The direct damage costs caused by the flood were estimated. This was achieved by synthesizing the flood inundation results of the RS and the hydraulic model, a semi-automated approach involving Artificial Intelligence (AI) for image segmentation and human checks to estimate the affected properties, and typical monetary values of the affected properties.

The direct flood damage costs involve the damages that occur due to the physical contact of objects with the floodwater [179,180], and are usually straightforward to asses, especially in cases with limited data availability [181,182]. To assess them, we conducted a semi-automated approach to count the elements affected by the flood.

First, the part of the Kineta town that was affected by the flood (namely the area within the validation polygon) was exported as an image. This was then used as an input to the AI tool "Segment Anything Model" (SAM) [183], a widely used application for image segmentation. The SAM uses a database of over 1billion masks on 11million licensed and privacy respecting images, to distinguish elements within new images (zero-shot segmentation) [184,185]. So, the SAM delineated the properties affected within the flood-affected area, in particular residential homes, commercial buildings, and agricultural fields.

As a cross-check, a human check was also performed by navigating in Google Street Maps and comparing the results to ensure that the identified elements were complete and correct, before counting them (Fig.17 and Table 5).

Figure 16: Estimating the cost of the flood damages per category of affected properties and infrastructure.

The counted elements affected from the flood are shown in Table 5, along with the approach followed to estimate the damage caused. In particular, to estimate the damage in residential homes, we used data from a relevant report of the Hellenic Association of Insurance Companies [186]. According to this report the average damage to homes from heavy precipitation in 2019 is 3,393€, which for the 541 counted houses damaged, translates into a total cost of 1,835,613€, and 2,095,531€ in 2023 value (considering the Greek cumulative inflation factor of 1.142 [187]). Regarding the impact of heavy precipitation on businesses, according to the same data, the average loss in 2019 was 21,203€. If we use this figure as an approximation for the average damage suffered by Kineta hotels, we have a total cost of 339,248€, which is 387,285€ in 2023 value.

According to the visual inspection study on the aftermath of the November 2019 flood of Kineta, extended damages were reported to private vehicles [114,188]. The average number of private vehicles is estimated to 1.2 per household, and the average insurance coverage is around 1100€. So, for the affected households and vehicles, the total cost is estimated to 714,120€ in 2023 value.

For the estimation of the direct costs of floods on agricultural fields in Kineta, Greece, we focused on the necessary cleanup expenses, as no direct loss of profits from production was incurred due to it being November when the fields were not cultivated. The total area affected by flooding, based on the flood model's simulation results was 549,308m², with around 67% (386,910m²) being agricultural land. The cost estimation involved calculating the labour costs for an unskilled worker, tasked with tools handling, transportation, drainage and the removal of sediments such as mud and wood debris. The typical hourly wage is 6.43€ and given that a worker could clean approximately 20m² per hour, a total of 17,853 hours was required for the entire affected area. Consequently, the estimated total labour cost for drainage and sediment removal the agricultural fields amounted to approximately 124,392€ in 2023 value [176–178,189].

For the calculation of the economic losses due to a blocked road from flooding, we used a general estimation model (Equation 4) which takes into account factors like the daily vehicle traffic, the additional distance of detour, vehicle operating costs, additional travel time, and the economic value of time and goods affected [190–194].

$$E = (V \times D \times Ct) + (T \times Cg) + I \qquad (4)$$

Where:

- V is the daily vehicle traffic (number of vehicles per day).
- D is the additional distance of the detour (in kilometres).
- Ct is the cost per vehicle per km (considering fuel, wear and tear, and other operating costs).
- T is the additional travel time caused by the detour (in hours).
- Cg is the cost per hour per vehicle (valuing the time of the passengers and goods).
- I represents any indirect costs such as loss of revenue, long-term economic impacts, etc.

For the case of Kineta, we assumed typical traffic data for the closed section of Athens-Corinth highway, for a working day. This is approximately 10,000 vehicles per day, with 25% being commercial vehicles. The detour caused an extra 2km and an additional 30 minutes of travel time for all vehicles. The direct costs were computed by assigning an operational cost of 0.5€/km for private vehicles and 0.8€/km for commercial vehicles, along with a value of time at 15€/hour for private vehicles and 50€/hour for commercial ones [190–194]. By applying these values in Equation (1) the total economic loss per day was calculated at 130,250€. No indirect costs considered due to data limitations (so, I=0). The road closure of the section of Athens-Corinth highway in the north of Kineta town lasted for two days [188,189]. Thus, the total cost was estimated to 260,500€ (in 2023 value).

Table 5. Estimating the cost of the flood damages per category of affected properties and infrastructure, for the "reality" scenario: Post-fire, No PEFTs.

Affected Properties and infrastructure	Quantity / Extent	Cost estimation approach	Estimated value (€ of 2023)
Residential homes	541	Based on the average damage cost to homes from heavy precipitation in 2019 as reported by the Hellenic Association of Insurance Companies	2,095,531
Commercial buildings (hotels)	16	Based on the 2019 average loss figure for businesses affected by heavy precipitation, also provided by the Hellenic Association of Insurance Companies	387,285
Private Vehicles	649.2	Based on the 2019 average loss figure for vehicles affected by natural disasters according to the Hellenic Association of Insurance Companies	714,120
Agricultural fields	386,910 m^2	Here, our approach focused on labour costs for cleanup and restoration, considering no direct profit loss from production, and was based on the costs for an unskilled worker to clear mud and debris, with an estimated area coverage rate and hourly wage.	124,392
Blocked roads	2 days	The estimation was based on general estimation formula that account for increased travel distance and time due to detours, with specific costs assigned per kilometer and per hour for private and commercial vehicles	260,500
Infrastructure	Roads, streams, land, drainage	Official estimated costs from the Region (Prefecture) of West Attica's Technical Works Observatory	21,643,068
		Total estimated cost	**25,215,275**

The total estimated cost so far (except of the last row on infrastructure of Table 5) sums at 3,572,206€. This value is very close to the reported reimbursements of 3,500,000€ for the Kineta flood [197].

Adding to that, the flood caused significant damages to the local infrastructure (last row of Table 2), including costs for cleaning the streams from sediments (increased volumes due to the wildfire), works of land stabilization, restoration of the road network and the drainage network [114]. As reported by the Region (Prefecture) of West Attica's Technical Works Observatory, the total repair costs for these damages reached 18,950,000€ (2021), i.e., 21,643,068€ in 2023 value [198]. So, our total estimated cost (€25.22mill.) is very close to those reported costs (€3.5mill. + €21.63mill. = €25.14mill.).

The same process was followed to estimate the flood damage costs for the other two scenarios, as summarized in Table 6 below.

Table 6: Estimates of direct flood damage costs under the three scenarios explored. Source: [175].

Affected Properties and infrastructure	Pre-fire, No PEFTs (wildfire effect scenario)		Post-fire, No PEFTs (reality scenario)		Post-fire, With PEFTs (protection scenario)	
	Quantity / Extent	**Estimated value (€ of 2023)**	**Quantity / Extent**	**Estimated value (€ of 2023)**	**Quantity / Extent**	**Estimated value (€ of 2023)**
Residential homes	412	1,595,857	541	2,095,531	405	1,568,743
Commercial buildings (hotels)	16	387,285	16	387,285	14	338,874
Private Vehicles	495	320,055	650	714,120	486	315,511
Agricultural fields	295,701 m^2	95,068	386,910 m^2	124,392	290,923 m^2	93,532
Blocked highway	2 days	260,500	2 days	260,500	2 days	260,500
Infrastructure	Roads, streams, land, drainage	16,429,135	Roads, streams, land, drainage	21,643,068	Roads, streams, land, drainage	16,273,769
Total Damage Cost:		**19,087,901**		**25,224,897**		**18,850,929**

The results of the PEFTs costs and flood damages are summarized as follows:

- **Pre-fire, No PEFTs:** Reduced count of residential homes, commercial buildings (hotels), private vehicles, and agricultural fields affected compared to the "reality" scenario; Same cost for the same highway closure; Reduced infrastructure cost based on the reduced flooded area, compared to the "reality" scenario. Cost of PEFTs = 0€. Flood damage cost = €19.1mill. The difference in the flood damage cost is 6,136,996€ (or 24.33% of the real event's damage), which is purely attributed to the wildfire.
- **Post-fire, No PEFTs:** The exact affected number of residential homes, commercial buildings (hotels), private vehicles, and agricultural fields; Actual cost for the Athens-Corinth highway closure; Actual infrastructure cost. Cost of PEFTs = 0€. Flood damage cost = €25.2mill. This represents the real case, which highlights the extensive financial burden on local authorities and communities, underscoring the need for effective flood management and mitigation strategies to reduce long-term economic impacts.
- **Post-fire, With PEFTs:** Reduced count of residential homes, commercial buildings (hotels), private vehicles, and agricultural fields; Same cost for the same highway closure; Reduced infrastructure cost based on the reduced flooded area. Cost of PEFTs = €3.45mill, Flood damage cost = €18.9mill. The difference in the flood damage cost is €6.4mill. This indicates that the PEFTs could have

reduced the actual real case's flood damage costs by 25.3%, completely offsetting the wildfire's impact.

11 Discussion: Flood Protection versus Flood Damages

The results of this integrated analysis refer to three main ‘sets’ [175]:

1) Modelling post-fire floods and PEFTs

The representation of the post-fire flood event, considering a combination of methods (meteorologic model, RS, hydraulic-hydrodynamic, and spatial PEFTs-design model) is a challenging and interdisciplinary modelling task. With this combined modelling approach, on the one hand, we provide a framework for similar analyses, as all models are freely available and can be used in combination (soft-linked) to represent other post-fire flood events. On the other hand, this approach led to accurate representation that enables building on the findings (flood inundation maps) to consider protection measures and enhance resilience. Also, the modelling of the PEFTs within HEC-RAS is a novel application. An interesting set of findings here is the wildfire's and the PEFTs' effects on flooding. The effect of wildfire on the flood extent is 24.1% (difference of the pre- and post-fire scenarios), which is not negligible for a small town. Regarding the effectiveness of the PEFTs, if the recommended measures were in place, 24.8% of the flooding would have been avoided, while most of the floodwaters would have been delayed, coming with reduced velocities and depths.

2) Exploring the effect of PEFTs

The analysis for the application of the most suitable PEFTs, their mapping, and cost-effectiveness is also a challenging task, as the literature on PEFTs is limited. To the best of our knowledge, this is the first attempt to model PEFTs based on spatially modelled physical characteristics and case-study-specific technical guidelines, along with a detailed assessment of their cost-effectiveness for flood mitigation. This approach illustrates how the PEFTs can be followed to other study areas, similarly, and give at least a preliminary picture/estimation of the potential post-fire measures. As mentioned, their effectiveness is significant, completely offsetting the wildfire's impact on flooding. Especially if we consider the significance of the downstream residential area, and take into account the overall effects in water extent, depth, velocity, and arrival times, as well as the relatively low costs, there is no doubt on the PEFTs' value.

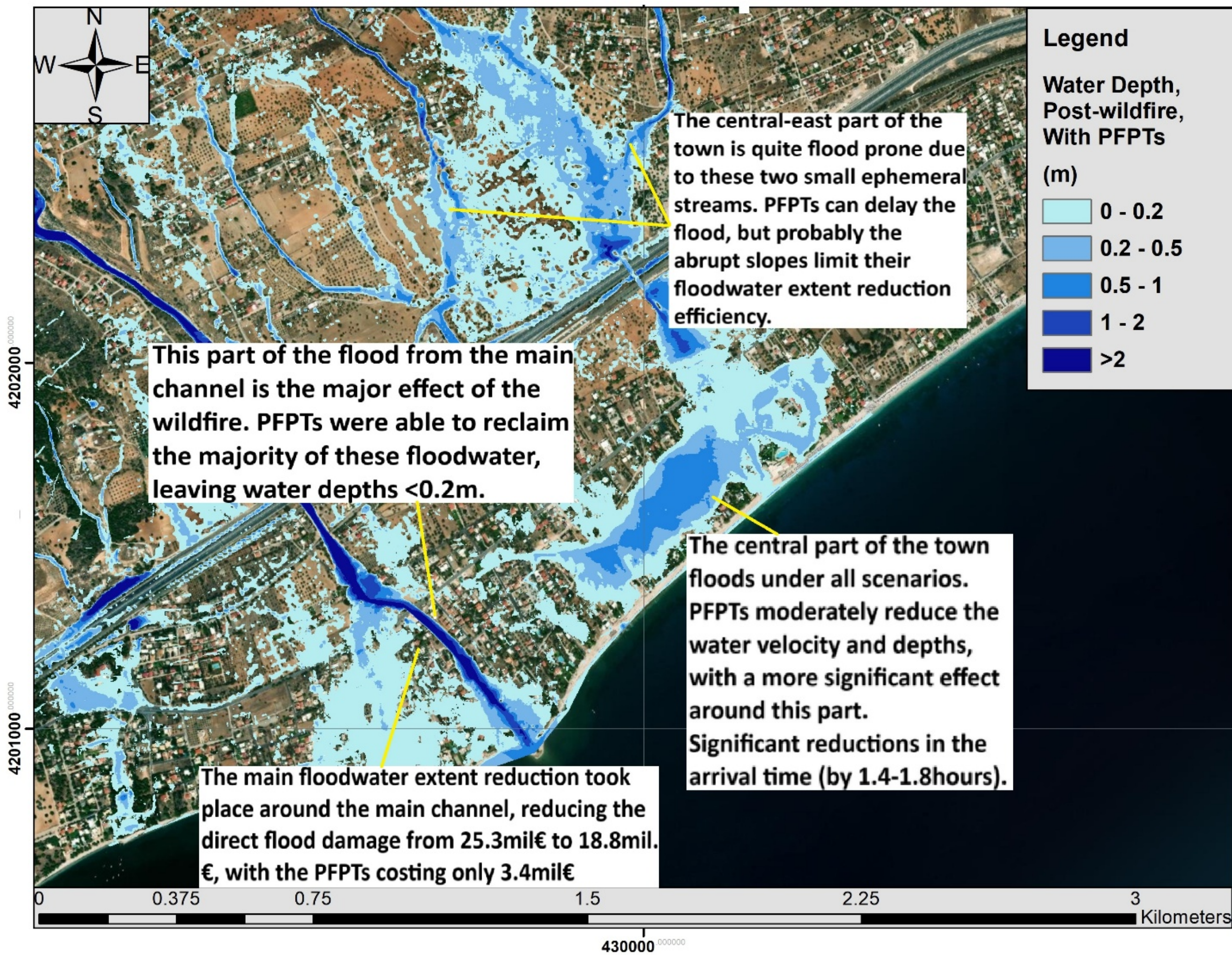

Figure 17: Summarizing the main findings on the effect of PEFTs, over the Post-fire With PEFTs scenario. Source: [175].

Overall, as Fig.17 summarizes, the PEFTs are particularly effective along the main stream, where well-established flowpaths and gentle slopes allow LEBs and WCD to intercept and attenuate floodwater over long reaches. This configuration not only reduces peak velocities but also meaningfully delays water arrival times, offering valuable lead-time for downstream communities. In contrast, PEFTs prove less efficient in the smaller Intermittent Rivers and Ephemeral Streams (IRES) in the northeast part of the catchment with steeper, more abrupt slopes. These were responsible for the majority of the flooding, indicating the need to map IRES, as they are not mapped in Greece [156], and usually not considered in flood protection plans, however, as proved, these can cause severe damages, under all scenarios. Yet even here PEFTs can substantially slow the initial flood buildup, providing critical flood delay in the town center.

It is worth noting that the storm of November 2019 was a severe phenomenon, that would have caused flooding under all scenarios, underscoring the vulnerability of the area, and the need of perhaps even more strict flood protection works. The PEFTs largely mitigate the wildfire's hydrological impact, rather than the flood event itself: even under pre-fire conditions, this storm was severe enough to inundate much of the floodplain. Thus, additional and more robust flood defenses remain essential for events of this magnitude.

In simpler words, for such extreme storm events that can lead to floods anyway, although the PEFTs perfectly did what they are meant to do, namely avoiding the fire-induced flooding, they are not enough alone. The additional and more robust flood defenses include [199]:

- Early Warning Systems (EWS) to predict and warn for sudden floods in advance.
- The role of intermittent rivers and streams (IRES) is crucial for dry areas. These are waterways that remain dry most of the time but flood after heavy rain. Without accurate mapping (an overlooked topic in many countries) showing where they are and how much water they can carry, it's nearly impossible to design effective flood defences.
- Infrastructure planning and land use: Measures such as moving levees further away from rivers, allowing natural floodplains to absorb overflow, or deepening riverbeds to increase their flowing capacity, along with sustainable land-use practices like reforestation and sustainable farming helping the soil absorb water and reduce runoff, are key. It's also critical to stop building on flood-prone land near rivers, a practice still common in Greece.
- Drainage and irrigation upgrades are other crucial interventions. Maintaining and modernizing dikes, canals, and irrigation systems can help regulate water flow during both droughts and floods. In Greece specifically, this means rethinking how we design flood, drainage, and even road infrastructure. Simply rebuilding what existed before a flood isn't enough, as those older designs were based on rainfall patterns from decades ago, which no longer apply, as climate changes and we have to adapt to more extreme rainfalls. That's why we keep seeing repeated failures in the same places.
- Nature-Based Solutions (NBS) can also help in sustainable ways with multiple co-benefits [200,201]. These include smaller-scale, 'smart' projects like restoring riverbanks and floodplains, reconnecting rivers to their natural flood zones, and planting vegetation to slow down runoff. Removing manmade barriers that disrupt river flow, creating wetlands to reduce peak water flow, and using urban sustainable drainage systems (SuDS).

<u>3) Economic assessment</u>

The cost of the PEFTs, the direct flood damage cost, and ultimately their comparison, were insightful for the cost-effectiveness of protection investments. The cost of the examined PEFTs resulted to €3.45mill, while the direct flood damage cost was estimated to €25.2mill (around 7.5 times higher). This indicates a considerable difference, with the cost of the measures aiming at the flood damage mitigation (PEFTs) being just 13.7% of (only) the direct flood damage costs. This is a 'lesson in preparedness', highlighting that investing in mitigation works can help reduce much larger hazard-induced damages.

At this point, the limitations should be mentioned. Due to unavailable data, we did not consider certain components of the flood damage cost – in particular, those beyond the direct costs: The economic impact of business interruption caused by the flood (this includes lost revenue, additional expenses incurred due to downtime, and potential long-term impacts on business operations) has not been considered. Moreover, the health impacts of the flood, including medical expenses, emergency response costs, and potential long-term health effects were not taken into account in the flood damage cost estimations. Other environmental damages such as pollution, habitat destruction, and cleanup costs, were not considered. Finally, the community and social costs were also ignored (including displacement of residents, loss of community services, and psychological effects).

So, our flood damage cost estimates are quite conservative (just the direct costs), and in reality, they are way higher – significantly more than five times the investment in post-fire flood protection. Moreover, the flood damage estimation was primarily based on the flooded area. In the protection scenario (Post-fire, With PEFTs), we observed that even if there was floodwater in some parts, the depth was lower than 20-10cm, and the velocity was also negligible, indicating that in reality the damage cost might have been less than €18.9mill. At the same time, the PEFT measures proposed for the case of Kineta are also conservative (i.e., a dense network of LEBs and wooden check-dams was proposed), but other approaches might consider less PEFTs, significantly lowering their costs. Having a 'low-end' estimate of flood damage cost, and a 'high-end' estimate of the PEFTs' costs, and still proving their significant difference, highlights even more the fact that 'precaution' seems to be a wiser decision than 'cure'.

PART B: The governance problem and a transformative roadmap for stakeholders

1 The governance problem

There is inertia in the adoption and implementation of PEFTs by local actors responsible for managing natural hazards and disaster risks [202,203]. The response of local governance and the necessary behavioural changes to adapt to combined hazards often lag, resulting in numerous instances of inadequate flood protection. Integrating modelling insights with local governance and stakeholder perspectives poses significant challenges, necessitating multidisciplinary and transdisciplinary approaches [204,205]. These approaches require qualitative, discursive methods intended to understand complex factors, such as values, psychology, norms, and regulations, that influence human responses to new and highly uncertain risks, that are driven by climate change [206].

It is vital to account for the decision contexts (defined by the interconnected systems of values, rules, and knowledge) into which scientific information must be integrated for it to be credible, legitimate, and relevant in policy and planning processes. Addressing the knowledge-to-policy gaps by combining improved quantitative and qualitative tools is crucial for creating resilient societies [207].

2 Lessons and knowledge transfer potential from Australia

The need to bring such model-driven insights into policies implementing PEFTs, led us to augment the modelling approach with a governance framework followed in Australia, which has many similar hazard and governance characteristics to those of Greece [208]. Greece and Australia were selected because they have similar conditions of local governance-led flood protection approaches and projections of increasing wildfire and flood hazards under climate change [209,210].

Similar to Greece, many fire-prone regions of Australia have been experiencing increasing wildfire threats due to climate change. Many of these regions also have Mediterranean climates characterized by hot, dry summers and mild, wet winters [211]. These conditions, coupled with dense vegetation and rugged terrain, create an environment highly susceptible to wildfires – which are called bushfires in Australia – during the dry season and flash-floods during the wet season [212].

The frequency, extent and intensity of mega-fires across Australia have increased in recent decades due to climate change. The most recent of these occurred between November and February 2019/20 in southeast Australia, where more than 23% of temperate forests in the region were burned [213]. In mid-February 2020, a severe rainstorm occurred in the region, which combined with the absence of vegetation cover due to years of drought and the widespread wildfires, led to severe flooding, landslips and landslides across the southeast coast. The post-fire floods significantly impacted residential and commercial properties in New South Wales (NSW), resulting in over 98,000 insurance claims and an estimated insured loss of about $1.67 billion [214].

Because of these similarities in the climate, topography, vegetation and natural hazard behaviours, we draw upon Australian wildfire-flooding experiences to inform lessons for Greek policymakers on the importance of timely and proactive flood mitigation measures.

Additionally, both countries have similar governance approaches making comparisons of lessons useful for enhancing practice in each country. In Greece, the Ministry of Environment provides at the national level generic guidelines for hazard protection, and the Regions are responsible for implementing such plans. In Australia, the governance arrangements involve the Federal Government establishing the overall strategic policy environment and providing funding support for pre- and post-disaster activities, which include emergency management, disaster recovery, and strategic disaster risk reduction. The State and Local governments are responsible for local land-use planning, approving development applications, disaster management, and the supply of local services (e.g., water, sewage, local roads, etc.). In both countries, local authorities (i.e., municipality-level), individually or in groups, are the first to take the initiative to design and implement PEFTs.

3 The governance framework

Integrating the proposed modelling approach and the insights about flood risks and PEFTs into relevant decision-making processes is challenging and has not occurred in the case study of Kineta. Increasing awareness and use of this modelling approach and outputs requires understanding the formal and informal rules governing how decisions are made, the values, preferences, interests and priorities of relevant decision-makers, and the knowledge bases that these decision-makers consider to be credible and legitimate. A deeper understanding of these three dimensions – values, rules and knowledge – and their interactions, has been repeatedly shown in a range of context to be effective at revealing strategies for how these can be 'shifted' to accommodate new knowledge (e.g., about novel risks and interventions) or value priorities. This perspective on decision contexts is the values-rules-knowledge (VRK) perspective/model and is applied to the Kineta case study to reveal leverage points for improving the uptake and use of the modelling insights in flood risk management (Fig.18).

The VRK model of decision contexts assists in diagnosing constraints and barriers to interventions or decisions, particularly novel ones, and better prepare decision-makers for significant and uncertain changes [215]. The VRK framework emphasizes that prevailing systems of values, rules and knowledge can affect (positively or negatively) the options available to decision-makers. The effects merge over time through complex social, cultural, behavioural processes in organizations or communities. The intersection of these three factors, which is called the decision context, forms the envelope or space for a set of practical and permissible (legitimate–V, legal–R, and credible–K) decisions/interventions that can be made. When these three factors are aligned, a decision-maker is legally able to choose from a variety of options that are also viewed to be credible and legitimate amongst relevant stakeholders. However, when the societal values, rules or knowledge are misaligned, decision-makers may find themselves constrained by their decision context and forced to select from a limited array of less effective options. This includes the rejection of potentially effective novel solutions and a reliance on business-as-usual options. A fundamental assumption of this model is that shifts in decision-making can only arise after modifications in values, rules, and knowledge occur at the organizational, community or societal levels.

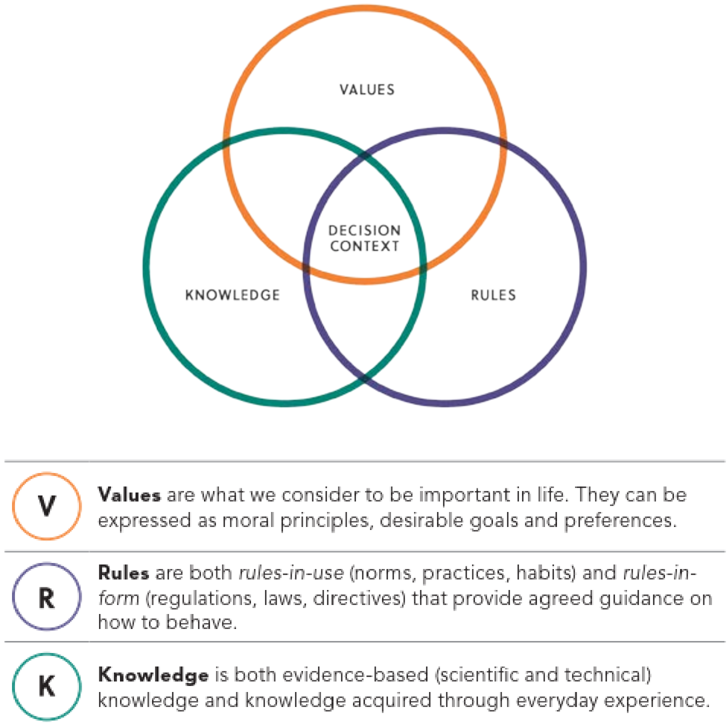

Figure 18: Illustration of decision contexts as the intersection of the societal systems of values, rules and knowledge (VRK). Adapted from [208,215]

The entailments of this approach for situations of emerging risks such as post-fire flooding, where novel solutions need to be adopted (e.g, PEFTs), are [208,216]:

i) the application of the VRK model as a diagnostic tool to identify the main V, R, or K barriers and to indicate leverage points that overcome these barriers and

ii) the need for proactive inclusive engagement with stakeholders that supports the deliberative co-production of knowledge about risks and adaptive learning about the effectiveness of novel responses.

We use the VRK model in this study as a lens on the local decision contexts in Kineta to help diagnose the constraints (and opportunities) leading to the inaction and to reveal transferable insights and lessons that can encourage and support similar changes and initiatives in other areas of Greece [206,217].

4 Bridging the knowledge and implementation gaps: Targeted points for stakeholder workshops

The total cost of applying the suggested PEFTs in Kineta has been estimated at €3.45 million (2023 values), as analyzed in Part A. The direct flood damage cost was found around €25.2 million (2023 values) - for the flood damages to assets and infrastructure only. This means that the suggested preventive costs for the flood mitigation measures could amount to only 1/7 of the post-flood damages.

In retrospect, insufficient PEFTs have been installed after the wildfire to intercept possible forthcoming flood events. Also, no compensation has been granted from the government to the regional authorities for the flood-affected communities [218].

At the end of 2024, after extended protests, the case was brought to court, with the primary defendant being the Former Regional Governor of Attica [219]. This situation demonstrates a perverse outcome whereby the government has avoided both the cost of risk protection and post-disaster compensation, transferring these risks and costs to the impacted communities and businesses. This has happened in other Greek cases suffering from catastrophic flood damages due to insufficient protection, e.g. the region of Thessaly in Central Greece in September 2023, where the Former Regional Governor was found guilty and convicted [220].

In our case, we followed the VRK framework's principles to identify the governance gaps in Kineta. After informal communications with local authorities, we identified certain gaps in V(alues), R(ules) and K(nowledge) that can help explain the limited awareness and adoption of sufficient flood mitigation measures, as presented in Table 7.

Table 7: Factors limiting the VRK decision context for the Kineta case, which should be targeted in stakeholder engagement processes [208].

Factors reducing the VRK intersection spaces and hence constraining the decision context	Intersection space limited
Policymakers set low priorities (R & V) for PEFTs because they feel that they are unlikely to be widely publicised ("the media come for the disasters, but afterwards they don't care").	Values & Rules (VR)
Policymakers set low priorities (V) for PEFTs because their effectiveness will not be immediately evident (K) after implementation but after the first storms. In contrast, policymakers tend to prioritize (V) measures that have immediate results (K), to build their legacy quickly through advertising.	Values & Knowledge (VK)
Existing regulations (R) continue to require that flood-damaged infrastructure be restored to pre-disaster standards (R), which are generally based on outdated storm data (K) (+50 years ago) that no longer reflect the current and future (changing) climate (K).	Rules & Knowledge (RK)
The funding, staffing and training levels (V & K) of those responsible remain insufficient to support effective mitigation of the growing magnitude and frequency of the hazard risks.	Rules & Values (RK)
Unclear roles and responsibilities (i.e., accountability) (R) and siloed communications within and across organisations lead to uncoordinated decisions and inaction, particularly in diverse areas with uneven disaster impacts (V) and complex property rights (R & V). This is also often used as an excuse by local authorities that are responsible for implementing flood protection measures but feel unsure how to act.	Rules & Values (VR)
Although there are regulations (R) and national plans (R) for hazard mitigation and adaptation in place, there is little available information or assessments on the suitability and cost-effectiveness of PEFTs (K). This is especially the case in specific instances requiring novel PEFTs that are more effective at mitigating the changed hazard risk profiles. This knowledge gap (K) leads to generic regulations (R) around risk mitigation and leads to poor/limited implementation.	Knowledge & Rules (KR)
The widespread lack of awareness (K) about post-fire effects on the hydrological response of a burnt site to a subsequent storm or flood. The timely application of appropriate PEFTs can have many co-beneftisto flood protection (e.g. rapid recovery, reduced soil erosion, avoided damage etc.) but these are overlooked due to the lack of incentives (R) and awareness (K).	Rules & Knowledge (RK)

Local authorities continue with BAU mitigation practices (e.g., clearing the streams from sediment and rubbish) because these are associated with simple and easy implementation requirements (K) and levels of accountability (R), even though these are no longer as effective as they used to be.	Knowledge & Rules (KR)
Policymakers' ways of thinking and behaving (V, R & K) (i.e., prevailing poor or anachronistic understanding of compounding extreme hazards) have not changed to account for the "new normal" of radically different hazard behaviours under climate change (K). This is reflected in these 'extreme events' being considered exceptions and justifying BAU, which is hindering the adoption of necessary mitigation efforts.	Values, Rules & Knowledge (VRK)

It is evident that when it comes to the local stakeholders that are responsible for the implementation of protection measures, a combination of factors has been causing several issues, which can be summarized as: policymakers tend to be unaware or deprioritise PEFTs (VK); the lack of analytical depth and previous experiences with PEFTs (KR); low levels of awareness and acceptance that such extreme storm events are not exceptions but constitute the "new normal" in the context of climate change. This is sustained by a consistent lack of flood modelling insights and PEFT-design approaches or an insufficient level of detail) (KV). The above examples illustrate how prevailing interactions between 2 or more of the VRK elements of the decision context are excluding PEFTs from the set of options considered credible, legal and legitimate, as presented in Fig.18. This raises salient questions about what actions are taken, when, where and why, and helps explain the decision-making inertia around the novel PEFTs that has finally happened in the case of Kineta. This decision-making inertia is further aggravated by inadequate investment and lack of human and institutional capabilities needed to support hazard risk reduction initiatives.

Bridging the existing science-policy and knowledge-action gaps in Kineta requires participatory processes and knowledge co-production, including the adaptive development and testing of the simulation modelling approach that draws upon stakeholders' experiential knowledge and enhances their understanding and awareness.

The engagement process also needs to target the specific factors listed in Table 7 in ways which increase the overlaps between V, R and K through shifting prevailing and predominant paradigms, norms, practices, perceptions, and policies so these better account for the new and emerging dimensions of post-fire flood risks and PEFTs.

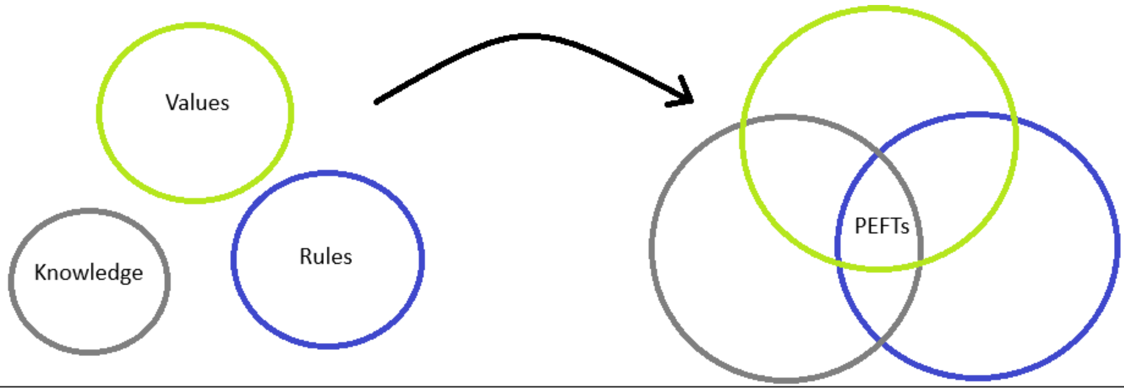

Values - low priority for PEFTs	Potential argumentation on the benefits and the policy co-benefits (e.g. protection, small and easy local scale works of low cost, creation of local jobs, etc.
Rules - lack of accountability & poor integration of PEFTs in the regulations	Potential argumentation on enhancement of communication skills, clarification of the governance processes, and use of tools like the modelling framework, or previous applications for the design of PEFTs.
Knowledge - awareness for combined hazards	Use of modelling tools, such as the one presented, to raise awareness on the interactions among wildfires - extreme storms - floods - protection works

Figure 19: An illustration of the values-rules-knowledge perspective on the decision context of those responsible for flood risk management in Kineta. The separation of the systems of v, r, and k on the left-hand side illustrates the prevailing situation where PEFTs are not seen by decision-makers to be credible or legitimate and policies don't exist to prioritise their adoption. The overlapping v, r and k on the right-hand side illustrates the situation where the simulation modelling insights about flood risks and suggested PEFTs for the Kineta case study are being effectively considered in policies and inform investment priorities.Source: [208].

The combined use of the modelling insights and the VRK application can assist decision-makers in recognising the need to focus on certain actions required to alter the boundaries of their decision context (i.e., increase the VRK overlap) to achieve the necessary adaptations (in this case, the PEFTs) for coping more effectively with the changed hazard risk profile (Fig.19).

As indicated above, there are several notable examples demonstrating the application of the VRK model with a range of government and non-government stakeholders in Australia and globally [215,221–223]. We believe that it is likely that Greece can also adopt such approaches and utilize combined modelling-governance insights in stakeholder participatory approaches. Recently, in Greece, the municipal authorities of the second largest city and its metropolitan area – Thessaloniki (1.1 million) - have made significant efforts to engage citizens in disaster risk reduction and resilience planning in the region.

However, more coordinated policies must be established by local, state, and national governments, as well as the private sector, focusing on redirecting funding mechanisms towards resilience planning, informed by deeper understanding of the VRK dynamics of the decision-making contexts of relevant stakeholders. We hope that the proposed approach combining modelling and VRK-based insights will be a useful roadmap for such future science-to-policy assessments.

6 Building capacity

At this stage, the insights of the modelling framework (representation of flood event and proposed protection measures), were used as inputs to a capacity building exercise, aiming to trigger a discussion that will identify the necessary behavioral changes for flood protection enhancement. In particular, the design of this transitional process was based on the Systems Innovation Approach (SIA) [224,225].

The SIA is a process designed for capacity building/ behavioral transition exercises (living labs), and consists of the following main steps:

a) Selection of the stakeholder group, and their assignment.

b) Analysis of the problem.

c) Analysis of existing solutions, with their strengths and weaknesses.

d) Identification of tipping points to apply solutions, or create new solutions. e) Stakeholder collaboration for solutions implementation.

For steps (a)-(c), the inputs of the modelling framework, and the broader scientific literature on the topic, are integral parts.

Steps (d) and (e) are in essence an analysis of both technical and policy gaps in order to use them as goals for the necessary capacity development, through solutions development.

The capacity development plan, using SIA's steps (Table 8) can largely use the modelling framework's results (steps a-c) to identify the stakeholders, analyze the problem, and the technical solutions. However, the focus of such a process would be on a broader behavioral change (step d).

First, it is crucial to understand that such extreme events (including combined fire-flood hazards) are not an exception, but the "new normal". There are several examples in Greece over the past four years, justifying this argument. A coordinated science-to-policy two-way informational process is key to build resilience in a socially acceptable way, maximizing the locals' welfare, that can be supported from existing funds and local assets (humans and raw materials).

Table 8. Designing a capacity development exercise for flood protection, according to the SIA [226].

Step:	Goal/ Expected Outcome
a) Selection of the stakeholder group	Representatives from central and regional government, scientists, experts on floods, and experienced professionals on protection works, citizen scientists.
b) Analysis of the problem	Climate change, wildfires and impacts on catchments, extreme storms and flood risks. Inadequate infrastructure and (post-fire) flood protection action and basic design of flood protection works based on outdated data that cannot cope with future's climate. Unclear responsibility and accountability for remote areas.

	Issues identified in Table 7 (based on the VRK framework) should be core targets for behavioural change.
c) Analysis of existing solutions	Analysis of post-fire flood protection techniques, and implementation processes (logistics, economics, regulations). Solutions such as PEFTs should be suggested as counter-arguments to the obstacles of Table 7.
d) Identify/ design solutions	Behavioural changes (understand severity and frequency, and necessity to act). Non-protection risks vs protection benefits narrative (drawing insights from the techno-economic analysis of Part A). Building technical expertise. Collaboration/ coordination to apply proposed post-fire cleaning and flood protection works (drawing insights from the techno-economic analysis of Part A). Emphasis on local stakeholders, using available regional funds, and proactive action.
e) Solutions implementation	Boosting local economy with the application of the proposed measures from local timber and workers. Coordinative action and responsibilities sharing after wildfires, including installation and maintenance. Again, drawing motivation from the promising performance of the PEFTs analyzed in Part A.
f) Dissemination	An important element at this stage is the dissemination and publicity of such efforts. Since policymakers give particular weight to the public perception of their low-cost and highly effective actions in the short-term, this effort should be communicated as such. The journalistic narrative should stress the immediate / short-term benefits of PEFTs as restoration and resilience actions.

Indeed, capacity development has been seen as a key component of the implementation of Sustainable Development Goal (SDG) 6, as highlighted in the SDG 6 Global Acceleration Framework as one of the key accelerators [227,228].

In this exercise we are referring to the ability of the government, organizations, and society as a whole, to manage combined extremes successfully. In this regard, major changes needed are the following:

a. Appropriate institutional arrangements should support the “new normal” of frequent wildfires and flooding

b. The central and regional government should be acquiring the knowledge to understand the new updated data and tools used to identify the problem and provide possible solutions and protection measures and improve its operational capacity to effectively respond in time or even better proactively.

c. Behavioral change is important to empower society to adapt to the “new normal” conditions taking into consideration local context and specifications, especially in vulnerable remote areas.

d. Proper communication and argumentation on the cost-effectiveness and multiple benefits of PEFTs protection.

PART C: Towards generalization at the national scale

The approach presented so far was based on the representation of an existing storm event (Girionis). However, the usual flood protection design is based on standards, namely design storms. Design storms are essential tools in engineering hydrology, guiding the design of stormwater infrastructure, flood control systems, and erosion protection. Manually generating them for each project is time-consuming and limits large-scale analysis and generalization of flood protection interventions.

To address this, we developed Catchment2Storm by Alamanos and Papaioannou [229], a Python-based tool that generates design storm hyetographs from watershed shapefiles using the official Greek gridded IDF parameters provided by the Ministry of Environment [230]. The tool overlays a user-defined catchment shapefile onto the national IDF grid, calculates area-weighted IDF parameters for each intersected sub-area, and synthesizes a complete hyetograph. The storm is reduced spatially using the Area-Reduction-Coefficient ϕ (Phi) and is temporally rearranged using the Alternating Block Method (ABM), resulting in a realistic design storm profile. The Catchment2Storm can provide a ready-to-use hyetograph for any user-specified return period, storm duration, and time interval. The output includes a plot, Excel step-by-step summaries, and rainfall input tables (either depth-based or intensity-based) formatted for direct use for HEC-HMS and HEC-RAS. This tool enables engineers and hydrologists to rapidly develop site-specific design storms from spatial inputs, ensuring compatibility with national standards and model-ready outputs.

Applied nationally to approx. 11,000 sub-catchments, we produced a comprehensive inventory across Greece. By comparing total rainfall depth and peak intensities under different return period scenarios, we reveal variations across urban centers, port cities, and agricultural zones. The findings indicate the need for localized urban drainage sizing, port stormwater resilience planning, and site-specific agricultural runoff control, rather than uniform national design standards.

1 The Catchment2Storm tool

The Catchment2Storm tool follows a structured geospatial-hydrologic workflow to generate customized design storm hyetographs. First, it loads the user-defined catchment shapefile and the national Greek IDF parameter grid ("ombrian parameters"), which is publicly available from the Greek Ministry of Environment [230].

First, it ensures that both shapefiles share a common coordinate reference system (so the catchment overlays the Greek IDF grid). This spatial overlay identifies which IDF grid cells intersect the user's catchment (Fig.20).

For each intersected polygon (sub-catchment), the script calculates its area and relative contribution to the total catchment, extracting the corresponding IDF parameters (α, η, ξ, λ, β). If any portion of the catchment lies outside the IDF grid, the nearest valid IDF cell is assigned.

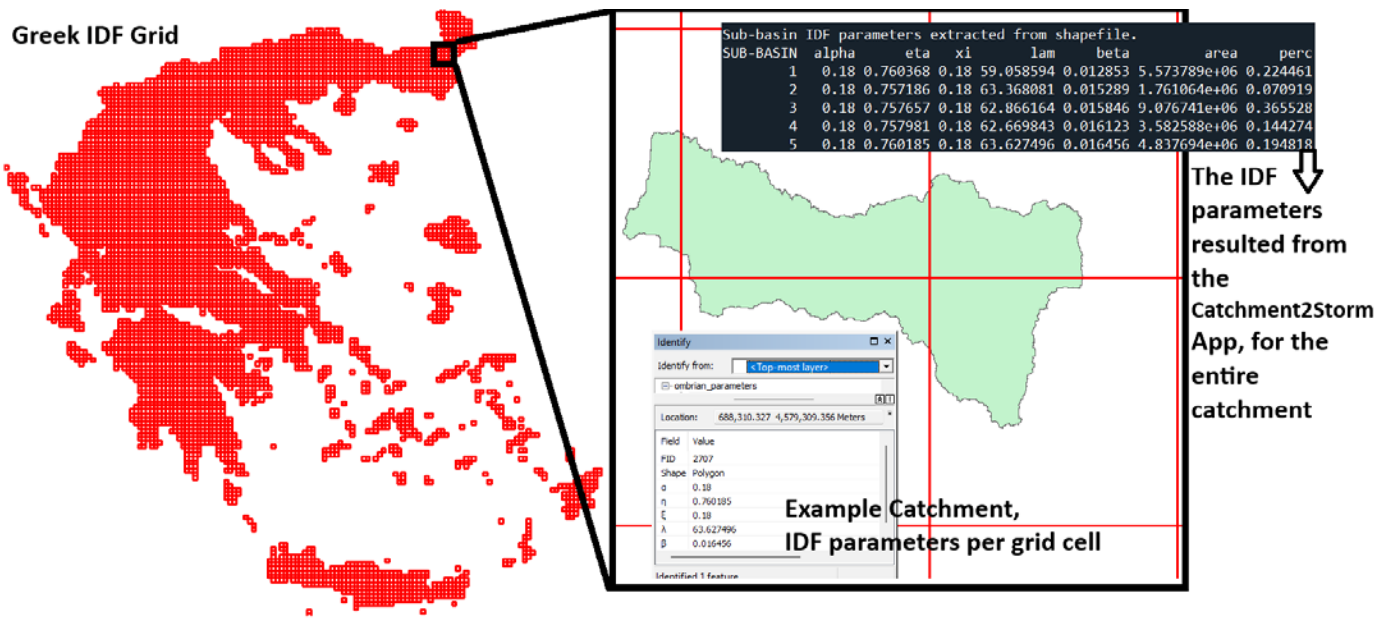

Figure 20: An example catchment, overlaying with the official Greek IDF Grid, where each cell has its own set of IDF parameters. The users do not have to open any spatial files, like in this figure. Instead, they can just load their catchment's shapefile in the Catchment2Storm App. They will get (as a first output) the (black) set of IDF parameters for their catchment. Source: [229].

The script then computes intensity (i) and precipitation depth (P) for each sub-area over the storm duration using the generalized IDF Equation 5.

The user defines the desirable return period (T), duration (D), and the time interval (t), so k is estimated as the time step {t, t+1, …, D}.

Area-weighted (based on each sub-catchment's area shares) intensities and depths are aggregated across sub-catchments for each time step.

To account for spatial variability, the area reduction coefficient φ is applied based on the total catchment area and duration, using the empirical formula by Koutsoyiannis and Ksanthopoulos [231] (Eq.6).

$$i(mm/hr) = \lambda \cdot \frac{\left(\frac{T}{\beta}\right)^{\xi} - 1}{\left(1 + \frac{k}{\alpha}\right)^{\eta}} \qquad (5)$$

$$\varphi = \max\{1 - \frac{0.048 \cdot A^{0.36-0.01 lnA}}{D^{0.35}}, 0.25\} \quad (6)$$

The resulting hyetograph is temporally distributed using the Alternating Block Method (ABM) [232], producing a center-peaked design storm.

Final outputs include a plot of the hyetograph, an Excel summary, and CSV tables formatted for direct use in HEC-HMS and HEC-RAS hydrologic and hydraulic models (Fig.21).

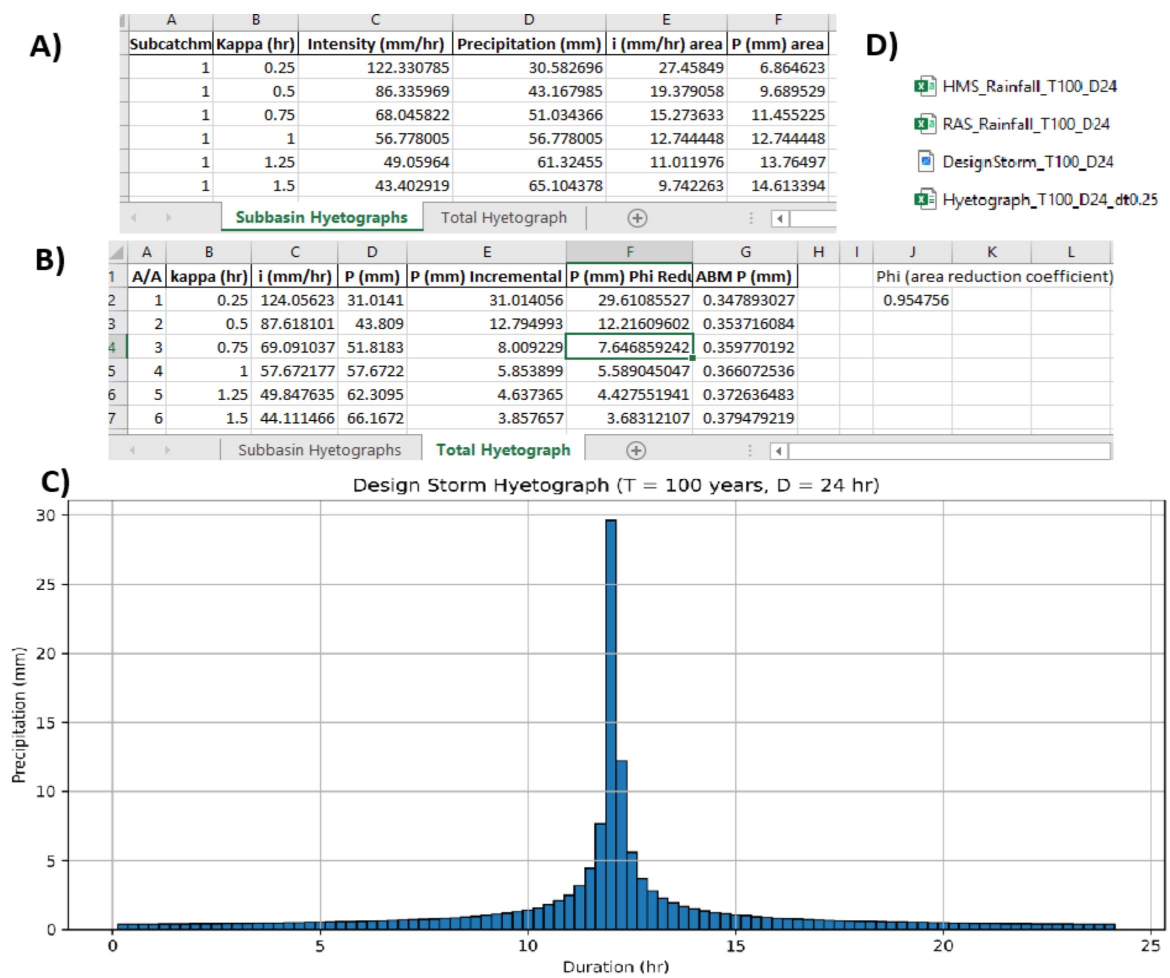

A)

Subcatchm	Kappa (hr)	Intensity (mm/hr)	Precipitation (mm)	i (mm/hr) area	P (mm) area
1	0.25	122.330785	30.582696	27.45849	6.864623
1	0.5	86.335969	43.167985	19.379058	9.689529
1	0.75	68.045822	51.034366	15.273633	11.455225
1	1	56.778005	56.778005	12.744448	12.744448
1	1.25	49.05964	61.32455	11.011976	13.76497
1	1.5	43.402919	65.104378	9.742263	14.613394

B)

A/A	kappa (hr)	i (mm/hr)	P (mm)	P (mm) Incremental	P (mm) Phi Redu	ABM P (mm)	Phi (area reduction coefficient)
1	0.25	124.05623	31.0141	31.014056	29.61085527	0.347893027	0.954756
2	0.5	87.618101	43.809	12.794993	12.21609602	0.353716084	
3	0.75	69.091037	51.8183	8.009229	7.646859242	0.359770192	
4	1	57.672177	57.6722	5.853899	5.589045047	0.366072536	
5	1.25	49.847635	62.3095	4.637365	4.427551941	0.372636483	
6	1.5	44.111466	66.1672	3.857657	3.68312107	0.379479219	

Figure 21: An Catchment2Storm detailed result reports: (A) per sub-catchment; B) for the entire catchment. C) The design storm plot. D) the resulted created files, with the additional ready-to-input HEC-HMS and HEC-RAS files. Source: [229].

The developed Catchment2Storm tool has been developed in Python, and we are considering its commercial use. It streamlines the traditionally complex and often manual process of generating design storms by automating geospatial analysis and storm synthesis directly from national IDF data. Thus, it enables engineers to produce accurate, model-ready hyetographs in seconds, ensuring consistency with official standards.

2 Applying the Catchment2Storm tool in Greece: A national-scale IDF-based design storm hyetograph inventory

We showcase how this tool can be also used for multiple catchments: We have applied the Catchment2Storm tool to all Greek sub-catchments, as provided by the Ministry of Environment (N=10,773), using a batch-run approach in Python, which also summarized key metrics for different hyetographs (Fig.22).

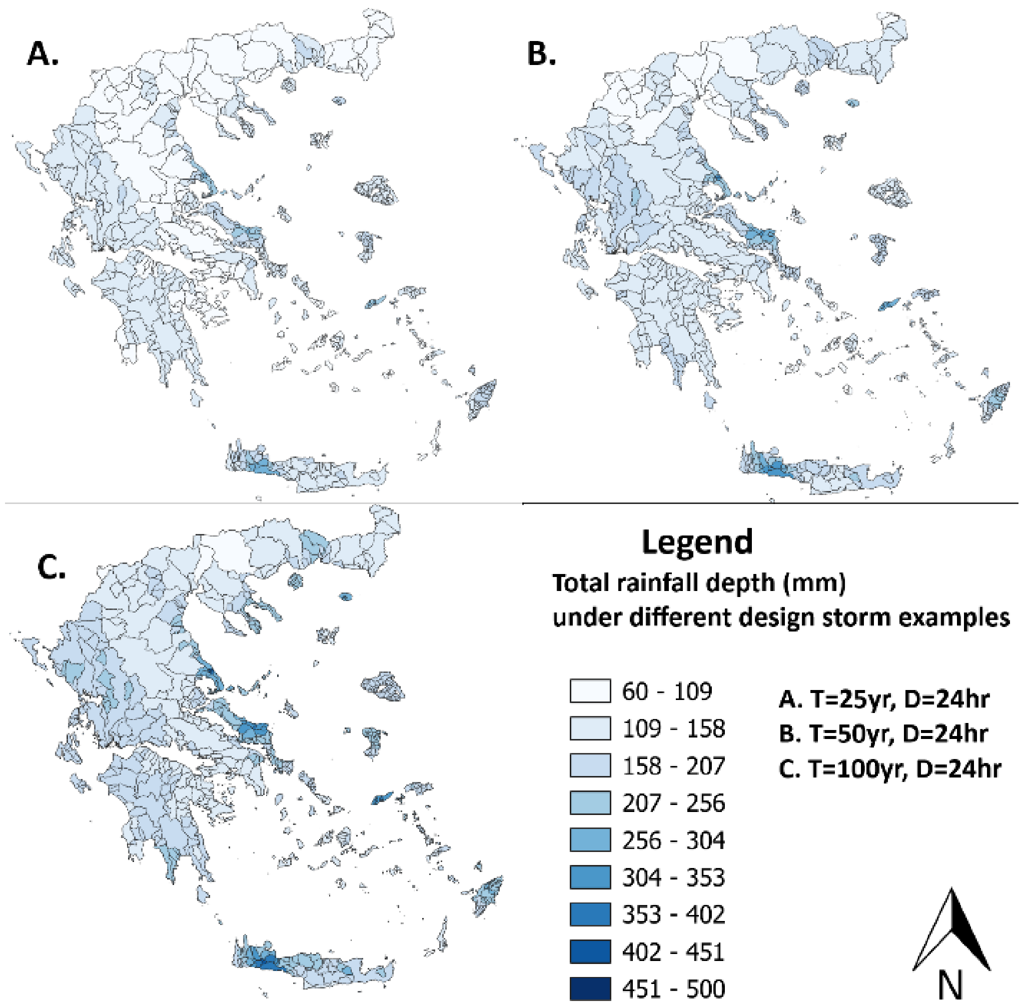

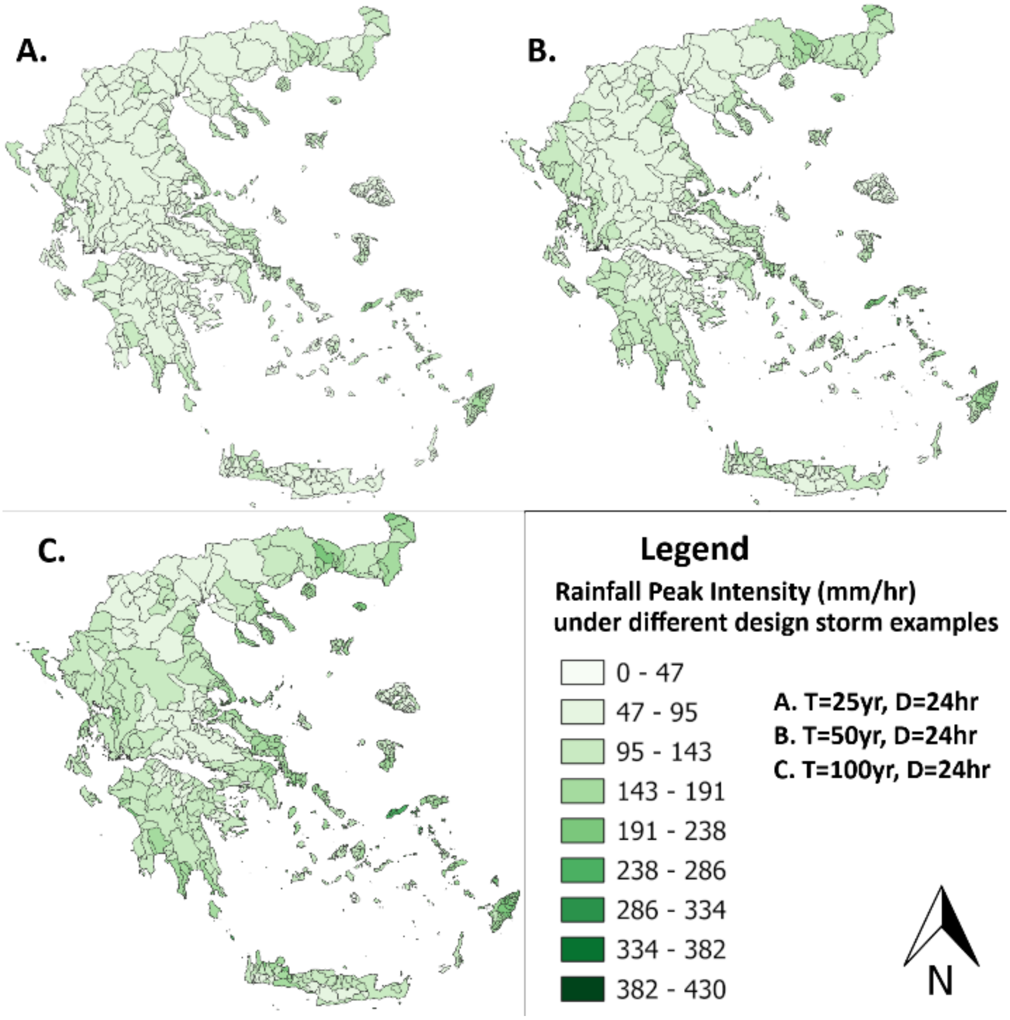

Figure 22: Indicative summary metrics of the design storms produced at the national scale. Upper: Total rainfall depth (sum of the design storm precipitation). Lower: Rainfall peak intensity (max intensity of the design storms). Source: [229,233].

Text Box 11:

Availability of data and code:
The developed Catchment2Storm tool has been developed in Python, and we are considering its commercial use.
All materials are stored in a private Github repository (https://github.com/Alamanos11/Catchment2Storm), including step-by-step guidance on running the Catchment2Storm tool, also for multiple catchments, summarizing key metrics of the results, and mapping them in QGIS, even in the case of missing values

See screenshot below:

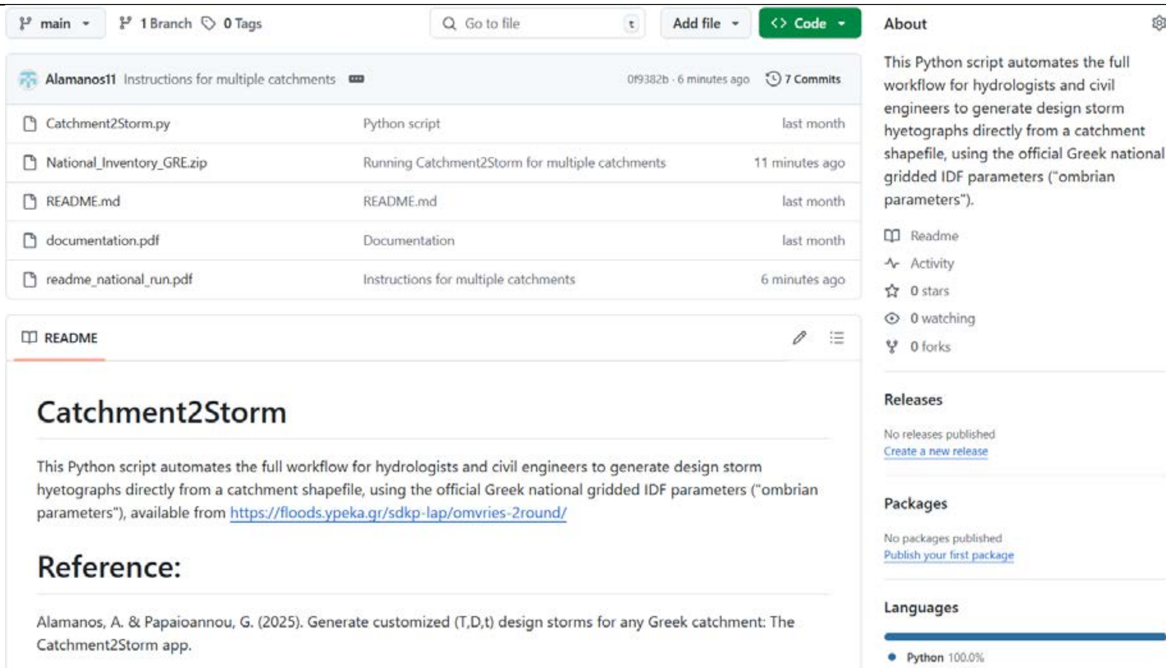

The presented tool streamlines the traditionally complex and often manual process of generating design storms by automating geospatial analysis and storm synthesis directly from national IDF data, at any catchment or scale. Thus, it enables engineers to produce accurate, model-ready hyetographs in seconds, ensuring consistency with official standards.

Applied nationally to approx. 11,000 sub-catchments, we produced a comprehensive inventory across Greece.

Results for specified catchments can be made available upon reasonable request to the authors.

3 Need for localized design approaches

Moreover, we compared total rainfall depth and peak intensities under different return period scenarios, for certain critical zones in Greece: urban centers, port cities, and agricultural zones [234]. The findings indicate variations that justify the need for localized urban drainage sizing, port stormwater resilience planning, and site-specific agricultural runoff control, rather than uniform national design standards.
In particular:

A. Major Cities / Urban Centers

Cities compared: Athens, Thessaloniki, Patras, Heraklion, Volos, Larissa

- Athens: Lies in Attica — moderate rainfall depths (~200–256 mm range).

- Thessaloniki: In Central Macedonia — shows lower depths, ~158–207 mm.
- Patras: West Greece — appears in a darker shade, ~256–304+ mm.
- Heraklion (Crete): Hotspot in T=100yr map (>353 mm).
- Volos/Larissa: Inland Thessaly — moderate-to-high (~256–304 mm).

Finding:
Greek urban centers are exposed to markedly different design storm magnitudes, suggesting that a single national standard storm (e.g., 100 mm in 24h) would under-design for Heraklion or Patras and overdesign for Thessaloniki. This supports the argument for regionally customized urban drainage design standards. While this happens by considering local design storms with return periods according to the project type guidelines, the storm durations might play a role. The Catchment2Storm tool, allows the easy consideration of several design storms for the analysts to test.

B. Major Ports

Ports compared: Piraeus, Thessaloniki, Patras, Heraklion, Alexandroupoli, Kavala, Igoumenitsa

- Piraeus: Same as Athens — mid-range.
- Thessaloniki: Low storm depth.
- Heraklion / Patras / Alexandroupoli: High — 304–451 mm zone.
- Igoumenitsa / Kavala: Also fall in elevated zones in NW and NE Greece.

Finding:

Coastal port cities in different basins face radically different design rainfall, despite similar sea-level settings. For port drainage, stormwater storage, and critical asset protection (e.g., container yards), regional IDF derivation is essential, not optional.

This could motivate a national Port Resilience Framework based on localized design storms.

C. Main Agricultural Areas

Sites compared: Thessaly Plain (Larissa, Karditsa), Central Macedonia, Evros, Argolis, Boeotia, Crete's Messara plain

- Thessaly & Central Macedonia: Moderate depths — 207–304 mm range
- Evros / NE Thrace: 158–207 mm — relatively low
- Crete (Messara): 353–402 mm — significantly high
- Peloponnese valleys: Mixed — some moderately high

Finding:
Agricultural catchments show less consistent patterns, meaning irrigation and drainage infrastructure design (e.g., field ditches, farm ponds, culverts) need local calibration. This spatial disparity argues

against a “one-size-fits-all” rural drainage policy. Also, Peak Intensities drive soil erosion and runoff loss. High-intensity storms in Crete and Western Peloponnese support erosion-focused water management in those basins.

The findings overall show that even under equal exposure assumptions (same T, D), different catchments reveal nonlinear hydrologic responses, suggesting spatial risk inequalities. Thus. resilience strategies tied to localized extremes, not national averages. This is especially timely under climate adaptation policies.

Conclusions

The findings of this modelling study, beyond the general framework provided for the integrated analysis of similar phenomena, argue for the importance of investing in the flood resilience of burnt sites. This study showed that the PEFTs would have been able to reduce the amount of fire-induced floodwater. Of course, this does not mean that if the PEFTs have been in place after the fire the flood would have been totally avoided, as it was an extreme event. But the effects of the fire were 'cancelled'. We proved that the flood would have been mitigated, saving at least €7mill from the damage. Again, this estimate is quite conservative, as explained in the discussion section; therefore, we believe that the investment in preparedness is definitely worthwhile.

The take-away message here is that after wildfires, PEFTs are absolutely necessary, and should be seen as a money-saving decision, relatively cheap, which can be achieved in local scales (e.g. at municipality scale), with local means.

Beyond that, the need to further mitigate flood hazards is evident. This means: designing based on past extremes, updated design storms, and considering enhanced protection measures, additionally to PEFTs.

An insight from this research is the need to map the Intermittent Rivers and Ephemeral Streams (IRES). In the case of Kineta, those were the ones that contributed most to the flood, so it is necessary to map them and consider enhanced protection measures.

A follow-up question from this research is why these protection measures are not applied? One explanation could be the lack of knowledge of the decision-makers, combined with the lack of communication (and perhaps trust) with those who have the knowledge [192, 193]. Following the wildfires in Kineta, Greek newspapers argued that a significant investment in preventive measures is necessary to address future flood risks, noting that even after the flood, there was still no protection work in place [236]. Often, flood damage compensation is not being paid in Greece, and restoration works are being significantly delayed. This also occurred in Kineta, where the latest reports on the case indicate that the compensation for the affected households was still pending [218]. Therefore, if there is a tendency to dismiss flood damage compensation, then the application of PEFTs seems indeed like an unnecessary and undesirable expense. As mentioned, at the end of 2024, after extended protests, the case of Kineta was brought to court, as no PEFTs were in place, nor compensations were granted. The primary defendant is the Former Regional Governor of Attica, and the case is underway [219].

The need to consider stakeholder engagement processes is recognized long ago. The Australian experiences of consultation with local and state governments, informed by the values-rules-knowledge model of decision contexts, have led to the collaborative development of comprehensive risk assessments, adaptation plans, and investment strategies. The application of the VRK framework shows a way to find specific gaps that need to be addressed in such processes, hence we provided a targeted capacity building roadmap. Due to the inherent uncertainties associated with future disaster risks and responses, there will always be a policy-making debate on "prevention versus cure", and contestation about the problem and solutions. However, from our experience in different contexts and countries, we believe that the gaps identified (Table 7) apply for most Greek areas, and the findings and roadmaps suggested are generalizable.

Building resilience to future similar hazards requires a fundamental shift in how knowledge about problems and solutions is viewed, produced, and used. We believe that a key point here is the awareness of extreme and combined hazards as a regular situation that policymakers should seriously address, supported by model-based assessments. To effectively confront complex problems like post-fire flood risks, researchers and policy makers shall co-develop and apply tools and frameworks to generate policy-relevant and scientifically robust insights. This urgency cannot be understated due to the high and growing stakes as climate change speeds up and exposure levels continue to grow.

With respect to the national scale application and design storm inventory, the use of tools such as the Catchment2Storm is essential to facilitate fast and accurate assessments. Using multiple design storms is the first crucial step to design protection under different conditions.

The findings of the Greek-wide application indicate that national-scale IDF standards are inadequate given the spatial variability and nonlinear scaling of design storms across the country. We recommend region-specific storm design, zoning of IDF curves, and resilience strategies tailored to localized extremes, particularly critical for urban, port, and agricultural regions. More specifically, urban centers like Athens and Thessaloniki fall within moderate to low ranges, while Patras and Heraklion experience much higher storm depths, indicating that a single national standard would be inadequate. Similarly, major ports (though at similar sea levels) show substantial variation, reinforcing the need for region-specific stormwater and resilience planning. In agricultural zones, spatial variability is even more pronounced. While some areas like Thessaly and Central Macedonia show moderate depths, others like Messara in Crete face intense storms, suggesting localized design for rural drainage and erosion control is essential.

Policy Recommendations

To summarize, the main Policy Recommendations arising from this work are listed in Table 9.

Table 9. List of recommendations per target-category.

For modelling analysis:
1. The simulation of storm events, burn conditions, and flood events, as demonstrated in this report, is crucial for accurately understanding post-fire floods and designing effective protection measures. Also, connecting models such as WRF and HEC-RAS, using the realistic rain-on-grid technique is now possible, offering highly granular results. It is recommended to conduct similar analyses, even before the wet season (e.g., considering design storms), to support timely and efficient protection efforts.
2. The Catchment2Storm tool is a reliable option with nation-wide coverage in Greece, allowing the fast generation of customize design storms, and hence the consideration of several scenarios. Its use and the consideration of different return periods (T) and durations (D) is recommended.
3. The use of new AI-based tools, such as the image segmentation methodology presented, has proven to be a valuable addition to the techno-economic analyses performed. At least, they should be used for a quick picture of the extent of the affected types of properties.

For local authorities, stakeholders and on-site work and analysis:
4. Post-fire Erosion and Flood-Protection Treatments (PEFTs): It is recommended to analyze the suitability and proper installation of appropriate PEFTs, as their effectiveness is highly case-specific. This ensures that the measures are tailored to the specific conditions and requirements of each site. Of course, modelling insights are complementary.
5. Stream and Drainage Network Condition: Our findings indicate the critical importance of cleaning streams and the drainage network, especially after a wildfire and before the wet season. This intervention helps reduce the risk of floods and ensures the proper functioning of drainage systems.
6. Map Intermittent Rivers and Ephemeral Streams (IRES) and integrate them in flood protection planning. We showed that these have been mainly responsible for several events, leading to ‘surprising’ floods. Considering the proper protection level for IRES is something that is completely absent in Greece.
7. Go beyond the basic mitigation practices: Clearing the streams from sediment and rubbish because these are associated with simple and easy implementation requirements and levels of accountability, are not enough. Engage with scientists, dialogue with model-based insights and expand the protection capacity with new and targeted flood defences.
8. Investment in PEFTs: The effectiveness of PEFTs in flood mitigation and their cost-efficiency indicate that they are worthy investments, compared to the flood damages, which account for much higher expenses. Timely application of these treatments, using local-based raw resources, following the analyses presented, is highly recommended to maximize their benefits and protect vulnerable areas.
For policymakers:
9. Set higher priority for flood protection investments: First, they need to understand their importance and necessity, then apply them, and finally publicize them with the appropriate narrative to get the visibility and immediate political traction.
10. Understanding: Move beyond anachronistic perceptions of randomness of extremes (e.g. “this will not happen again in the next 100 years”). Instead, realize that compounding extreme hazards are likely to be the “new normal” due to climate change.
11. Increase the awareness about post-fire effects on the hydrological response of a burnt site to a subsequent storm or flood, to mobilize the timely application of appropriate PEFTs.
12. Increase the awareness about PEFTs and their co-benefits to flood protection (e.g. rapid recovery, reduced soil erosion, avoided damage etc.). Same for the need and benefits for several protection actions, such as: Early Warning Systems (EWS), IRES mapping and protection – buffering, infrastructure planning and land use measures, Nature-Based Solutions (NBS), etc.
13. Applying PEFTs: PEFTs should be explicitly included into National Flood and Drought Management Plans, in order to increase the level of awareness and improve the technical capacity over the updating cycles of these Plans.

14. Communicating flood protection: Widely publicize flood protection actions and force media uptake. Present and explain the role of PEFTs and flood defences as results-based actions with both short- and long-term benefits, even naming specific protected areas.
15. Regulatory commitment to re-design works: Redesign flood-damaged infrastructure and drainage works using updated storm data reflecting the current and future climate.
16. Accountability: Set clear roles, responsibilities, and regular communication channels within and across organisations to maximize coordination and flood protection actions.
17. Invest in capable people: The necessary funding, staffing and training levels of the responsible authorities and consulting scientists should all meet certain standards, which must be ensured by the legislative framework and controlled regularly.

References

1. Alamanos, A. The Global Climate Hub. *Nat Sustain* **2024**, *7*, 375–376, doi:10.1038/s41893-024-01289-8.
2. Koundouri, P.; Alamanos, A.; Sachs, J. Innovating for Sustainability: The Global Climate Hub. *Athens University of Economics and Business* **2024**.
3. Time to Recover. *Nat Sustain* **2023**, *6*, 1027–1027, doi:10.1038/s41893-023-01228-z.
4. Alamanos, A.; Koundouri, P. Emerging Challenges and the Future of Water Resources Management. *Hydrolink 2022/10. Madrid: International Association for Hydro-Environment Engineering and Research (IAHR).* **2022**, doi:: https://hdl.handle.net/20.500.11970/110818.
5. Duane, A.; Castellnou, M.; Brotons, L. Towards a Comprehensive Look at Global Drivers of Novel Extreme Wildfire Events. *Climatic Change* **2021**, *165*, 43, doi:10.1007/s10584-021-03066-4.
6. Wang, X.; Swystun, T.; Oliver, J.; Flannigan, M.D. One Extreme Fire Weather Event Determines the Extent and Frequency of Wildland Fires. *Environ. Res. Lett.* **2021**, *16*, 114031, doi:10.1088/1748-9326/ac2f64.
7. Koundouri, P.; Alamanos, A.; Dellis, K.; Landis, C.; Stratopoulou, A. Ecosystem Services into Water Resource Planning and Management. In *Oxford Research Encyclopedia of Environmental Science*; 2024 ISBN 978-0-19-938941-4.
8. Koundouri, P.; Halkos, G.; Landis, C.F.M.; Alamanos, A. Ecosystem Services Valuation for Supporting Sustainable Life below Water. *Sustainable Earth Reviews* **2023**, *6*, 19, doi:10.1186/s42055-023-00068-1.
9. Alamanos, A.; Rolston, A.; Linnane, S. *Irish Bathing Sites Closures and Stormwater Overflows: Precipitation Forecasts, Extremes Analysis, and Comparison with Climate Change Projections*; Copernicus Meetings, 2021;
10. Papagiannaki, K.; Giannaros, T.M.; Lykoudis, S.; Kotroni, V.; Lagouvardos, K. Weather-Related Thresholds for Wildfire Danger in a Mediterranean Region: The Case of Greece. *Agricultural and Forest Meteorology* **2020**, *291*, 108076, doi:10.1016/j.agrformet.2020.108076.
11. Ruffault, J.; Curt, T.; Moron, V.; Trigo, R.M.; Mouillot, F.; Koutsias, N.; Pimont, F.; Martin-StPaul, N.; Barbero, R.; Dupuy, J.-L.; et al. Increased Likelihood of Heat-Induced Large Wildfires in the Mediterranean Basin. *Sci Rep* **2020**, *10*, 13790, doi:10.1038/s41598-020-70069-z.
12. Brogan, D.J.; Nelson, P.A.; MacDonald, L.H. Spatial and Temporal Patterns of Sediment Storage and Erosion Following a Wildfire and Extreme Flood. *Earth Surface Dynamics* **2019**, *7*, 563–590, doi:10.5194/esurf-7-563-2019.
13. Hasan, M.M.; Burian, S.; Barber, M.E. Determining The Impacts Of Wildfires On Peak Flood Flows In High Mountain Watersheds. *International Journal of Environmental Impacts* **2020**, *3(2020)*, 12, doi:10.2495/EI-V3-N4-339-351.
14. Liu, M.; Wei, H.; Dong, X.; Wang, X.-C.; Zhao, B.; Zhang, Y. Integrating Land Use, Ecosystem Service, and Human Well-Being: A Systematic Review. *Sustainability* **2022**, *14*, 6926, doi:10.3390/su14116926.
15. Havel, A.; Tasdighi, A.; Arabi, M. Assessing the Hydrologic Response to Wildfires in Mountainous Regions. *Hydrology and Earth System Sciences* **2018**, *22*, 2527–2550, doi:10.5194/hess-22-2527-2018.
16. Cos, J.; Doblas-Reyes, F.; Jury, M.; Marcos, R.; Bretonnière, P.-A.; Samsó, M. The Mediterranean Climate Change Hotspot in the CMIP5 and CMIP6 Projections. *Earth System Dynamics* **2022**, *13*, 321–340, doi:10.5194/esd-13-321-2022.
17. Alamanos, A. Megadroughts and Challenges for Water Resources Management. In *Elgar Encyclopedia of Water Policy, Economics and Management*; Edward Elgar Publishing, 2024; pp. 164–167 ISBN 978-1-80220-294-6.

18. Alamanos, A.; Loukas, A.; Mylopoulos, N.; Xenarios, S.; Vasiliades, L.; Latinopoulos, D. Climate Change Effects on Agriculture in Southeast Mediterranean: The Case of Karla Watershed in Central Greece. In Proceedings of the EGU General Assembly; Geophysical Research Abstracts: Vienna, Austria, 2019; Vol. 21.
19. Yilmaz, O.S.; Akyuz, D.E.; Aksel, M.; Dikici, M.; Akgul, M.A.; Yagci, O.; Balik Sanli, F.; Aksoy, H. Evaluation of Pre- and Post-Fire Flood Risk by Analytical Hierarchy Process Method: A Case Study for the 2021 Wildfires in Bodrum, Turkey. *Landscape Ecol Eng* **2023**, *19*, 271–288, doi:10.1007/s11355-023-00545-x.
20. Jong-Levinger, A.; Banerjee, T.; Houston, D.; Sanders, B.F. Compound Post-Fire Flood Hazards Considering Infrastructure Sedimentation. *Earth's Future* **2022**, *10*, e2022EF002670, doi:10.1029/2022EF002670.
21. Alamanos, A. Exploring the Impact of Future Land Uses on Flood Risks and Ecosystem Services, With Limited Data: Coupling a Cellular Automata Markov (CAM) Model, With Hydraulic and Spatial Valuation Models. *Qeios* **2024**, doi:10.32388/JJWWBD.
22. Folador, L.; Cislaghi, A.; Vacchiano, G.; Masseroni, D. Integrating Remote and In-Situ Data to Assess the Hydrological Response of a Post-Fire Watershed. *Hydrology* **2021**, *8*, 169, doi:10.3390/hydrology8040169.
23. Ebel, B.A.; Moody, J.A. Parameter Estimation for Multiple Post-Wildfire Hydrologic Models. *Hydrological Processes* **2020**, *34*, 4049–4066, doi:10.1002/hyp.13865.
24. Wang, W.; Yang, X.; Yao, T. Evaluation of ASTER GDEM and SRTM and Their Suitability in Hydraulic Modelling of a Glacial Lake Outburst Flood in Southeast Tibet. *Hydrological Processes* **2012**, *26*, 213–225, doi:10.1002/hyp.8127.
25. Ebel, B.A.; Shephard, Z.M.; Walvoord, M.A.; Murphy, S.F.; Partridge, T.F.; Perkins, K.S. Modeling Post-Wildfire Hydrologic Response: Review and Future Directions for Applications of Physically Based Distributed Simulation. *Earth's Future* **2023**, *11*, e2022EF003038, doi:10.1029/2022EF003038.
26. Godara, N.; Bruland, O.; Alfredsen, K. Simulation of Flash Flood Peaks in a Small and Steep Catchment Using Rain-on-Grid Technique. *Journal of Flood Risk Management* **2023**, *16*, e12898, doi:10.1111/jfr3.12898.
27. Chrysovergis, P.; Chrysovergis, S.; Chrysovergis, T. An Evaluation of Post-Wildfire Erosional and Flooding Damage in Southern California. **2021**, 116–128, doi:10.1061/9780784483688.012.
28. Theochari, A.-P.; Baltas, E. Holistic Hydrological Approach to the Fire Event on August 2021 in Evia, Greece. *Euro-Mediterr J Environ Integr* **2022**, *7*, 287–298, doi:10.1007/s41207-022-00304-8.
29. Mitsopoulos, G.; Diakakis, M.; Panagiotatou, E.; Sant, V.; Bloutsos, A.; Lekkas, E.; Baltas, E.; Stamou, A.I. 'How Would an Extreme Flood Have Behaved If Flood Protection Works Were Built?' The Case of the Disastrous Flash Flood of November 2017 in Mandra, Attica, Greece. *Urban Water Journal* **2022**, *19*, 911–921, doi:10.1080/1573062X.2022.2103002.
30. Mitsopoulos, G.; Diakakis, M.; Bloutsos, A.; Lekkas, E.; Baltas, E.; Stamou, A. The Effect of Flood Protection Works on Flood Risk. *Water* **2022**, *14*, 3936, doi:10.3390/w14233936.
31. Ebel, B.A.; Martin, D.A. Meta-Analysis of Field-Saturated Hydraulic Conductivity Recovery Following Wildland Fire: Applications for Hydrologic Model Parameterization and Resilience Assessment. *Hydrological Processes* **2017**, *31*, 3682–3696, doi:10.1002/hyp.11288.
32. Alamanos, A.; Linnane, S. Systems Resilience to Floods: A Categorisation of Approaches.; May 27 2022.
33. Gibson, R.K.; Mitchell, A.; Chang, H.-C. Image Texture Analysis Enhances Classification of Fire Extent and Severity Using Sentinel 1 and 2 Satellite Imagery. *Remote Sensing* **2023**, *15*, 3512, doi:10.3390/rs15143512.

34. Gibson, R.; Danaher, T.; Hehir, W.; Collins, L. A Remote Sensing Approach to Mapping Fire Severity in South-Eastern Australia Using Sentinel 2 and Random Forest. *Remote Sensing of Environment* **2020**, *240*, 111702, doi:10.1016/j.rse.2020.111702.
35. Quintano, C.; Fernández-Manso, A.; Fernández-Manso, O. Combination of Landsat and Sentinel-2 MSI Data for Initial Assessing of Burn Severity. *International Journal of Applied Earth Observation and Geoinformation* **2018**, *64*, 221–225, doi:10.1016/j.jag.2017.09.014.
36. García-Llamas, P.; Suárez-Seoane, S.; Fernández-Guisuraga, J.M.; Fernández-García, V.; Fernández-Manso, A.; Quintano, C.; Taboada, A.; Marcos, E.; Calvo, L. Evaluation and Comparison of Landsat 8, Sentinel-2 and Deimos-1 Remote Sensing Indices for Assessing Burn Severity in Mediterranean Fire-Prone Ecosystems. *International Journal of Applied Earth Observation and Geoinformation* **2019**, *80*, 137–144, doi:10.1016/j.jag.2019.04.006.
37. Alamanos, A.; Koundouri, P. Monitoring and Mapping the Sustainable Life on Land (SDG15) Changes in Europe with Freely Available Data and Tools. In *DEOS Working Papers - 2410, Athens University of Economics and Business*; 2024.
38. Bhattacharya, B.; Mazzoleni, M.; Ugay, R. Flood Inundation Mapping of the Sparsely Gauged Large-Scale Brahmaputra Basin Using Remote Sensing Products. *Remote Sensing* **2019**, *11*, 501, doi:10.3390/rs11050501.
39. Shen, X.; Wang, D.; Mao, K.; Anagnostou, E.; Hong, Y. Inundation Extent Mapping by Synthetic Aperture Radar: A Review. *Remote Sensing* **2019**, *11*, 879, doi:10.3390/rs11070879.
40. Lin, Y.; Wang, J.; Yue, M. Equity-Based Grid Resilience: How Do We Get There? *The Electricity Journal* **2022**, *35*, 107135, doi:10.1016/j.tej.2022.107135.
41. Alamanos, A.; Linnane, S. Drought Monitoring, Precipitation Statistics, and Water Balance with Freely Available Remote Sensing Data: Examples, Advances, and Limitations. In Proceedings of the Irish National Hydrology Conference 2021; Athlone, Ireland, 2021; pp. 1–13.
42. Kabenge, M.; Elaru, J.; Wang, H.; Li, F. Characterizing Flood Hazard Risk in Data-Scarce Areas, Using a Remote Sensing and GIS-Based Flood Hazard Index. *Nat Hazards* **2017**, *89*, 1369–1387, doi:10.1007/s11069-017-3024-y.
43. Moreno, H.A.; Gourley, J.J.; Pham, T.G.; Spade, D.M. Utility of Satellite-Derived Burn Severity to Study Short- and Long-Term Effects of Wildfire on Streamflow at the Basin Scale. *Journal of Hydrology* **2020**, *580*, 124244, doi:10.1016/j.jhydrol.2019.124244.
44. Kurbanov, E.; Vorobev, O.; Lezhnin, S.; Sha, J.; Wang, J.; Li, X.; Cole, J.; Dergunov, D.; Wang, Y. Remote Sensing of Forest Burnt Area, Burn Severity, and Post-Fire Recovery: A Review. *Remote Sensing* **2022**, *14*, 4714, doi:10.3390/rs14194714.
45. Chuvieco, E.; Aguado, I.; Salas, J.; García, M.; Yebra, M.; Oliva, P. Satellite Remote Sensing Contributions to Wildland Fire Science and Management. *Curr Forestry Rep* **2020**, *6*, 81–96, doi:10.1007/s40725-020-00116-5.
46. Chawan, A.C.; Kakade, V.K.; Jadhav, J.K. Automatic Detection of Flood Using Remote Sensing Images. *Journal of Information Technology and Digital World* **2020**, *2*, 11–26.
47. Hashemi-Beni, L.; Gebrehiwot, A.A. Flood Extent Mapping: An Integrated Method Using Deep Learning and Region Growing Using UAV Optical Data. *IEEE Journal of Selected Topics in Applied Earth Observations and Remote Sensing* **2021**, *14*, 2127–2135, doi:10.1109/JSTARS.2021.3051873.
48. Hamidi, E.; Peter, B.G.; Muñoz, D.F.; Moftakhari, H.; Moradkhani, H. Fast Flood Extent Monitoring With SAR Change Detection Using Google Earth Engine. *IEEE Transactions on Geoscience and Remote Sensing* **2023**, *61*, 1–19, doi:10.1109/TGRS.2023.3240097.
49. Skamarock, C.; Klemp, B.; Dudhia, J.; Gill, O.; Liu, Z.; Berner, J.; Wang, W.; Powers, G.; Duda, G.; Barker, D.; et al. A Description of the Advanced Research WRF Model Version 4.3. **2021**, doi:10.5065/1dfh-6p97.

50. Zhou, J.; Zhang, H.; Zhang, J.; Zeng, X.; Ye, L.; Liu, Y.; Tayyab, M.; Chen, Y. WRF Model for Precipitation Simulation and Its Application in Real-Time Flood Forecasting in the Jinshajiang River Basin, China. *Meteorol Atmos Phys* **2018**, *130*, 635–647, doi:10.1007/s00703-017-0542-9.
51. Emmanouil, G.; Vlachogiannis, D.; Sfetsos, A. Exploring the Ability of the WRF-ARW Atmospheric Model to Simulate Different Meteorological Conditions in Greece. *Atmospheric Research* **2021**, *247*, 105226, doi:10.1016/j.atmosres.2020.105226.
52. Toros, H.; Kahraman, A.; Tilev-Tanriover, S.; Geertsema, G.; Cats, G. Simulating Heavy Precipitation with HARMONIE, HIRLAM and WRF-ARW: A Flash Flood Case Study in İstanbul, Turkey. *EJOSAT* **2018**, 1–12, doi:10.31590/ejosat.417535.
53. Patel, P.; Ghosh, S.; Kaginalkar, A.; Islam, S.; Karmakar, S. Performance Evaluation of WRF for Extreme Flood Forecasts in a Coastal Urban Environment. *Atmospheric Research* **2019**, *223*, 39–48, doi:10.1016/j.atmosres.2019.03.005.
54. Varlas, G.; Papadopoulos, A.; Papaioannou, G.; Markogianni, V.; Alamanos, A.; Dimitriou, E. Integrating Ensemble Weather Predictions in a Hydrologic-Hydraulic Modelling System for Fine-Resolution Flood Forecasting: The Case of Skala Bridge at Evrotas River, Greece. *Atmosphere* **2024**, *15*, 120, doi:10.3390/atmos15010120.
55. Junior, J.; Oliveira, V.D.P.; Sales, D. RAINFALL INPUT FROM WRF-ARW ATMOSPHERIC MODEL COUPLED WITH MOHID LAND HYDROLOGICAL MODEL FOR FLOW SIMULATION IN THE PARAÍBA DO SUL RIVER - BRAZIL. *Journal of Urban and Environmental Engineering* **2021**, *15*, 188–203, doi:10.4090/juee.20219.v15n2.188203.
56. Hydrologic Engineering Center (HEC) *River Analysis Systems - HEC-RAS (Version 6.3.1). U.S. Army Corps of Engineers.*; 2022;
57. Papaioannou, G.; Vasiliades, L.; Loukas, A.; Alamanos, A.; Efstratiadis, A.; Koukouvinos, A.; Tsoukalas, I.; Kossieris, P. A Flood Inundation Modeling Approach for Urban and Rural Areas in Lake and Large-Scale River Basins. *Water* **2021**, *13*, 1264, doi:10.3390/w13091264.
58. Alamanos, A.; Papaioannou, G.; Varlas, G.; Markogianni, V.; Papadopoulos, A.; Dimitriou, E. Representation of a Post-Fire Flash-Flood Event Combining Meteorological Simulations, Remote Sensing, and Hydraulic Modeling. *Land* **2024**, *13*, 47, doi:10.3390/land13010047.
59. Alamanos, A.; Papaioannou, G. Developing a Hydrological Model for Grand River Watershed, Ontario. In Proceedings of the 3rd IAHR Young Professionals Congress. Online; IAHR: Online, November 2022.
60. Milišić, H.; Hadžić, E.; Šuvalija, S.; Jahić, E. Floodplain Mapping Using HEC-RAS and Lidar Data: A Case Study of Bistrica River (Vrbas River Basin in B&H). In Proceedings of the New Technologies, Development and Application IV; Karabegović, I., Ed.; Springer International Publishing: Cham, 2021; pp. 1093–1103.
61. Costabile, P.; Costanzo, C.; Ferraro, D.; Macchione, F.; Petaccia, G. Performances of the New HEC-RAS Version 5 for 2-D Hydrodynamic-Based Rainfall-Runoff Simulations at Basin Scale: Comparison with a State-of-the Art Model. *Water* **2020**, *12*, 2326, doi:10.3390/w12092326.
62. Yalcin, E. Assessing the Impact of Topography and Land Cover Data Resolutions on Two-Dimensional HEC-RAS Hydrodynamic Model Simulations for Urban Flood Hazard Analysis. *Nat Hazards* **2020**, *101*, 995–1017, doi:10.1007/s11069-020-03906-z.
63. Alamanos, A.; Papaioannou, G.; Markogianni, V.; Plataniotis, A.; Varlas, G. The Impacts of a Forest Wildfire on Flooding and Economic Damages.; Online, September 2024.
64. Bailey, R.W.; Copeland, O.L. Vegetation and Engineering Structures in Flood and Erosion Control; U.S. Forest Service, Intermountain Forest and Range Experiment Station: Ogden, Utah, 1961. **1961**.
65. DeBano, L.F.; Neary, D.G.; Ffolliott, P.F. *Fire Effects on Ecosystems; 1st Ed.; Wiley, 1998*; 1998;

66. Moody, J.A.; Martin, D.A. Post-Fire, Rainfall Intensity–Peak Discharge Relations for Three Mountainous Watersheds in the Western USA. *Hydrological Processes* **2001**, *15*, 2981–2993, doi:10.1002/hyp.386.
67. Blake, D.; Nyman, P.; Nice, H.; D'Souza, F.M.L.; Kavazos, C.R.J.; Horwitz, P. Assessment of Post-Wildfire Erosion Risk and Effects on Water Quality in South-Western Australia. *Int. J. Wildland Fire* **2020**, *29*, 240–257, doi:10.1071/WF18123.
68. Dai, D.; Alamanos, A.; Cai, W.; Sun, Q.; Ren, L. Assessing Water Sustainability in Northwest China: Analysis of Water Quantity, Water Quality, Socio-Economic Development and Policy Impacts. *Sustainability* **2023**, *15*, 11017, doi:10.3390/su151411017.
69. Dai, D.; Alamanos, A. Modeling the Impact of Land Use Changes and Wastewater Treatment on Water Quality and Ecosystem Services in the Yongding River Basin, North China. *Water* **2024**, *16*, 1701, doi:10.3390/w16121701.
70. Robichaud, P.R.; Beyers, J.L.; Neary, D.G. *Evaluating the Effectiveness of Postfire Rehabilitation Treatments; US Department of Agriculture, Forest Service, Rocky Mountain Research Station: Fort Collins, CO, USA*; 2000;
71. Santi, P.M.; deWolfe, V.G.; Higgins, J.D.; Cannon, S.H.; Gartner, J.E. Sources of Debris Flow Material in Burned Areas. *Geomorphology* **2008**, *96*, 310–321, doi:10.1016/j.geomorph.2007.02.022.
72. Girona-García, A.; Vieira, D.C.S.; Silva, J.; Fernández, C.; Robichaud, P.R.; Keizer, J.J. Effectiveness of Post-Fire Soil Erosion Mitigation Treatments: A Systematic Review and Meta-Analysis. *Earth-Science Reviews* **2021**, *217*, 103611, doi:10.1016/j.earscirev.2021.103611.
73. Nasirzadehdizaji, R.; Akyuz, D.E. Predicting the Potential Impact of Forest Fires on Runoff and Sediment Loads Using a Distributed Hydrological Modeling Approach. *Ecological Modelling* **2022**, *468*, 109959, doi:10.1016/j.ecolmodel.2022.109959.
74. Cheung, D.J.; Giardino, J.R. Debris Flow Occurrence under Changing Climate and Wildfire Regimes: A Southern California Perspective. *Geomorphology* **2023**, *422*, 108538, doi:10.1016/j.geomorph.2022.108538.
75. Ebel, B.A. The Statistical Power of Post-Fire Soil-Hydraulic Property Studies: Are We Collecting Sufficient Infiltration Measurements after Wildland Fires? *Journal of Hydrology* **2022**, *612*, 128019, doi:10.1016/j.jhydrol.2022.128019.
76. Kemter, M.; Fischer, M.; Luna, L.V.; Schönfeldt, E.; Vogel, J.; Banerjee, A.; Korup, O.; Thonicke, K. Cascading Hazards in the Aftermath of Australia's 2019/2020 Black Summer Wildfires. *Earth's Future* **2021**, *9*, e2020EF001884, doi:10.1029/2020EF001884.
77. Nyman, P. *Yeates, P.; Langhans, C.; Schärer, C.; Noske, P.J.; Lane, P.N.J.; Haydon, S.; Sheridan, G.J. A Novel Approach for Determining Risk of Water Supply Disruptions Due to Post-Wildfire Debris Flows . In Proceedings of the 7th International Conference on Debris-Flow Hazards Mitigation; Golden, Colorado, USA, June 2019.*; 2019;
78. Roering, J.J.; Gerber, M. Fire and the Evolution of Steep, Soil-Mantled Landscapes. *Geology* **2005**, *33*, 349–352, doi:10.1130/G21260.1.
79. Stavi, I. Wildfires in Grasslands and Shrublands: A Review of Impacts on Vegetation, Soil, Hydrology, and Geomorphology. *Water* **2019**, *11*, 1042, doi:10.3390/w11051042.
80. Langhans, C.; Nyman, P.; Noske, P.J.; Van der Sant, R.E.; Lane, P.N.J.; Sheridan, G.J. Post-Fire Hillslope Debris Flows: Evidence of a Distinct Erosion Process. *Geomorphology* **2017**, *295*, 55–75, doi:10.1016/j.geomorph.2017.06.008.
81. Andreu, V.; Imeson, A.C.; Rubio, J.L. Temporal Changes in Soil Aggregates and Water Erosion after a Wildfire in a Mediterranean Pine Forest. *CATENA* **2001**, *44*, 69–84, doi:10.1016/S0341-8162(00)00177-6.

82. Fernández, C.; Vega, J.A.; Jiménez, E.; Fonturbel, T. Effectiveness of Three Post-Fire Treatments at Reducing Soil Erosion in Galicia (NW Spain). *Int. J. Wildland Fire* **2011**, *20*, 104–114, doi:10.1071/WF09010.
83. Swanson, F. *Fire and Geomorphic Processes. In Proceedings of the Fire Regimes and Ecosystem Properties; Mooney, H., Bonnicksen, T.M., Christensen, N.L., Lotan, J.E., Reiners, W.A., Eds.; U.S. Department of Agriculture, Forest Service: Honolulu, December 11 1981; Pp. 410–420.*; 1981;
84. Rust, A.J.; Hogue, T.S.; Saxe, S.; McCray, J. Post-Fire Water-Quality Response in the Western United States. *Int. J. Wildland Fire* **2018**, *27*, 203–216, doi:10.1071/WF17115.
85. Jolly, W.M.; Cochrane, M.A.; Freeborn, P.H.; Holden, Z.A.; Brown, T.J.; Williamson, G.J.; Bowman, D.M.J.S. Climate-Induced Variations in Global Wildfire Danger from 1979 to 2013. *Nat Commun* **2015**, *6*, 7537, doi:10.1038/ncomms8537.
86. Basheer, M.; Oommen, T. PyLandslide: A Python Tool for Landslide Susceptibility Mapping and Uncertainty Analysis. *Environmental Modelling & Software* **2024**, *177*, 106055, doi:10.1016/j.envsoft.2024.106055.
87. Robinne, F.-N.; Hallema, D.W.; Bladon, K.D.; Buttle, J.M. Wildfire Impacts on Hydrologic Ecosystem Services in North American High-Latitude Forests: A Scoping Review. *Journal of Hydrology* **2020**, *581*, 124360, doi:10.1016/j.jhydrol.2019.124360.
88. Kastridis, A.; Kamperidou, V. Evaluation of the Post-Fire Erosion and Flood Control Works in the Area of Cassandra (Chalkidiki, North Greece). *J. For. Res.* **2015**, *26*, 209–217, doi:10.1007/s11676-014-0005-9.
89. Posner, A.J.; Georgakakos, K.P. Quantifying the Impact of Community-Scale Flood Mitigation. *International Journal of Disaster Risk Reduction* **2017**, *24*, 189–208, doi:10.1016/j.ijdrr.2017.06.001.
90. Alamanos, A.; Koundouri, P. Science-Supported Policies to Achieve Environmental Sustainability under Crises. In *Elgar Encyclopedia of Water Policy, Economics and Management*; Edward Elgar Publishing, 2024; pp. 230–233 ISBN 978-1-80220-294-6.
91. | How to Talk to Your Community About Their 'Flood After Fire' Risk Available online: https://agents.floodsmart.gov/articles/how-talk-your-community-about-their-flood-after-fire-risk (accessed on 22 July 2025).
92. Alamanos, A. The Global Climate Hub. *Nature Sustainability* **2024**, *7*, doi:10.1038/s41893-024-01289-8.
93. UNSDSN CLIMATE GLOBAL HUB - Home Page Available online: https://32520579.isolation.zscaler.com/profile/f1651b6c-5a7a-4e25-a61a-66f8cd23da60/zia-session/?controls_id=a2bf14b6-b675-4c18-9553-90171d0d67dd&region=fra&tenant=2c2f6c39ed9e&user=834d4a7bae43b4509739f9c9805308b06228807b6d93e0506f308945488948d5&original_url=https%3A%2F%2Funsdsn.globalclimatehub.org%2F&key=sh-1&hmac=1f3523d60fb5a9c01da29637992868411bf36d87784198720c36c2da71d617df (accessed on 20 June 2024).
94. Koundouri, P.; Alamanos, A.; Plataniotis, A.; Stavridis, C.; Perifanos, K.; Devves, S. Assessing the Sustainability of the European Green Deal and Its Interlinkages with the SDGs. *npj Clim. Action* **2024**, *3*.
95. Koundouri, P.; Alamanos, A.; Sachs, J.D. A Global Climate Hub to Bridge Science and Society. In Proceedings of the International Conference on Sustainable Development (ICSD); SDSN: Online, 2024.
96. Rentschler, J.; Salhab, M.; Jafino, B.A. Flood Exposure and Poverty in 188 Countries. *Nat Commun* **2022**, *13*, 3527, doi:10.1038/s41467-022-30727-4.

97. Hasegawa, T.; Fujimori, S.; Shin, Y.; Tanaka, A.; Takahashi, K.; Masui, T. Consequence of Climate Mitigation on the Risk of Hunger. *Environ. Sci. Technol.* **2015**, *49*, 7245–7253, doi:10.1021/es5051748.
98. Koundouri, P.; Dellis, K.; Miziaki, O. The Multi-Faceted Effects of Green Innovation in the Crop & Livestock Sector in Greece: Evidence with the FABLE Calculator. *Preprint (DEOS Working Papers) 2412. Athens University of Economics and Business* **2024**.
99. Du, W.; FitzGerald, G.J.; Clark, M.; Hou, X.-Y. Health Impacts of Floods. *Prehospital and Disaster Medicine* **2010**, *25*, 265–272, doi:10.1017/S1049023X00008141.
100. Koundouri, P.; Plataniotis, A.; Alamanos, A. 9: Clean Water and Sanitation for All: SDG 6 Performance in Global, European and Regional Level. In; 2024 ISBN 978-1-80220-294-6.
101. Alamanos, A. Job–Environment Feedbacks. *Nat Sustain* **2024**, *7*, 525–526, doi:10.1038/s41893-024-01348-0.
102. AE4RIA AE4RIA & Huawei Report: "Twin Skills for the Twin Transition: Defining Green Digital Skills and Jobs" - Ae4ria Available online: https://32520579.isolation.zscaler.com/profile/f1651b6c-5a7a-4e25-a61a-66f8cd23da60/zia-session/?controls_id=5aed7c54-c445-4da7-862a-dce263201540&region=fra&tenant=2c2f6c39ed9e&user=834d4a7bae43b4509739f9c9805308b06228807b6d93e0506f308945488948d5&original_url=https%3A%2F%2Fae4ria.org%2Fae4ria-huawei-report-twin-skills-for-the-twin-transition-defining-green-digital-skills-and-jobs%2F&key=sh-1&hmac=42005f2c26c3196ff17d4a66c0fa742ce2632b11952d3493eb5fac0970b35b83 (accessed on 31 January 2024).
103. Bowes, B.D.; Tavakoli, A.; Wang, C.; Heydarian, A.; Behl, M.; Beling, P.A.; Goodall, J.L. Flood Mitigation in Coastal Urban Catchments Using Real-Time Stormwater Infrastructure Control and Reinforcement Learning. *Journal of Hydroinformatics* **2020**, *23*, 529–547, doi:10.2166/hydro.2020.080.
104. Alamanos, A. Water Resources Planning under Climate and Economic Changes in Skiathos Island, Aegean. *AQUA - Water Infrastructure, Ecosystems and Society* **2021**, *70*, 1085–1093, doi:https://doi.org/10.2166/aqua.2021.061.
105. Alamanos, A.; Sfyris, S.; Fafoutis, C.; Mylopoulos, N. Urban Water Demand Assessment for Sustainable Water Resources Management, under Climate Change and Socioeconomic Changes. *Water Supply* **2019**, *20*, 679–687, doi:10.2166/ws.2019.199.
106. Alamanos, A.; Linnane, S. Towards a Unifying Framework for Balancing Different SDGs and Objectives, and Achieving Sustainability: New Technologies, Socio-Hydrology, and Multi-Disciplinarity in Data-Scarce Areas.; September 6 2021.
107. Thaler, T. Developing Partnership Approaches for Flood Risk Management: Implementation of Inter-Local Co-Operations in Austria. *Water International* **2014**, *39*, 1018–1029, doi:10.1080/02508060.2014.992720.
108. Kourgialas, N.N. A Critical Review of Water Resources in Greece: The Key Role of Agricultural Adaptation to Climate-Water Effects. *Science of The Total Environment* **2021**, *775*, 145857, doi:10.1016/j.scitotenv.2021.145857.
109. Angeli, A.; Karkani, E.; Alamanos, A.; Xenarios, S.; Mylopoulos, N. Hydrological, Socioeconomic, Engineering and Water Quality Modeling Aspects for Evaluating Water Security: Experience from Greek Rural Watersheds. In Proceedings of the EGU General Assembly; EGU: Vienna, Austria, 2020.
110. CORINE CORINE Land Cover Available online: https://land.copernicus.eu/en/products/corine-land-cover (accessed on 13 December 2023).
111. Mononews New updates from Kineta: One dead from the fire, two injured and one missing. *mononews.gr* 2017.

112. Eleftheros typos The fire in Kineta started from the electricity piles - Details of the report. *Eleftheros Typos* 2019.
113. Souliotis, G. The mistakes started from Kineta. *Kathimerini* 2019.
114. Lekkas, E.; Spyrou, N.; Filis, C.; Diakakis, M.; Vassilakis, E.; Katsetsiadou, A.; Milios, D.; Arianoutsou, M.; Faragitakis, G.; Christopoulou, A.; et al. *The November 25, 2019 Kineta (Western Attica) Flood.*; Athens, Greece, 2019;
115. Vimaonline Kineta is a barren land after the fire - The fire was rekindled. *Vimaonline*.
116. Protothema Storm "Girionis": How Kineta was burned - Visual inspection in the area. *ProtoThema* 2019.
117. Copernicus The Sentinels Scientific Data Hub Available online: https://scihub.copernicus.eu/maintenance.html#/home (accessed on 2 February 2023).
118. Barrett, D.C.; Frazier, A.E. Automated Method for Monitoring Water Quality Using Landsat Imagery. *Water* **2016**, *8*, 257, doi:10.3390/w8060257.
119. Japitana, M.V.; Demetillo, A.T.; Burce, M.E.C.; B. Taboada, E. Catchment Characterization to Support Water Monitoring and Management Decisions Using Remote Sensing. *Sustainable Environment Research* **2019**, *29*, 8, doi:10.1186/s42834-019-0008-5.
120. Key, C.; Benson, N. *Landscape Assessment (LA); USDA Forest Service, Rocky Mountain Research Station: Ogden, UT, USA, 2006*; 2006;
121. Petropoulos, G.P.; Griffiths, H.M.; Kalivas, D.P. Quantifying Spatial and Temporal Vegetation Recovery Dynamics Following a Wildfire Event in a Mediterranean Landscape Using EO Data and GIS. *Applied Geography* **2014**, *50*, 120–131, doi:10.1016/j.apgeog.2014.02.006.
122. Rahman, S.; Chang, H.-C.; Hehir, W.; Magilli, C.; Tomkins, K. Inter-Comparison of Fire Severity Indices from Moderate (Modis) and Moderate-To-High Spatial Resolution (Landsat 8 & Sentinel-2A) Satellite Sensors. In Proceedings of the IGARSS 2018 - 2018 IEEE International Geoscience and Remote Sensing Symposium; July 2018; pp. 2873–2876.
123. Tewari, M.; Boulder, C.; Chen, F.; Wang, W.; Dudhia, J.; LeMone, M.; Mitchell, K.; Ek, M.; Gayno, G.; Wegiel, J.; et al. Implementation and Verification of the Unified Noah Land Surface Model in the WRF Model. In Proceedings of the 20th Conference on Weather Analysis and Forecasting/16th Conference on Numerical Weather Prediction; 2004; Vol. Formerly Paper Number 17.5.
124. Barlage, M.; Chen, F.; Tewari, M.; Ikeda, K.; Gochis, D.; Dudhia, J.; Rasmussen, R.; Livneh, B.; Ek, M.; Mitchell, K. Noah Land Surface Model Modifications to Improve Snowpack Prediction in the Colorado Rocky Mountains. *Journal of Geophysical Research: Atmospheres* **2010**, *115*, doi:10.1029/2009JD013470.
125. Iacono, M.J.; Delamere, J.S.; Mlawer, E.J.; Shephard, M.W.; Clough, S.A.; Collins, W.D. Radiative Forcing by Long-Lived Greenhouse Gases: Calculations with the AER Radiative Transfer Models. *Journal of Geophysical Research: Atmospheres* **2008**, *113*, doi:10.1029/2008JD009944.
126. Hong, S.-Y.; Dudhia, J.; Chen, S.-H. A Revised Approach to Ice Microphysical Processes for the Bulk Parameterization of Clouds and Precipitation. *Monthly Weather Review* **2004**, *132*, 103–120, doi:10.1175/1520-0493(2004)132<0103:ARATIM>2.0.CO;2.
127. Grell, G.A.; Freitas, S.R. A Scale and Aerosol Aware Stochastic Convective Parameterization for Weather and Air Quality Modeling. *Atmospheric Chemistry and Physics* **2014**, *14*, 5233–5250, doi:10.5194/acp-14-5233-2014.
128. Hong, S.-Y.; Noh, Y.; Dudhia, J. A New Vertical Diffusion Package with an Explicit Treatment of Entrainment Processes. *Monthly Weather Review* **2006**, *134*, 2318–2341, doi:10.1175/MWR3199.1.
129. Meteo MeteoSearch Available online: https://meteosearch.meteo.gr/ (accessed on 8 November 2023).

130. Boschetti, M.; Nutini, F.; Manfron, G.; Brivio, P.A.; Nelson, A. Comparative Analysis of Normalised Difference Spectral Indices Derived from MODIS for Detecting Surface Water in Flooded Rice Cropping Systems. *PLOS ONE* **2014**, *9*, e88741, doi:10.1371/journal.pone.0088741.
131. Memon, A.A.; Muhammad, S.; Rahman, S.; Haq, M. Flood Monitoring and Damage Assessment Using Water Indices: A Case Study of Pakistan Flood-2012. *The Egyptian Journal of Remote Sensing and Space Science* **2015**, *18*, 99–106, doi:10.1016/j.ejrs.2015.03.003.
132. Smith, A.R. Color Gamut Transform Pairs. In Proceedings of the Proceedings of the 5th annual conference on Computer graphics and interactive techniques; Association for Computing Machinery: New York, NY, USA, August 23 1978; pp. 12–19.
133. Pekel, J.-F.; Vancutsem, C.; Bastin, L.; Clerici, M.; Vanbogaert, E.; Bartholomé, E.; Defourny, P. A near Real-Time Water Surface Detection Method Based on HSV Transformation of MODIS Multi-Spectral Time Series Data. *Remote Sensing of Environment* **2014**, *140*, 704–716, doi:10.1016/j.rse.2013.10.008.
134. Pekel, J.-F.; Cottam, A.; Gorelick, N.; Belward, A.S. High-Resolution Mapping of Global Surface Water and Its Long-Term Changes. *Nature* **2016**, *540*, 418–422, doi:10.1038/nature20584.
135. Konapala, G.; Kumar, S.V.; Khalique Ahmad, S. Exploring Sentinel-1 and Sentinel-2 Diversity for Flood Inundation Mapping Using Deep Learning. *ISPRS Journal of Photogrammetry and Remote Sensing* **2021**, *180*, 163–173, doi:10.1016/j.isprsjprs.2021.08.016.
136. Xu, H. Modification of Normalised Difference Water Index (NDWI) to Enhance Open Water Features in Remotely Sensed Imagery. *International Journal of Remote Sensing* **2006**, *27*, 3025–3033, doi:10.1080/01431160600589179.
137. Kalyanapu, A.; Burian, S.; McPherson, T. Effect of Land Use-Based Surface Roughness on Hydrologic Model Output. *Journal of Spatial Hydrology* **2009**, *9*.
138. Weltz, M.A.; Arslan, A.B.; Lane, L.J. Hydraulic Roughness Coefficients for Native Rangelands. *Journal of Irrigation and Drainage Engineering* **1992**, *118*, 776–790, doi:10.1061/(ASCE)0733-9437(1992)118:5(776).
139. Moore, D.; Todea, N.; Cerrelli, G.; Yochum, S.; Norman, J.; Hoeft, C. *Hydrologic Analyses of Post-Wildfire Conditions*; 2016; p. 146;.
140. Canfield, H.E.; Goodrich, D. Suggested Changes to AGWA to Account for Fire (V 2.1).; 2005.
141. Canfield, H.E.; Goodrich, D.C.; Burns, I.S. Selection of Parameters Values to Model Post-Fire Runoff and Sediment Transport at the Watershed Scale in Southwestern Forests. **2012**, 1–12, doi:10.1061/40763(178)48.
142. Lefrancq, M.; Van Dijk, P.; Jetten, V.; Schwob, M.; Payraudeau, S. Improving Runoff Prediction Using Agronomical Information in a Cropped, Loess Covered Catchment. *Hydrological Processes* **2017**, *31*, 1408–1423, doi:10.1002/hyp.11115.
143. Sanz-Ramos, M.; Bladé, E.; González-Escalona, F.; Olivares, G.; Aragón-Hernández, J.L. Interpreting the Manning Roughness Coefficient in Overland Flow Simulations with Coupled Hydrological-Hydraulic Distributed Models. *Water* **2021**, *13*, 3433, doi:10.3390/w13233433.
144. Senarath, S.U.S.; Ogden, F.L.; Downer, C.W.; Sharif, H.O. On the Calibration and Verification of Two-Dimensional, Distributed, Hortonian, Continuous Watershed Models. *Water Resources Research* **2000**, *36*, 1495–1510, doi:10.1029/2000WR900039.
145. Pradhan, N.R.; Floyd, I. Event Based Post-Fire Hydrological Modeling of the Upper Arroyo Seco Watershed in Southern California. *Water* **2021**, *13*, 2303, doi:10.3390/w13162303.
146. Eleftheros typos Satellite images of the post-flood destructed Kineta. *Ελεύθερος Τύπος* 2019.
147. UPstories Kineta Greece after Disaster. Up Stories - YouTube Available online: https://www.youtube.com/watch?v=EDr5sZqQMnw (accessed on 12 November 2023).

148. Di Baldassarre, G.; Schumann, G.; Bates, P.D.; Freer, J.E.; Beven, K.J. Flood-Plain Mapping: A Critical Discussion of Deterministic and Probabilistic Approaches. *Hydrological Sciences Journal* **2010**, *55*, 364–376, doi:10.1080/02626661003683389.
149. Horritt, M.S.; Di Baldassarre, G.; Bates, P.D.; Brath, A. Comparing the Performance of a 2-D Finite Element and a 2-D Finite Volume Model of Floodplain Inundation Using Airborne SAR Imagery. *Hydrological Processes* **2007**, *21*, 2745–2759, doi:10.1002/hyp.6486.
150. Zotou, I.; Karamvasis, K.; Karathanassi, V.; Tsihrintzis, V.A. Potential of Two SAR-Based Flood Mapping Approaches in Supporting an Integrated 1D/2D HEC-RAS Model. *Water* **2022**, *14*, 4020, doi:10.3390/w14244020.
151. Loukas, A.; Katsiolas, A.; Papaioannou, G. *Investigating the Effects of Initial Soil Moisture and the Uncertainty of Manning Friction Coefficient on Flood Hazard Estimation and Mapping.*; Copernicus Meetings, 2024;
152. Sampson, C.C.; Smith, A.M.; Bates, P.D.; Neal, J.C.; Alfieri, L.; Freer, J.E. A High-Resolution Global Flood Hazard Model. *Water Resources Research* **2015**, *51*, 7358–7381, doi:10.1002/2015WR016954.
153. Shastry, A.; Durand, M.; Neal, J.; Fernández, A.; Phang, S.C.; Mohr, B.; Jung, H.C.; Kari, S.; Moritz, M.; Mark, B.G.; et al. Small-Scale Anthropogenic Changes Impact Floodplain Hydraulics: Simulating the Effects of Fish Canals on the Logone Floodplain. *Journal of Hydrology* **2020**, *588*, 125035, doi:10.1016/j.jhydrol.2020.125035.
154. Nandam, V.; Patel, P.L. A Framework to Assess Suitability of Global Digital Elevation Models for Hydrodynamic Modelling in Data Scarce Regions. *Journal of Hydrology* **2024**, *630*, 130654, doi:10.1016/j.jhydrol.2024.130654.
155. Napper, C. *Burned Area Emergency Response Treatments (BAER) Catalog; US Forest Service: Washington, DC, USA; San Dimas Technology and Development Center: San Dimas, CA, USA.*; 2006;
156. Pastor, A.V.; Tzoraki, O.; Bruno, D.; Kaletová, T.; Mendoza-Lera, C.; Alamanos, A.; Brummer, M.; Datry, T.; De Girolamo, A.M.; Jakubínský, J.; et al. Rethinking Ecosystem Service Indicators for Their Application to Intermittent Rivers. *Ecological Indicators* **2022**, *137*, 108693, doi:10.1016/j.ecolind.2022.108693.
157. Papaioannou, G.; Alamanos, A.; Maris, F. Evaluating Post-Fire Erosion and Flood Protection Techniques: A Narrative Review of Applications. *GeoHazards* **2023**, *4*, 380–405, doi:10.3390/geohazards4040022.
158. Robichaud, P.R.; Storrar, K.A.; Wagenbrenner, J.W. Effectiveness of Straw Bale Check Dams at Reducing Post-Fire Sediment Yields from Steep Ephemeral Channels. *Science of The Total Environment* **2019**, *676*, 721–731, doi:10.1016/j.scitotenv.2019.04.246.
159. Inbar, A.; Ben-Hur, M.; Sternberg, M.; Lado, M. Using Polyacrylamide to Mitigate Post-Fire Soil Erosion. *Geoderma* **2015**, *239–240*, 107–114, doi:10.1016/j.geoderma.2014.09.026.
160. Prats, S.A.; Malvar, M.C.; Wagenbrenner, J.W. Compaction and Cover Effects on Runoff and Erosion in Post-Fire Salvage Logged Areas in the Valley Fire, California. *Hydrological Processes* **2021**, *35*, e13997, doi:10.1002/hyp.13997.
161. Prats, S.A.; Martins, M.A. dos S.; Malvar, M.C.; Ben-Hur, M.; Keizer, J.J. Polyacrylamide Application versus Forest Residue Mulching for Reducing Post-Fire Runoff and Soil Erosion. *Science of The Total Environment* **2014**, *468–469*, 464–474, doi:10.1016/j.scitotenv.2013.08.066.
162. Boix-Fayos, C.; de Vente, J.; Martínez-Mena, M.; Barberá, G.G.; Castillo, V. The Impact of Land Use Change and Check-Dams on Catchment Sediment Yield. *Hydrological Processes* **2008**, *22*, 4922–4935, doi:10.1002/hyp.7115.
163. Girona-García, A.; Cretella, C.; Fernández, C.; Robichaud, P.R.; Vieira, D.C.S.; Keizer, J.J. How Much Does It Cost to Mitigate Soil Erosion after Wildfires? *J Environ Manage* **2023**, *334*, 117478, doi:10.1016/j.jenvman.2023.117478.

164. Pizzeghello, D.; Zanella, A.; Carletti, P.; Nardi, S. Chemical and Biological Characterization of Dissolved Organic Matter from Silver Fir and Beech Forest Soils. *Chemosphere* **2006**, *65*, 190–200, doi:10.1016/j.chemosphere.2006.03.001.
165. Margiorou, S.; Kastridis, A.; Sapountzis, M. Pre/Post-Fire Soil Erosion and Evaluation of Check-Dams Effectiveness in Mediterranean Suburban Catchments Based on Field Measurements and Modeling. *Land* **2022**, *11*, 1705, doi:10.3390/land11101705.
166. Foltz, R.B. *Robichaud, P.R.; Rhee, H. A Synthesis of Postfire Road Treatments for BAER Teams: Methods, Treatment Effectiveness, and Decisionmaking Tools for Rehabilitation. Gen. Tech. Rep. MRS-GTR-228; Fort Collins, CO: U.S, 2009*; 2009;
167. Reid, L.M. *Understanding and Evaluating Cumulative Watershed Impacts. In Cumulative Watershed Effects of Fuel Management in the Western United States. Gen. Tech. Rep. RMRS-GTR-231; Elliot, W.J., Miller, I.S., Audin, L., Eds.; Department of Agriculture, Forest Service, Rocky Mountain Research Station: Collins, CO: U.S., 2010; Pp. 277–298*; 2010;
168. Dobrowski, S.Z.; Aghai, M.M.; Chichilnisky du Lac, A.; Downer, R.; Fargione, J.; Haase, D.L.; Hoecker, T.; Kildisheva, O.A.; Murdoch, A.; Newman, S.; et al. 'Mind the Gap'—Reforestation Needs vs. Reforestation Capacity in the Western United States. *Front. For. Glob. Change* **2024**, *7*, doi:10.3389/ffgc.2024.1402124.
169. Myronidis, D.I.; Arabatzis, G. Evaluation of Greek Post-Fire Erosion Mitigation Policy through Spatial Analysis. *Pol. J. Environ. Stud.* **2009**, *18*, 865–872.
170. Myronidis, D.I.; Emmanouloudis, D.A.; Mitsopoulos, I.A.; Riggos, E.E. Soil Erosion Potential after Fire and Rehabilitation Treatments in Greece. *Environ Model Assess* **2010**, *15*, 239–250, doi:10.1007/s10666-009-9199-1.
171. Greek Ministry of Environment and Energy *Hellenic Technical Specification on the Technical Guidelines for Temporary Erosion Control Structures Utilizing Locally Available Timber. ICS: 93.040; Athens Greece, 2009.*; 2009;
172. Papakonstantinou, S.; Kalliris, M. *Flood and Soil-Erosion Protection Works in Forests Burned by the Wildfire of 27-07-2013 at the Communities of Istrio, Profilias, Arnithas, Vatiou, and Apolakkias, in Southern Rhodes. Decentralized Administration of the Aegean (in Greek).*; 2013;
173. Marougklianis, C.; Ranis, G. *Final Study for the Construction of Wooden Check-Dams in the Forests of the Catchments of Rahonio, Prinou, Sotiros, and Kallirachis, Affected by the Wildfire of 10-09-2016 in Thasos Island. Decentralized Administration of Macedonia and Thrace (in Greek).*; 2018;
174. Alamanos, A.; Papaioannou, G.; Varlas, G.; Markogianni, V.; Plataniotis, A.; Papadopoulos, A.; Dimitriou, E.; Koundouri, P. Designing Post-Fire Flood Protection Techniques for a Real Event in Central Greece. *Prevention and Treatment of Natural Disasters* **2024**, *3*.
175. Papaioannou, G.; Alamanos, A.; Basheer, M.; Nagkoulis, N.; Markogianni, V.; Varlas, G.; Plataniotis, A.; Papadopoulos, A.; Dimitriou, E.; Koundouri, P. A Lesson in Preparedness: Assessing the Effectiveness of Low-Cost Post-Wildfire Flood Protection Measures for the Catastrophic Flood in Kineta, Greece. *Hydrologic and Earth Systems Science (under review)* **2025**.
176. Koudoumakis, P.; Keramitsoglou, K.; Protopapas, A.L.; Dokas, I. A General Method for Multi–Hazard Intensity Assessment for Cultural Resources: Implementation in the Region of Eastern Macedonia and Thrace, Greece. *International Journal of Disaster Risk Reduction* **2024**, *100*, 104197, doi:10.1016/j.ijdrr.2023.104197.
177. Politi, N.; Vlachogiannis, D.; Sfetsos, A.; Gounaris, N.; Varela, V. Investigation of Fire Weather Danger under a Changing Climate at High Resolution in Greece. *Sustainability* **2023**, *15*, 2498, doi:10.3390/su15032498.
178. Greek Ministry of Environment and Energy *Study on Soil-Erosion and Flood Protection Works at the Burnt Area of the Avantas Catchment and Surounding Settlements. Decentralized Administration of Macedonia and Thrace. (in Greek)*; 2023;

179. Thieken, A.H.; Ackermann, V.; Elmer, F.; Kreibich, H.; Kuhlmann, B.; Kunert, U.; Maiwald, H.; Merz, B.; Müller, M.; Piroth, K.; et al. Methods for the Evaluation of Direct and Indirect Flood Losses.; Deutsches GeoForschungsZentrum GFZ, 2009.
180. Merz, B.; Kreibich, H.; Thieken, A.; Schmidtke, R. Estimation Uncertainty of Direct Monetary Flood Damage to Buildings. *Natural Hazards and Earth System Sciences* **2004**, *4*, 153–163, doi:10.5194/nhess-4-153-2004.
181. Brémond, P.; Grelot, F.; Agenais, A.-L. Review Article: Economic Evaluation of Flood Damage to Agriculture – Review and Analysis of Existing Methods. *Natural Hazards and Earth System Sciences* **2013**, *13*, 2493–2512, doi:10.5194/nhess-13-2493-2013.
182. Zabret, K.; Hozjan, U.; Kryžanowsky, A.; Brilly, M.; Vidmar, A. Development of Model for the Estimation of Direct Flood Damage Including the Movable Property. *Journal of Flood Risk Management* **2018**, *11*, S527–S540, doi:10.1111/jfr3.12255.
183. Kirillov, A.; Mintun, E.; Ravi, N.; Mao, H.; Rolland, C.; Gustafson, L.; Xiao, T.; Whitehead, S.; Berg, A.C.; Lo, W.-Y.; et al. Segment Anything 2023.
184. He, Y.; Wang, J.; Zhang, Y.; Liao, C. An Efficient Urban Flood Mapping Framework towards Disaster Response Driven by Weakly Supervised Semantic Segmentation with Decoupled Training Samples. *ISPRS Journal of Photogrammetry and Remote Sensing* **2024**, *207*, 338–358, doi:10.1016/j.isprsjprs.2023.12.009.
185. Baziak, B.; Bodziony, M.; Szczepanek, R. Mountain Streambed Roughness and Flood Extent Estimation from Imagery Using the Segment Anything Model (SAM). *Hydrology* **2024**, *11*, 17, doi:10.3390/hydrology11020017.
186. Hellenic Association of Insurance Companies *1993 – 2023: Analysis of the damages of disastrous events*; Athens, Greece, 2024; p. 27;.
187. Macrotrends Greece Inflation Rate 1960-2024 Available online: https://www.macrotrends.net/global-metrics/countries/GRC/greece/inflation-rate-cpi (accessed on 27 April 2024).
188. IEFIMERIDA.GR The causes of the disaster in Kineta Available online: https://www.iefimerida.gr/ellada/aytopsia-lekka-stin-kineta-aitia-tis-katastrofis (accessed on 27 April 2024).
189. Kalabokidis, K.; Soulakellis, N.; Zouros, N.; Kavroudakis, D.; et al. *Evaluation of the disaters in south Lesvos and recommendations for restoration and development after the recent wildfires*; University of the Aegean: Mytilene, Greece, 2024; p. 375;.
190. McCarthy, P.S. *Transportation Economics: Theory and Practice : A Case Study Approach*; Blackwell Publishers, 2001; ISBN 978-0-631-22181-4.
191. US Department of Transportation *Revised Departmental Guidance on Valuation of Travel Time in Economic Analysis | US Department of Transportation*; Washington, DC, USA, 2016; p. 26;.
192. Fletcher, D.R.; Ekern, D.S. *Transportation System Resilience: Research Roadmap and White Papers*; Transportation Research Board: Washington, D.C., 2021; ISBN 978-0-309-48457-2.
193. Pregnolato, M.; Ford, A.; Wilkinson, S.M.; Dawson, R.J. The Impact of Flooding on Road Transport: A Depth-Disruption Function. *Transportation Research Part D: Transport and Environment* **2017**, *55*, 67–81, doi:10.1016/j.trd.2017.06.020.
194. Dutta, D.; Herath, S.; Musiake, K. A Mathematical Model for Flood Loss Estimation. *Journal of Hydrology* **2003**, *277*, 24–49, doi:10.1016/S0022-1694(03)00084-2.
195. Greek Parliament *Greek Parliament Minutes of the 27 November 2019*; Athens, Greece, 2019; p. 120;.
196. Protothema Storm “Girionis”: Flooded Kineta and Katerini - Closed the Athens-Corinth Highway. *ProtoThema* 2019.

197. IEFIMERIDA.GR Kineta: 3.5 million euro needed for the flood damage recovery Available online: https://www.iefimerida.gr/ellada/kineta-erga-35-ekat-eyro-gia-apokatastasi-zimion (accessed on 27 April 2024).
198. West Attica Region *Restoration of damages for the local community of Kineta. West Attica's Technical Works Observatory.*; 2021;
199. Koundouri, P.; Alamanos, A. Running Dry, Then Underwater: Greece's Path to Building Resilience against Climate Threats - 360. *360info* 2025.
200. Turkelboom, F.; Demeyer, R.; Vranken, L.; De Becker, P.; Raymaekers, F.; De Smet, L. How Does a Nature-Based Solution for Flood Control Compare to a Technical Solution? Case Study Evidence from Belgium. *Ambio* **2021**, *50*, 1431–1445, doi:10.1007/s13280-021-01548-4.
201. Alamanos, A.; Papaioannou, G. A GIS Multi-Criteria Analysis Tool for a Low-Cost, Preliminary Evaluation of Wetland Effectiveness for Nutrient Buffering at Watershed Scale: The Case Study of Grand River, Ontario, Canada. *Water* **2020**, *12*, 3134, doi:10.3390/w12113134.
202. Birchall, S.J.; Kehler, S.; Weissenberger, S. "Sometimes, I Just Want to Scream": Institutional Barriers Limiting Adaptive Capacity and Resilience to Extreme Events. *Global Environmental Change* **2025**, *91*, 102967, doi:10.1016/j.gloenvcha.2025.102967.
203. McNaught, R.; Nalau, J.; Hales, R.; Pittaway, E.; Handmer, J.; Renouf, J. Innovation and Deadlock in Governing Disasters and Climate Change Collaboratively - Lessons from the Northern Rivers Region of New South Wales, Australia. *International Journal of Disaster Risk Reduction* **2024**, *105*, 104366, doi:10.1016/j.ijdrr.2024.104366.
204. Alamanos, A. Public Policy to Support Environmental Sustainability and Circular Economy: Efforts towards Integrated Approaches. In Proceedings of the 2nd Symposium on on Circular Economy and Sustainability; Alexandroupolis, Greece, July 15 2021.
205. Garcia, J.A.; Alamanos, A. A Multi-Objective Optimization Framework for Water Resources Allocation Considering Stakeholder Input. *Environmental Sciences Proceedings* **2023**, *25*, 32, doi:10.3390/ECWS-7-14227.
206. Alamanos, A.; Koundouri, P. Multi-Stakeholder Platforms for Water Management: Connecting Policy and Science. In Proceedings of the Proceedings of the 10th Annual International Conference on Sustainable Development (ICSD); Online, 2022.
207. Nagkoulis, N.; Alamanos, A.; Koundouri, P.; Nisiforou, O. The Floodport App for Interactive Coastal Flooding Training. Https://Auebports.Shinyapps.Io/Floodport DOI: 10.13140/RG.2.2.27425.72809 2025.
208. Alamanos, A.; Wise, R.M.; Xenarios, S.; Papaioannou, G.; Markogianni, V.; Varlas, G.; Plataniotis, A.; Papadopoulos, A.; Dimitriou, E.; Koundouri, P. A Prevention versus Cure Dilemma: Protection from Post-Wildfire Flood Hazards Combining Experiences from Greece and Australia. *Environmental Communications Letters (under review)* **2025**.
209. Cunningham, C.X.; Williamson, G.J.; Bowman, D.M.J.S. Increasing Frequency and Intensity of the Most Extreme Wildfires on Earth. *Nat Ecol Evol* **2024**, *8*, 1420–1425, doi:10.1038/s41559-024-02452-2.
210. Jones, M.W.; Abatzoglou, J.T.; Veraverbeke, S.; Andela, N.; Lasslop, G.; Forkel, M.; Smith, A.J.P.; Burton, C.; Betts, R.A.; van der Werf, G.R.; et al. Global and Regional Trends and Drivers of Fire Under Climate Change. *Reviews of Geophysics* **2022**, *60*, e2020RG000726, doi:10.1029/2020RG000726.
211. Seager, R.; Wu, Y.; Cherchi, A.; Simpson, I.R.; Osborn, T.J.; Kushnir, Y.; Lukovic, J.; Liu, H.; Nakamura, J. Recent and Near-term Future Changes in Impacts-relevant Seasonal Hydroclimate in the World's Mediterranean Climate Regions. *International Journal of Climatology* **2024**, doi:10.1002/joc.8551.

212. Bradshaw, S.D.; Dixon, K.W.; Lambers, H.; Cross, A.T.; Bailey, J.; Hopper, S.D. Understanding the Long-Term Impact of Prescribed Burning in Mediterranean-Climate Biodiversity Hotspots, with a Focus on South-Western Australia. *Int. J. Wildland Fire* **2018**, *27*, 643–657, doi:10.1071/WF18067.
213. Abram, N.J.; Henley, B.J.; Sen Gupta, A.; Lippmann, T.J.R.; Clarke, H.; Dowdy, A.J.; Sharples, J.J.; Nolan, R.H.; Zhang, T.; Wooster, M.J.; et al. Connections of Climate Change and Variability to Large and Extreme Forest Fires in Southeast Australia. *Commun Earth Environ* **2021**, *2*, 1–17, doi:10.1038/s43247-020-00065-8.
214. Australian Parliament *Inquiry into Response to Major Flooding across New South Wales in 2022*; Sydney, Australia, 2022;
215. Gorddard, R.; Colloff, M.J.; Wise, R.M.; Ware, D.; Dunlop, M. Values, Rules and Knowledge: Adaptation as Change in the Decision Context. *Environmental Science & Policy* **2016**, *57*, 60–69, doi:10.1016/j.envsci.2015.12.004.
216. Prober, S.M.; Colloff, M.J.; Abel, N.; Crimp, S.; Doherty, M.D.; Dunlop, M.; Eldridge, D.J.; Gorddard, R.; Lavorel, S.; Metcalfe, D.J.; et al. Informing Climate Adaptation Pathways in Multi-Use Woodland Landscapes Using the Values-Rules-Knowledge Framework. *Agriculture, Ecosystems & Environment* **2017**, *241*, 39–53, doi:10.1016/j.agee.2017.02.021.
217. Word Bank *Citizen Engagement and Open Data for Disaster Risk Reduction in Thessaloniki*; 2018;
218. Papadopoulou, E. Shocking Testimonies about the Flood in Kineta in 2019 Available online: https://www.efsyn.gr/ellada/dikaiosyni/456701_sygklonistikes-martyries-gia-tin-plimmyra-stin-kineta-2019#goog_rewarded (accessed on 25 March 2025).
219. Protothema *The Trial for the Kineta Flood Begins This Autumn. Patoulis to Be the First Defendant.*; Athens, Greece, 2024;
220. ERTnews K. Agorastos and three other defendants found guilty of causing a flood through negligence in the “Ianos” trial. *ertnews.gr* 2024.
221. Dubo, T.; Palomo, I.; Zingraff-Hamed, A.; Bruley, E.; Collain, G.; Lavorel, S. Levers for Transformative Nature-Based Adaptation Initiatives in the Alps. *PLOS Climate* **2023**, *2*, e0000193, doi:10.1371/journal.pclm.0000193.
222. Fleming, A.; Wise, R.M.; Hansen, H.; Sams, L. The Sustainable Development Goals: A Case Study. *Marine Policy* **2017**, *86*, 94–103, doi:10.1016/j.marpol.2017.09.019.
223. Colloff, M.J.; Wise ,Russell M.; Palomo ,Ignacio; Lavorel ,Sandra; and Pascual, U. Nature’s Contribution to Adaptation: Insights from Examples of the Transformation of Social-Ecological Systems. *Ecosystems and People* **2020**, *16*, 137–150, doi:10.1080/26395916.2020.1754919.
224. Alamanos, A.; Koundouri, P.; Papadaki, L.; Pliakou, T. A System Innovation Approach for Science-Stakeholder Interface: Theory and Application to Water-Land-Food-Energy Nexus. *Frontiers in Water* **2022**, *3*.
225. Alamanos, A.; Koundouri, P.; Papadaki, L.; Pliakou, T.; Toli, E. Water for Tomorrow: A Living Lab on the Creation of the Science-Policy-Stakeholder Interface. *Water* **2022**, *14*, 2879, doi:10.3390/w14182879.
226. Alamanos, A.; Kolokytha, E.; Mylopoulos, Y. A SCIENCE-TO-POLICY CAPACITY DEVELOPMENTPROCESS FOR FLOOD PROTECTION. In Proceedings of the 41st IAHR World Congress; Singapore, June 24 2025.
227. Capacity Development for Water. *SIWI - Leading expert in water governance*.
228. SDG 6 Capacity Development Initiative Available online: https://www.unwater.org/our-work/sdg-6-capacity-development-initiative (accessed on 22 July 2025).
229. Alamanos, A.; Papaioannou, G. Generating Customized Design Storms for Any Greek Catchment Based on Official IDF Parameters: The Catchment2Storm Python App. In Proceedings of the 6th IAHR Young Professionals Congress; Online, December 3 2025.
230. YPEKA *IDF Curves under the 2nd Cycle of the Flood Risk Management Plans*; 2023;

231. Koutsoyianis, D.; Ksanthopoulos, T. *Technical Hydrology [Undergraduate Manual].*; Kallipos, Open Academic Publishing. https://dx.doi.org/10.57713/kallipos-715;
232. Chow, V.T.; Maidment, D.R.; Mays, L.W. *Applied Hydrology. International Edition, McGraw-Hill Book Company, New York*;
233. Alamanos, A.; Papaioannou, G. A National-Scale IDF-Based Design Storm Hyetograph Inventory: Applying the Catchment2Storm Tool in Greece. In Proceedings of the The 9th International Electronic Conference on Water Sciences Recent Advances in Water Sciences under a Variable and Changing Environment; Online, November 11 2025.
234. Alamanos, A.; Nisiforou, O. Regional Rainfall Disparities across Greece Calling for Localized Design Standards for Major Urban Centres, Ports and Farming Sites: Insights from National-Scale Hyetograph Modelling. In Proceedings of the IWA World Water Forum & Exhibition; Glaskow, UK, October 4 2025.
235. Sarpong, H.A.; Rolston, A.; Linnane, S.; Getty, D.; Alamanos, A. 47: Public Communication of Water Scarcity from Water Supply Agencies. In; 2024 ISBN 978-1-80220-294-6.
236. Chaini, A. No flood protection works in Kineta: the causes of the disaster. *Ecozen* 2019.